Mémoire

Auteur : Bomans, Victor
Promoteur(s) : Cudell, Jean-Rene
Faculté : Faculté des Sciences
Diplôme : Master en sciences spatiales, à finalité approfondie
Année académique : 2020-2021
URI/URL : http://hdl.handle.net/2268.2/12181

Consequences of an extension of General Relativity on gravitational waves

Master thesis presented for the purpose of the obtention of the academic grade of master in space sciences

Author Bomans Victor
Academic year 2020-2021

Acknowledgements

I would like to thanks my supervisor Jean-René Cudell for his support along this very difficult and unpleasant academic year of 2020-2021. I would like to express my thanks also to all the professors of the AGO department of the university of Liège and the physics department of the university of Bruxelles for the well organised lectures despite the pandemic.

Contents

Introduction

Origins of gravitational waves

The following section is based on [1] and [2].

In 1905, after Einstein published his famous article *Zur Elektrodynamik bewegter Körper* [3], Henri Poincaré proposed the existence of gravitational waves analogous to the electromagnetic waves [4]. Later Einstein also had the idea that these waves could exist. But he wasn't convinced of there existence, essentially because there are no dipole in gravitation due to the absence of negative mass [5].

However, he tried to find wave solutions to his equations in 1916 and did find such solutions [6]. But he made a mistake that led him to the conclusions that three types of gravitational waves exist. He had made a calculational mistake and realized it later in 1918 [7]. He published another paper that year with the correct derivation of gravitational waves. However, the scientific community, including Einstein, remained doubtful about their existence. The reason was the possibility that these waves are a spurious artefact from the coordinate system.

In 1936, Einstein and his collaborator Rosen sent an article which concluded that gravitational waves don't exist [8]. The reviewer is believed to have been Robertson, who found mistakes in the development but Rosen refused to listen to the critics and published his paper in another journal. Einstein remained sceptical. In the late 1950's the works of Pirani, Bondi, Hartmann and Robinson proved that gravitational waves are a real phenomenon predicted by General Relativity and not some spurious result linked to the choice of the coordinate system.

If gravitational waves exist one could prove their existence by observing them. To that end, one must first know their effects and whether these effects can effectively be observed. So until the end of the 1950's the big question was: Do gravitational waves carry energy? The complex formalism of the theory of General Relativity was at the center of the difficulty that scientists encountered at that time. However, the answer that convinced the majority was very simple and given by Feynman [9]. The effect of gravitational waves was already known at that time: they squeeze one of the two dimensions perpendicular to their propagation direction and stretch the other. In 1957 the university of North California organised the first edition of a series of discussions named the Chapel Hill Conference, on the most recent questions related to gravity. Feynman explained that if a bar, on which two rings are placed, lies in the plane transverse to the propagation of the wave the rings would move along the bar back and forth. Thus if there is friction between the rings and the bar, energy is produced. This thought experiment proved that gravitational wave carry energy and can thus be detected in principle.

The observability of gravitational waves being established, scientists were left with the last part of the problem: How can one practically detect these waves? As a gravitational wave passes by, it deforms a ring of free particles into an ellipse. But solids don't deform like free

particles due to their internal mechanical properties. So it seemed very difficult to detect the passage of a gravitational wave if one uses a solid but not impossible according to the work done on bar detector during the second half of the XX^{th} century. Moreover the order of magnitude of the amplitude h of the wave was expected to be very small (The amplitude of the wave that we detect nowadays is of the order of 10^{-23}). This dimensionless quantity is linked to some extent to the variation of the distance between a pair of free particles:

$$h \simeq 2\frac{\Delta l}{L} \tag{1}$$

where Δl is the increase in distance between the two particles and L the distance between the same particles before the wave deformed space-time.

The first device built to detect gravitational waves came from an idea of Weber. He was an engineer and attended the Chapel Hill Conference. After this meeting, Weber decided to build a detector for gravitational waves. His idea consisted in building a big aluminium cylinder, some kind of "antenna". His detector was maintained above the ground hanging to a support absorbing vibrations. When passing through his device, a gravitational wave would deform the cylinder and thus create a resonant signal. These vibrations would be monitored by a belt of piezoelectric sensors. Weber claimed later to detect gravitational waves [10]. His claimed detections gained popularity and many groups of scientists tried to detect gravitationnal waves using devices similar to the one designed by Weber. But no signals were detected by anyone but Weber and the scientific community agreed on the spurious nature of Weber's detections, to the exeption of Weber himself. This episode ended in a loss of motivation for the scientists to continue searching for gravitational waves.

In 1979, a regain of interest in the search for gravitational waves came from an new observation. Taylor and Hulse [11] confirmed indirectly the existence of gravitational waves through their observation of the period of the binary pulsar $PSRB1913+16$ in 1979. The energy lost by the system, deduced from the observation in the electromagnetic spectrum, was in agreement with the energy loss through gravitational waves predicted by General Relativity.

After the conference at Chapel Hill, Weber thought about several methods to detect gravitational waves. Among these methods were the interferometric ones. But as mentionned in the previous section, Weber tried his method based on an aluminum cylinder which was not fruitful. However, the first time the interferometry technique was suggested was in 1962 [12], by two Russian physicist Gertsenshtein and Pustovoid but their idea didn't go further in their case.

The basic working principle of an interferometer for the detection of gravitational waves is the following. If a gravitational wave passes through the detector with an adequate polarization the deformation of space-time will squeeze one arm and stretch the other. The two light beams coming from the two arms will thus have a phase shift with respect to each other. This phase shift will modify the interference image. The detector is initially set near a dark fringe and one measures the deviation from this lock.

In the early seventies, one of Weber's former students, Forward, built an interferometer with arms 8.5 meters long with funding from the Hughes Research Laboratory in Malibu, California [13]. Forward didn't detect gravitational waves. During the same period, Weiss built a 1.5-meter long interferometer in the Research Laboratory of Electronics at MIT [14]. He found his inspiration in a paper written by Pirani [15]. Pirani did seminal work on the effect of gravitational waves in the 1950's. In particular he worked on the choice of a coordinate

system convenient for laboratory measurement (the proper detector frame). Previous work on gravitational waves used coordinates that simplified theoretical calculations but these were not appropriate for experiments in a laboratory.

In 1974, Weiss submitted a proposal to build a larger prototype interferometer with 9-meter long arms to the US National Science Foundation [16]. The idea of the interferometer started to interest research groups in Europe. Two groups, one at the Max Planck Institute for Astrophysics in Garching [17] and one at the University of Glasgow [18], decided to build their own interferometer. The first group, directed by Heinz Billing built a 3-meter and then a 30 meter interferometer. The second, directed by Drever and Hough, built a 1-meter and then a 10-meter interferometer. In order to get sufficient funding, these two groups collaborated to build an 600-meter device called GEO600. This detector is located in the south of Hannover in Germany and is still operational.

Then, in the early 1980's, NSF financed two prototypes. One was located at MIT and the other at Caltech under the supervision of Thorne. In addition NSF funded Weiss's study about the design and technical feasibility of two interferometers with arms of a few kilometers and separated by several thousands of kilometers. The report, including all the results of the study, is known as the "Blue Book" [19]. It set the basis of a large scale project involving both MIT and Caltech. The project was led by Weiss, Drever and Thorne. These two interferometers became one observatory named LIGO: Laser Interferometer Gravitational-Wave Observatory. In the late 1980's, a large-scale French-Italian interferometer project started. It is now known as the Virgo observatory. LIGO and Virgo have collaborated since 2007. Both LIGO and Virgo have been improved in terms of sensitivity. The two current versions of these detectors are called Advanced LIGO (aLIGO) and Advanced Virgo (aVirgo).

Advanced LIGO and Advanced Virgo

The perturbation metric h that we want to measure is so small that we need to build an interferometer with extremely long arms. As seen before, the perturbation of space-time is related to the length of the arms of the detector by $\Delta l \simeq L \times (h/2)$. The amplitude h is of the order of 10^{-23}, as mentioned before, gravitational wave detectors must have arms with a length of about 750 km to detect a gravitational wave with a frequency of 100 Hz [2]. In addition to this difficulty comes the noise suppression in order to have a high enough sensitivity. Sources of noise include thermal deformations of the mirrors, external vibrations, photon shot noise, external gravitational perturbations, etc. In order to detect a gravitational wave a lot of technological improvements of the basic Michelson interferometer were needed. Among these improvements: active control systems to isolate the mirrors from external vibrations, power recycling mirrors, Fabry-Pérot cavities [2].

A Fabry-Pérot cavity is used to increase dramatically the optical path of an arm. The concept is simple, the light beam is reflected a lot of times before leaving the cavity. Thus the light path is much longer and the phase shift due to the gravitational wave is more important. A Fabry-Pérot cavity can increase the phase shift several hundreds of time. In the case of LIGO this factor is about 300 leading to an optical path of more than 1000 km for an arms only 4 km long [2].

To be able to detect gravitational waves one needs to use a high power light beam. The required power is several hundreds of kilowatts [20]. This is necessary to reduces the photon shot noise. This noise, which reduces with increasing power, limits the interferometer when

considering the detection of high frequency gravitational waves. But building a laser with such a high emitting power is practically impossible. To effectively increase the power of the laser a power recycling mirror is used. Basically it reflects the light coming back to the source of the laser. The Fabry-Pérot cavities and the power recycling mirrors are the main departures from the Michelson interferometer design. This type of detectors is called a Dual Recycled, Fabry-Pérot Michelson interferometer (see Fig. 1).

Vibrations are cancelled using active and passive controls. The detectors are also equipped with thousands of sensors of various type to monitor seismic, acoustic, electromagnetic and other external perturbations.

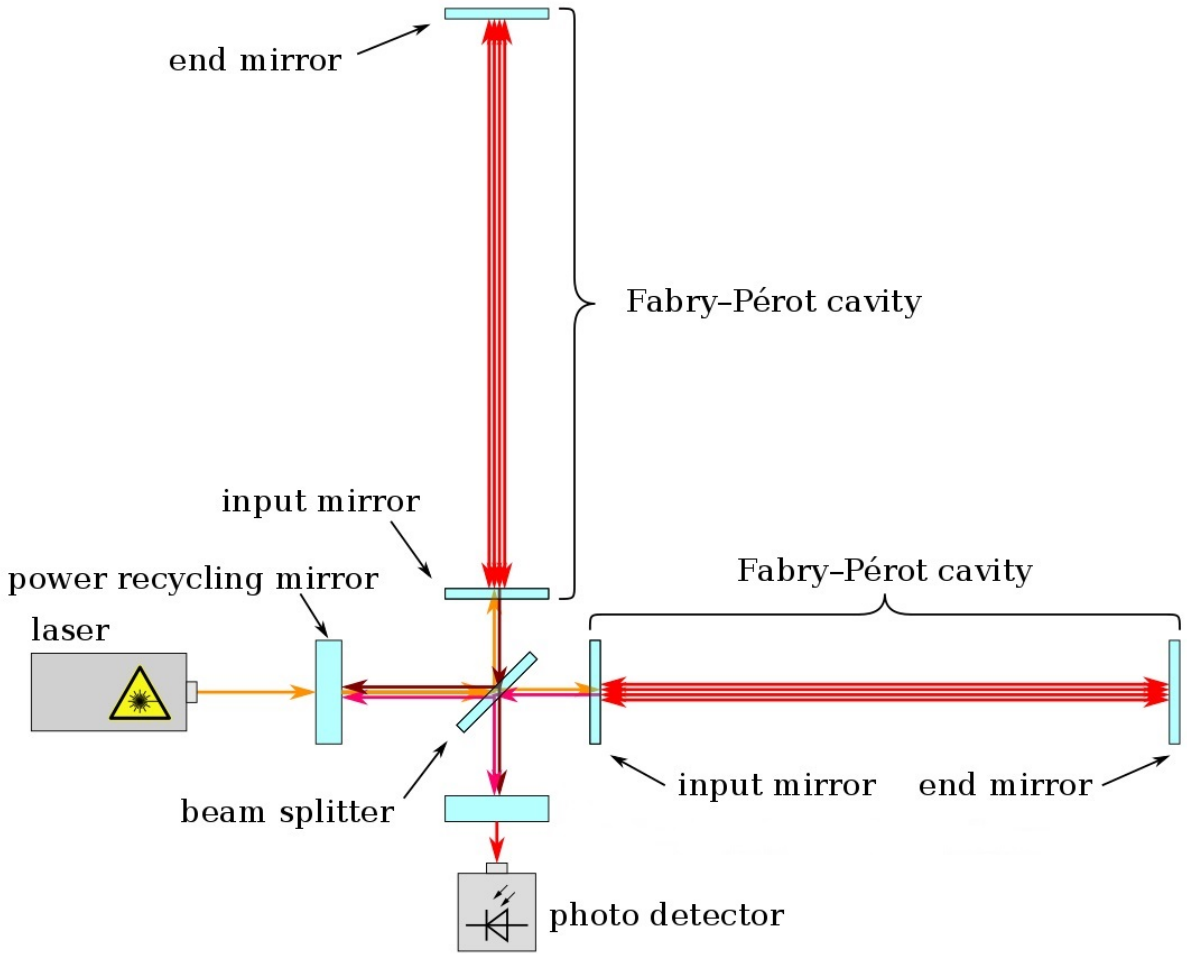

Figure 1: LIGO interferometer, simplified scheme, adaptated from [21]

One of the two inteferometers of LIGO is located in Hanford, Washington, the other one in Linvingston, Louisiana. They are separed by 3000 km. The LIGO sensitivity ranges from more than 20 Hz to several thousands of Hertz [2]. The European detector Virgo is located near Pisa in Italy. The frequency spectrum that Virgo can detect is slightly narrower than for LIGO (see Fig. 2). Using these three detectors one can locate the region from where the wave was emitted by triangulation. The event that can be detected using these interferometers are binary black holes, binary neutron stars, binary systems with a neutron star and a black hole, supernovae, rotating neutron stars, among others (see Fig. 3).

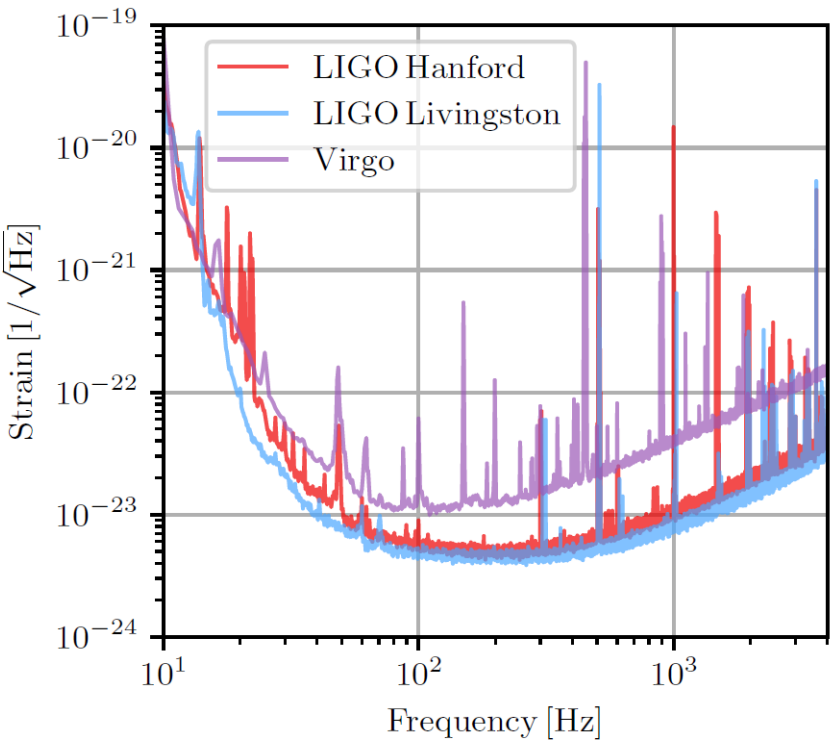

Figure 2: Sensitivity curve of the LIGO and Virgo observatories during the O3 run (2017), from [22]

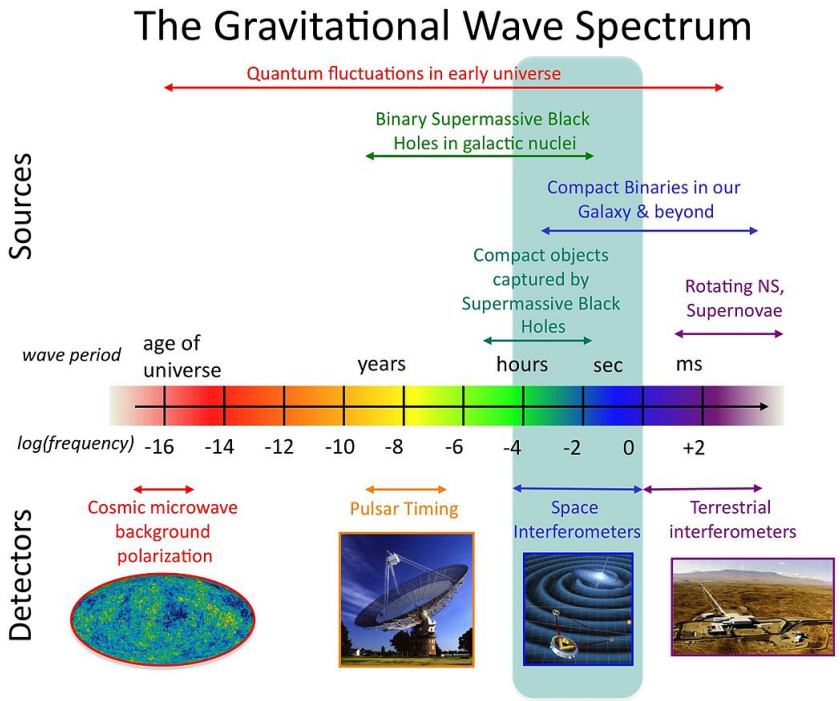

Figure 3: The gravitational wave spectrum, from [23]

There are four categories of gravitational wave sources according to Riles [24]. The category in which a source belongs depends on the duration of the signal emitted and on the quality of the modelling of the source. Sources that are short-lived and well-modelled are typically binary systems involving massive and compact objects. Such sources constitute the events detected so far by LIGO and Virgo. The signal is a succession of an inspiral phase and a merger phase followed by a ringdown. From these signals one can extract the masses of each star or black hole, the total effective spin, a characteristic quantity called the chirp mass and some others.

Another category contains short-lived but poorly known sources. These sources come from some asymmetry in events, like supernovae for example, that are very difficult to model. The signal emitted by these events could be detected by the ground-based observatories.

Eventually there is a category for the long-lived sources. The well-modelled sources are rotating neutron stars. If a neutron star is asymmetric it will emit a very stable nearly monochromatic gravitational wave. These could be detected by the ground-based interferometers if the sources are located in our galaxy. The last category consists of the primordial black holes and the cosmic gravitational wave background that is a diffuse emission from the Big Bang and previous mergers.

In the future, new interferometers will extend the possibility of detection. The KAmioka GRAvitational wave detector (KAGRA), a Japanese detector developed at the University of Tokyo will join LIGO and Virgo in the following years. This will be followed by LIGO-India. The Einstein telescope will extend the observation of gravitational waves to lower frequencies. Cosmic Explorer, a U.S. telescope will reach a sensitivity much better than LIGO. Eventually the Laser Interferometer Space Antenna (LISA) is expected to be launched in the early 2030s. LISA will be sensitive to frequency much lower than what is accessible with ground-based observatories, i.e. $10^{-4} - 10^{-1}$ Hz.

We are at the very beginning of an new era in astronomy. The observation of gravitational waves allows us to characterise new astrophysical phenomena and complement observations in the electromagnetic spectrum. The first observations allowed astronomers to test and constrain the theory of General Relativity with higher precision [25]. The cataclysmal events that are now observable could reveal deviation from General Relativity and eventually pave the way towards new physics.

Origin of extra dimensions

This section is based on [26].

One of the major objectives of physics is to describe nature with a unique and consistent theory. The theories that fit best our observations about the world are General Relativity and quantum-field theory which describe with great accuracy the observation of phenomena respectively at large and small scales. From this point, the way towards a final theory, if such a theory exists, starts with finding a single theory able to reproduce the prediction of both General Relativity and quantum-field theory.

One possibility to achieve this goal might be to work with more spatial dimensions than the three usual ones included in the four dimensional space-time of the two current theories. The origin of this very strange idea dates back to 1919. Kaluza, a German physicist, found that

adding a fifth dimension in the theoretical framework of General Relativity allows, under a few hypotheses, the unification of gravitation and classical electromagnetism.

The addition of classical electromagnetism is achieved through the Christoffel symbols linked to the fifth dimension. The Christoffel symbols are given by

$$\Gamma^{\lambda}_{\mu\nu} = g^{\lambda\alpha}\Gamma_{\alpha\mu\nu} = \frac{1}{2}g^{\lambda\alpha}\left(\partial_\mu g_{\alpha\nu} + \partial_\nu g_{\mu\alpha} - \partial_\alpha g_{\mu\nu}\right) \tag{2}$$

with $g_{\mu\nu}$ the metric tensor and $g^{\mu\nu}$ its inverse. If one identifies the 4-vector potential of electromagnetism to the metric component linked to the fifth dimension,

$$A_\mu \equiv g_{\mu 5}, \tag{3}$$

and makes the hypothesis that the metric components are independent of the new spatial dimension, one finds:

$$\begin{aligned}
\Gamma_{\mu\nu 5} &= \frac{1}{2}\left(\partial_\nu g_{\mu 5} + \partial_5 g_{\nu\mu} - \partial_\mu g_{\nu 5}\right) \\
&= \frac{1}{2}\left(\partial_\nu A_\mu + \partial_5 g_{\nu\mu} - \partial_\mu A_\nu\right) \\
&= \frac{1}{2}\left(\partial_\nu A_\mu - \partial_\mu A_\nu\right) \\
&= \frac{1}{2}F_{\nu\mu}
\end{aligned} \tag{4}$$

One can thus make the Faraday tensor appear in the connection linked to the fifth dimension.

However the work isn't done yet. One also needs to postulate a metric of the form

$$ds^2 = g_{\mu\nu}dx^\mu dx^\nu + \left(dx^5 + A_\mu dx^\mu\right)^2 \tag{5}$$

Imposing such a restriction on the metric form thus breaks the invariance of the theory under all diffeomorphisms. It can be shown that to enforce invariance of this metric expression one can only use the following diffeomorphisms in addition to any diffeomorphism affecting only the four dimensions of the usual space-time:

$$x^5 \to x^5 + f(x^\mu) \tag{6}$$

with the following transformation rule for the A_μ

$$A'_\mu \to A_\mu - \partial_\mu f \tag{7}$$

We recognize this transformation as being the gauge transformation of the 4-vector potential A_μ in the classical theory of electromagnetism. Thus this restriction on the metric breaks general covariance in 5 dimensions and leaves the theory invariant under any diffeoporphism on the usual four-dimensional space-time, like General Relativity does, and is invariant under the electromagnetism gauge transformation with respect to the fifth dimension. Eventually, one can also compute the lagrangian density of this theory and one finds:

$$\mathcal{L} = \mathcal{L}_{GR} - \frac{1}{4}F_{\mu\nu}F^{\mu\nu} \tag{8}$$

where $\mathcal{L}_{GR}$ is the Hilbert-Einstein lagrangian to which is added the lagrangian of electromagnetism. Eventually the geodesic equations of this theory can reproduce the behaviour of

particles having a mass and an electric charge. Thus the Kaluza theory reproduces gravitation and classical electromagnetism.

Beside unifying gravity and electromagnetism, this theory comes with serious conceptual issues. Is this fourth spatial dimension real and how can one justify the hypothesis that are needed to lead to electromagnetism while breaking general covariance? In order to solve the problem of the existence of an additional space dimension that nobody ever observed so far, the Swedish physicist Klein had the idea of writing the Kaluza theory with a fifth dimension assumed to be compact and small. Doing so allows one to explain why this extra dimension doesn't seem to exist in our everyday life: it is simply to small to be observed.

Since then, the idea of adding extra dimensions has been used in several attempts to find a unified theory of gravity and quantum physics. The most famous one is string theory. It is important to note that adding dimensions seems a very promising way to unify physics because of the Kaluza-Klein theory but the latter doesn't solve the issue encountered when one tries to quantify gravity: the Kaluza-Klein theory successfully unifies the theory of gravity with electromagnetism but it remains classical. Thus, the present work is about physics with extra dimensions despite the fact that it doesn't solve the incompatibility of General Relativity and quantum physics. The reason we will focus on extra dimensions is because current attempts tend to show that a theory of quantum gravity will probably involve extra dimensions. If it has to be true these extra dimensions will affect gravitational waves. The question is thus to know whether these effects can be detected in the four-dimensional part of gravitational waves.

Chapter 1

Linearised Einstein equation with extra dimensions

1.1 Linearised Einstein theory

The first step to analyse the effects of extra dimensions on gravitational waves is to derive the wave equation with these extra dimensions. Before that, I will remind the reader of the main steps of the derivation of gravitational waves in 4 dimensions with no sources on a Minkowski background metric, neglecting the cosmological constant. This derivation is based on [27].

We start from Einstein equation:

$$R_{\mu\nu} - \frac{R}{2} g_{\mu\nu} = 8\pi T_{\mu\nu} \tag{1.1}$$

Considering no sources simply means that $T_{\mu\nu} = 0$. Gravitational waves are small perturbations of a "background metric". The latter is assumed to be much larger than the perturbation and to vary much more slowly. In the present section it doesn't vary at all as we consider a Minkowski background. The field is said to be weak with respect to the Minkowski background if it can be written in the following form:

$$g_{\mu\nu} = \eta_{\mu\nu} + h_{\mu\nu} \tag{1.2}$$

with

$$|h_{\mu\nu}| \ll 1 \quad |\partial_\alpha h_{\mu\nu}| \ll 1 \quad |\partial_\alpha \partial_\beta h_{\mu\nu}| \ll 1 \tag{1.3}$$

where $\eta_{\mu\nu}$ is the Minkowski metric tensor. The convention we will follow for $\eta_{\mu\nu}$ is $(-,+,+,+)$. The inverse metric tensor is given by:

$$g^{\mu\nu} = \eta^{\mu\nu} - h^{\mu\nu} + \mathcal{O}(h^2) \tag{1.4}$$

In order to maintain the decomposition (1.2), we need to restrict ourself to some diffeomorphism. The two types of diffeomorphism that are allowed are:

1. The Lorentz transformations:
$$\underline{x}^\alpha = \Lambda^\alpha{}_\beta x^\beta \tag{1.5}$$

2. Infinitesimal "gauge" transformations:
$$\underline{x}^\alpha = x^\alpha + \xi^\alpha\left(x^\beta\right) \ , \ |\partial_\beta \xi^\alpha| \ll 1 \tag{1.6}$$

We can easily understand the origins of these transformations. The Lorentz transformations are obviously allowed because they correspond to a change from a inertial reference frame to another. These are the only transformations that link inertial reference frames. Thus the gauge transformations correspond to a change from an inertial frame to a non inertial frame. However these gauge transformations are allowed because they are infinitesimal transformations that can be reabsorbed in the metric perturbation. In other words, the only object that has a physical signification is the metric $g^{\mu\nu}$ and we impose this metric to be almost Minkowski and the transformations that links these almost Minkowski reference frames are the Lorentz and the gauge transformations. If we had imposed the metric $g^{\mu\nu}$ to be strictly Minkowski the gauge transformations would not be allowed.

The perturbation $h_{\mu\nu}$ must then change in order to preserve the decomposition of (1.2). The transformation rules are:

1. Lorentz transformation of the metric $g_{\mu\nu}$:

$$\underline{h}_{\alpha\beta} = \Lambda^{\mu}{}_{\alpha}\Lambda^{\nu}{}_{\beta}h_{\mu\nu} \tag{1.7}$$

2. Gauge transformation of the metric $g_{\mu\nu}$:

$$\underline{h}_{\mu\nu} = h_{\mu\nu} - \partial_{\nu}\xi_{\mu} - \partial_{\mu}\xi_{\nu} \tag{1.8}$$

The Christoffel symbols, the Rieman tensor, the Ricci tensor and the scalar curvature are then given by:

$$\Gamma^{\alpha}_{\beta\gamma} = \frac{1}{2}\eta^{\alpha\delta}\left(\partial_{\gamma}h_{\delta\beta} + \partial_{\beta}h_{\delta\gamma} - \partial_{\delta}h_{\beta\gamma}\right) + \mathcal{O}(h^2_{\mu\nu}) \tag{1.9}$$

$$R_{\alpha\beta\gamma\delta} = \frac{1}{2}\left(\partial_{\beta}\partial_{\gamma}h_{\alpha\delta} + \partial_{\alpha}\partial_{\delta}h_{\beta\gamma} - \partial_{\alpha}\partial_{\gamma}h_{\beta\delta} - \partial_{\beta}\partial_{\delta}h_{\alpha\gamma}\right) + \mathcal{O}(h^2_{\mu\nu}) \tag{1.10}$$

$$R_{\alpha\beta} = -\frac{1}{2}\left(\partial_{\alpha}\partial_{\beta}h^{\gamma}{}_{\gamma} + \partial^{\gamma}\partial_{\gamma}h_{\alpha\beta} - \partial_{\gamma}\partial_{\beta}h^{\gamma}{}_{\alpha} - \partial_{\gamma}\partial_{\alpha}h^{\gamma}{}_{\beta}\right) + \mathcal{O}(h^2_{\mu\nu}) \tag{1.11}$$

$$R = -\partial^{\beta}\partial_{\beta}h^{\alpha}{}_{\alpha} + \partial_{\alpha}\partial_{\beta}h^{\alpha\beta} + \mathcal{O}(h^2_{\mu\nu}) \tag{1.12}$$

All the second order terms are neglected because of the hypothesis of a weak field (1.3). The linearised Einstein equation can be written:

$$-\frac{1}{2}\Box\overline{h}_{\mu\nu} - \frac{1}{2}\left(-\partial^{\alpha}\partial_{\nu}\overline{h}_{\alpha\mu} - \partial^{\alpha}\partial_{\mu}\overline{h}_{\alpha\nu} + \eta_{\mu\nu}\partial^{\alpha}\partial^{\beta}\overline{h}_{\alpha\beta}\right) = 0 \tag{1.13}$$

where the following notations have been introduced:

$$\overline{h}_{\mu\nu} \equiv h_{\mu\nu} - \frac{h}{2}\eta_{\mu\nu} \tag{1.14}$$

$$h \equiv h^{\alpha}{}_{\alpha} \tag{1.15}$$

and $\Box$ is the d'Alembertian operator.

Thanks to the degrees of freedom due to the gauge transformation, the De Donder gauge condition can be imposed:

$$\partial_{\nu}\overline{h}^{\mu\nu} = 0 \tag{1.16}$$

which simplifies the equation even more:

$$\Box \overline{h}_{\mu\nu} = 0 \tag{1.17}$$

There is not one unique gauge satisfying (1.16) and all the gauges that satisfies the De Donder condition are linked by gauge transformation for which

$$\Box \xi^{\alpha} = 0 \tag{1.18}$$

1.2 The linearised theory in D dimensions

In this section, we detail the different steps leading to the equation describing gravitational waves in D dimensions. This derivation follows the one in [28]. The goal is to compare the behaviour of these waves with those in a 4 dimensional space-time. We used in the previous section the Einstein equation with no cosmological constant. Here, we will start from the general case of a non-zero cosmological constant because such a constant might have important effects on the extra dimensions. In D dimensions, and with a cosmological constant, the Einstein equation is:

$$R_{MN} - \frac{R}{2} g_{DMN} + \Lambda g_{DMN} = 8\pi T_{MN} \tag{1.19}$$

where the indices M and N take value from 0 to $D-1$ and g_D is the N-dimensional metric tensor.

Again we consider a vacuum space-time: $T_{MN} = 0$ so that we can compare the result with the four-dimensional case. Considering no sources thus allows us to avoid making some guess on the behaviour of matter in these dimensions.

$$R_{MN} - \frac{R}{2} g_{DMN} + \Lambda g_{DMN} = 0 \tag{1.20}$$

If we compute the trace by multiplying (1.20) by the inverse of the metric g_D^{MN} we find:

$$R = \frac{2D}{D-2} \Lambda \tag{1.21}$$

This result allows us to rewrite (1.20) as:

$$R_{MN} - \frac{2\Lambda}{D-2} g_{DMN} = 0 \tag{1.22}$$

To derive an equation for gravitational waves we need to split the metric into a background part which is dominant and varies slowly with time and a perturbation component that varies much faster than the background metric. As we don't know anything about the physics in the extra dimensions, we have no reason to suppose that the background metric is a "Minkowski" metric in D dimensions. So it is better to keep a general background metric g_{MN}.

$$g_{DMN} = g_{MN} + h_{MN} \tag{1.23}$$

The field perturbation is supposed to be weak:

$$|h_{MN}| \ll |g_{MN}| \tag{1.24}$$

and all higher terms with respect to h_{MN} can be neglected. Thus the inverse metric tensor is given by:

$$g_D{}^{MN} = g^{MN} - h^{MN} + \mathcal{O}(h_{MN}^2) \tag{1.25}$$

The decomposition of the metric (1.23) is left unchanged under some gauge transformations as in the four-dimensional case:

$$\underline{h}_{MN} = h_{MN} - \nabla_N \xi_M - \nabla_M \xi_N \tag{1.26}$$

These are the only transformations allowed if we want to keep the decomposition (1.23) of the metric. The Lorentz transformations aren't allowed as we keep the background metric general.

Now we introduce the decomposition (1.23) of the metric in the Einstein equation. From this point we can make the hypothesis that the Einstein equation can be split into an equation of order zero in the perturbation and an equation of first order in the perturbation:

$$R^{(0)}_{MN} - \frac{2\Lambda}{D-2} g_{MN} = 0 \tag{1.27}$$

$$R^{(1)}_{MN} - \frac{2\Lambda}{D-2} h_{MN} = 0 \tag{1.28}$$

In the four dimensional case, we are left with only one equation for the perturbation metric because the background equation is trivial as we impose a Minkoswki background metric.

In the following all the mathematical objects that are denoted with the upper indices (0) are built using only the background geometry. For example $\nabla^{(0)}_P$ is the covariant derivative with respect to x^P accounting only for the background, i.e. using only the order zero part of the Christoffel symbols: $\Gamma^{(0)}$. The Christoffel symbols and the Ricci tensor are given by:

$$\Gamma^M_{NP} = {\Gamma^{(0)}}^M_{NP} + \frac{1}{2} g^{MQ} \left(\nabla^{(0)}_N h_{QP} + \nabla^{(0)}_P h_{QN} - \nabla^{(0)}_Q h_{NP} \right) \tag{1.29}$$

$$R_{MN} = R^{(0)}_{MN} - \frac{1}{2} \nabla^{(0)}_P \left(g^{PQ} \nabla^{(0)}_Q h_{MN} \right) + \nabla^{(0)}_P \left(g^{PQ} \nabla^{(0)}_M h_{NQ} \right) - \frac{1}{2} \nabla^{(0)}_N \nabla^{(0)}_M h_D \tag{1.30}$$

with

$${\Gamma^{(0)}}^M_{NP} = \frac{1}{2} g^{MQ} \left(\partial_N g_{QP} + \partial_P g_{QN} - \partial_Q g_{NP} \right) \tag{1.31}$$

$$R^{(0)}_{MN} = \partial_A {\Gamma^{(0)}}^A_{MN} + {\Gamma^{(0)}}^A_{AE} {\Gamma^{(0)}}^E_{MN} - \partial_N {\Gamma^{(0)}}^A_{MA} - {\Gamma^{(0)}}^A_{NE} {\Gamma^{(0)}}^E_{MA} \tag{1.32}$$

and where the following notation have been introduced:

$$h_D \equiv h_{QP} g^{QP} \tag{1.33}$$

The linearised Einstein equation for the first-order perturbation of the background metric is then obtained by replacing the Ricci tensor (1.30) in equation (1.28) using $R^{(1)}_{MN} = R_{MN} - R^{(0)}_{MN}$:

$$\begin{aligned} -\frac{1}{2} \nabla^{(0)}_P \left(g^{PQ} \nabla^{(0)}_Q h_{MN} \right) + \frac{1}{2} \nabla^{(0)}_P \left(g^{PQ} \nabla^{(0)}_M h_{NQ} \right) + \frac{1}{2} \nabla^{(0)}_P \left(g^{PQ} \nabla^{(0)}_N h_{MQ} \right) \\ - \frac{1}{2} \nabla^{(0)}_N \nabla^{(0)}_M h_D - \frac{2\Lambda}{D-2} h_{MN} = 0 \end{aligned} \tag{1.34}$$

If we take into account the fact that the metric tensor commutes with the covariant derivative and we introduce the notation $\Box^{(0)} \equiv g^{PQ} \nabla^{(0)}_P \nabla^{(0)}_Q$, the previous equation can be written:

$$-\frac{1}{2}\Box^{(0)}h_{MN}+\frac{1}{2}\nabla^{(0)}_P\nabla^{(0)}_M g^{PQ}h_{NQ}+\frac{1}{2}\nabla^{(0)}_P\nabla^{(0)}_N g^{PQ}h_{MQ} \\ -\frac{1}{2}\nabla^{(0)}_N\nabla^{(0)}_M h_D-\frac{2\Lambda}{D-2}h_{MN}=0 \tag{1.35}$$

As in the four-dimensional case the linearised Einstein equation doesn't look like a wave equation at first sight. We would like to impose a gauge condition similar to the de Donder gauge condition (1.16) in four dimensions. To that end, we use the definition of the Riemann curvature tensor to evaluate:

$$\nabla^{(0)}_P\nabla^{(0)}_M g^{PQ}h_{QN}=\nabla^{(0)}_M\nabla^{(0)}_P g^{PQ}h_{QN}+R^{(0)}_{MP}g^{PQ}h_{QN}+g_{NS}R^{(0)\,S}{}_{RPM}g^{PQ}h_{QU}g^{UR} \tag{1.36}$$

and its symmetries to evaluate:

$$g_{NS}R^{(0)\,S}{}_{RPM}g^{PQ}h_{QU}g^{UR}=R^{(0)\,S}{}_{MNP}g^{PQ}h_{QS} \tag{1.37}$$

Eventually, introducing the notation

$$\mathcal{G}_N\equiv\nabla^{(0)}_P g^{PQ}h_{QN}-\frac{1}{2}\nabla^{(0)}_N h_D \tag{1.38}$$

allows us to rewrite equation (1.35) as :

$$-\frac{1}{2}\Box^{(0)}h_{MN}+R^{(0)}_{MP}g^{PQ}h_{QN}+R^{(0)\,S}{}_{MNP}g^{PQ}h_{QS} \\ +\frac{1}{2}\nabla^{(0)}_M\mathcal{G}_N+\frac{1}{2}\nabla^{(0)}_N\mathcal{G}_M-\frac{2\Lambda}{D-2}h_{MN}=0 \tag{1.39}$$

The equation can now easily be simplified through the background Einstein equation (1.27) to express the second term in (1.39) in terms of the perturbation only and see that it cancels with the last term:

$$\begin{aligned}R^{(0)}_{MP}g^{PQ}h_{QN}&=\frac{2\Lambda}{D-2}g_{MP}g^{PQ}h_{QN}\\&=\frac{2\Lambda}{D-2}\delta^Q_M h_{QN}\\&=\frac{2\Lambda}{D-2}h_{MN}\end{aligned} \tag{1.40}$$

The last step is to impose the de Donder gauge condition $\mathcal{G}_N=0$. We end up with the following equation:

$$-\frac{1}{2}\Box^{(0)}h_{MN}+R^{(0)\,S}{}_{MNP}g^{PQ}h_{QS}=0 \tag{1.41}$$

Again we obtain the wave equation but this time with a source term due to the background curvature.

As we didn't impose any restriction on the extra dimension this derivation is identical to that in four dimensions with a curved background. As mentioned in this section, the difference is that we can assume a Minkowski background in four dimensions, provided we restrict ourself to the study of waves travelling over distances that are short enough to neglect the curvature of space-time. With extra dimensions this doesn't hold anymore because we don't know anything about these dimensions.

Background metric specification

In order to solve equation (1.41), we need to specify the background metric. As we want the four dimensional part of the D dimensional space-time to have the same properties as in General Relativity, we choose a background metric such that the four dimensional background is maximally symmetric. According to [28], the most general metric satisfying this requirement is given by:

$$ds^2 = e^{2A(y)}\tilde{g}_{\mu\nu}(x)dx^\mu dx^\nu + g_{mn}(y)dy^m dy^n \tag{1.42}$$

where the x coordinates represent the four dimensional space-time and the y coordinates represent the extra dimensions. Thus the Greek indices can take the values 0, 1, 2, 3 and the Latin indices can take values from 4 to N-1. The manifold including only the extra dimensions will be denoted by $\mathcal{M}$ in the following. The factor $e^{2A(y)}$ is called the warp factor. It allows to have a scaling factor of the four-dimensional metric that is different depending on the position in the $\mathcal{M}$ manifold.

Each point in $\mathcal{M}$ corresponds to a different four dimensional space-time. Each of them will be referred to as a *brane*. We set the coordinate of the four dimensional brane we live in to $(x_\mu, 0)$. Fig. 1.1 represents the situation for a three dimensional space. An hypothetical observer see its universe as being two dimensional. In addition to these two dimension that can be perceived there exists a third extra dimension. In prevision of the compactification of the extra dimensions in the next chapter the extra dimension in the figure is compact. This means that the point $y = 0$ and $y = L$ in $\mathcal{M}$ are the same.

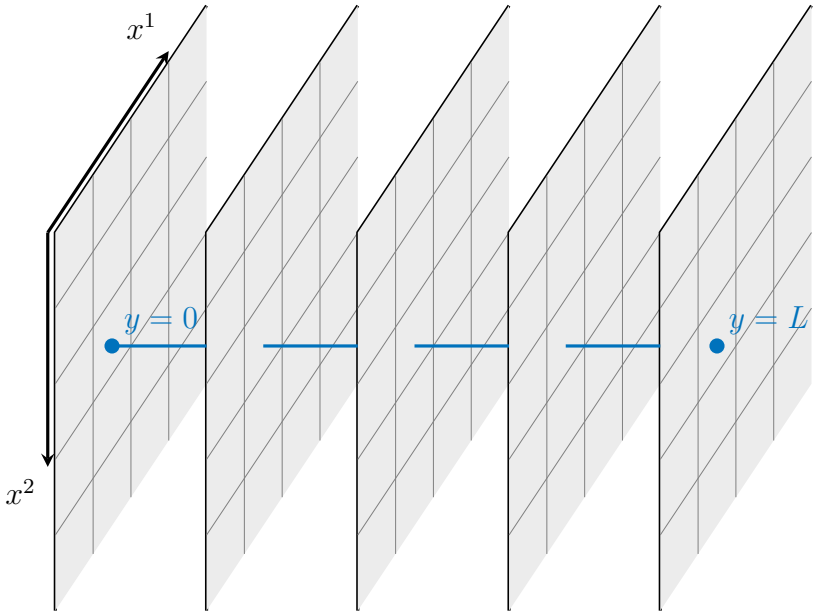

Figure 1.1: Illustration of differents two dimensional branes (represented in gray), along a compact extra dimension (represented in blue).

It is important to note that imposing the metric (1.42) breaks the general covariance in D dimensions. The only restriction on $\tilde{g}_{\mu\nu}$ is that it doesn't depend on the coordinate of the extra dimensions y^m. The diffeomorphisms left are thus all the diffeomorphism including only the four-dimensional coordinates x^μ. For this reason $\tilde{g}_{\mu\nu}$ is a four-dimensional tensor. The same reasoning can be made for g_{mn}. This is a tensor with respect to all the diffeomorphisms implying only the extra-dimensional coordinates y^m.

We can now take into account the form of the metric (1.42) to rewritte the wave equation (1.41). First we calculate the Christoffel symbols:

$$\begin{aligned}\Gamma^{\mu}_{\nu\pi} &= \tilde{\Gamma}^{\mu}_{\nu\pi} \\ \Gamma^{\mu}_{\nu p} &= \tilde{\Gamma}^{\mu}_{p\nu} = \frac{1}{2}\delta^{\mu}_{\nu} e^{-2A}\partial_p e^{2A} \\ \Gamma^{m}_{\nu\pi} &= -\frac{1}{2}\tilde{g}_{\nu\pi} g^{mn}\partial_n e^{2A}\end{aligned} \tag{1.43}$$

where $\tilde{\Gamma}^{\mu}_{\nu\pi}$ are the Christoffel symbols built from the metric $\tilde{g}_{\mu\nu}$ and Γ^{m}_{np} those built from g_{mn}. Then we can calculate the covariant derivatives of the pertubation metric and write them as follows:

$$\nabla_\pi h_{\mu\nu} = \tilde{\nabla}_\pi h_{\mu\nu} + \frac{1}{2}\tilde{g}_{\pi\mu}h_{\nu m}g^{mn}\partial_n e^{2A} + \frac{1}{2}\tilde{g}_{\pi\nu}h_{\mu m}g^{mn}\partial_n e^{2A} \tag{1.44a}$$

$$\nabla_\pi h_{\mu n} = \tilde{\nabla}_\pi h_{\mu n} + \frac{1}{2}\tilde{g}_{\pi\mu}h_{mn}g^{mp}\partial_p e^{2A} - \frac{1}{2}h_{\mu\pi}e^{-2A}\partial_n e^{2A} \tag{1.44b}$$

$$\nabla_\pi h_{mn} = \partial_\pi h_{mn} - \frac{1}{2}e^{-2A}h_{\pi m}\partial_n e^{2A} - \frac{1}{2}e^{-2A}h_{\pi n}\partial_m e^{2A} \tag{1.44c}$$

$$\nabla_q h_{\mu\nu} = \partial_q h_{\mu\nu} - h_{\mu\nu}e^{-2A}\partial_q e^{2A} \tag{1.44d}$$

$$\nabla_q h_{m\nu} = \nabla_q h_{m\nu} - \frac{1}{2}h_{m\nu}e^{-2A}\partial_q e^{2A} \tag{1.44e}$$

where $\tilde{\nabla}_\pi$ and ∇_q are the covariant derivatives built from the Christoffel symbols $\tilde{\Gamma}^{\mu}_{\nu\pi}$ and Γ^{m}_{nq} respectively. We can now calculate the d'Alembertian of the perturbation metric h_{MN}. Introducing the notations $\tilde{\Box}_4 = \tilde{g}^{\mu\nu}\tilde{\nabla}_\mu\tilde{\nabla}_\nu$ and $\Delta_{\mathcal{M}} = g^{pq}\nabla_p\nabla_q$, the d'Alembertian $\Box^{(0)}_D h_{MN}$ can be rewritten as follow:

$$\begin{aligned}\Box^{(0)}_D h_{\mu\nu} &= e^{-2A}\tilde{\Box}_4 h_{\mu\nu} + \Delta_{\mathcal{M}}h_{\mu\nu} - h_{\mu\nu}\Delta_{\mathcal{M}}\ ln\ e^{2A} - \frac{3}{2}e^{-4A}h_{\mu\nu}g^{mn}\partial_m e^{2A}\partial_n e^{2A} \\ &+e^{-2A}\tilde{\nabla}_\mu h_{\nu m}g^{mn}\partial_n e^{2A} + e^{-2A}\tilde{\nabla}_\nu h_{\mu m}g^{mn}\partial_n e^{2A} + \frac{1}{2}e^{-2A}\tilde{g}_{\mu\nu}h_{mn}g^{mr}g^{np}\partial_r e^{2A}\partial_p e^{2A}\end{aligned} \tag{1.45a}$$

$$\begin{aligned}\Box^{(0)}_D h_{\mu n} &= e^{-2A}\tilde{\Box}_4 h_{\mu n} + \Delta_{\mathcal{M}}h_{\mu n} + e^{-2A}g^{pq}\nabla_p h_{\mu n}\partial_q e^{2A} - \frac{3}{2}e^{-4A}h_{\mu m}g^{mp}\partial_p e^{2A}\partial_n e^{2A} \\ &-e^{-4A}h_{\mu n}g^{pq}\partial_p e^{2A}\partial_q e^{2A} - \frac{1}{2}h_{\mu n}\Delta_{\mathcal{M}}\ ln\ e^{2A} \\ &-e^{-4A}\tilde{g}^{\pi\rho}\tilde{\nabla}_\pi h_{\mu\rho}\partial_n e^{2A} + e^{-2A}g^{pq}\partial_\mu h_{np}\partial_q e^{2A}\end{aligned} \tag{1.45b}$$

$$\begin{aligned}\Box^{(0)}_D h_{mn} &= e^{-2A}\tilde{\Box}_4 h_{mn} + \Delta_{\mathcal{M}}h_{mn} + 2e^{-2A}g^{pq}\partial_p e^{2A}\nabla_q h_{mn} - 2e^{-4A}g^{pq}\partial_p e^{2A}h_{qm}\partial_n e^{2A} \\ &-e^{-4A}\tilde{g}^{\pi\rho}\tilde{\nabla}_\pi h_{\rho m}\partial_n e^{2A} - e^{-4A}\tilde{g}^{\pi\rho}\tilde{\nabla}_\pi h_{\rho n}\partial_m e^{2A} + \frac{e^{-4A}}{2}h_4\partial_m e^{2A}\partial_n e^{2A}\end{aligned} \tag{1.45c}$$

The last step is to calculate the background Riemann tensor. We note $\tilde{R}^{\pi}{}_{\mu\nu\sigma}$ and $R^{p}{}_{mns}$ the Riemann curvature tensors built from $\tilde{\Gamma}^{\mu}_{\nu\pi}$ and Γ^{m}_{np}. We find:

$$\begin{aligned}R^{(0)P}{}_{\mu\nu S} = \delta^{\sigma}_{S}\delta^{P}_{\pi}\Bigg(\tilde{R}^{\pi}{}_{\mu\nu\sigma} + \frac{1}{2}e^{-2A}\delta^{\pi}_{\sigma}\tilde{g}_{\nu\mu}g^{pq}\partial_p e^{2A}\partial_q e^{2A} - \frac{1}{2}e^{-2A}\delta^{\pi}_{\nu}\tilde{g}_{\sigma\mu}g^{pq}\partial_p e^{2A}\partial_q e^{2A}\Bigg) \\ +\delta^{s}_{S}\delta^{P}_{n}\frac{1}{2}\tilde{g}_{\mu\nu}g^{np}\left(\nabla_s\partial_p e^{2A} - \frac{1}{2}e^{-2A}\partial_p e^{2A}\partial_s e^{2A}\right)\end{aligned} \tag{1.46}$$

$$R^{(0)P}{}_{\mu mS} = \delta^{\sigma}_{S}\delta^{P}_{n}\frac{1}{2}\tilde{g}_{\sigma\mu}g^{np}\left(-\nabla_m\partial_p e^{2A} + \frac{1}{2}e^{2A}\partial_p e^{2A}\partial_m e^{2A}\right) \tag{1.47}$$

$$R^{(0)P}{}_{mnS} = \delta^{s}_{S}\delta^{P}_{p}R^{p}{}_{mns} + \delta^{\sigma}_{S}\delta^{P}_{\pi}\frac{1}{2}\delta^{\pi}_{\sigma}\left(\nabla_n\left(e^{-2A}\partial_m e^{2A}\right) + \frac{1}{2}e^{-4A}\partial_m e^{2A}\partial_n e^{2A}\right) \tag{1.48}$$

Eventually, we can write all the components of the Einstein equation:

$$\begin{aligned} &e^{-2A}\tilde{\Box}_4 h_{\mu\nu} + \Delta_{\mathcal{M}}h_{\mu\nu} - h_{\mu\nu}\Delta_{\mathcal{M}}\ ln\ e^{2A} - 2\tilde{R}^{\pi}{}_{\mu\nu\sigma}g^{\sigma\rho}h_{\rho\pi} \\ &\quad -\frac{1}{2}e^{-2A}g^{pq}\partial_p e^{2A}\partial_q e^{2A}\left(\tilde{g}_{\nu\mu}h_4 + 2h_{\nu\mu}e^{-2A}\right) \\ &\quad +e^{-2A}\tilde{\nabla}_\mu h_{\nu m}g^{mn}\partial_n e^{2A} + e^{-2A}\tilde{\nabla}_\nu h_{\mu m}g^{mn}\partial_n e^{2A} \\ &\quad -\tilde{g}_{\mu\nu}h_{mn}g^{mr}g^{np}\left(\nabla_r\partial_p e^{2A} - e^{-2A}\partial_r e^{2A}\partial_p e^{2A}\right) = 0 \end{aligned} \tag{1.49}$$

$$\begin{aligned} &e^{-2A}\tilde{\Box}_4 h_{\mu n} + \Delta_{\mathcal{M}}h_{\mu n} + e^{-2A}g^{pq}\nabla_p h_{\mu n}\partial_q e^{2A} \\ &+e^{-2A}h_{\mu m}g^{mp}\nabla_n\partial_p e^{2A} - 2e^{-4A}h_{\mu m}g^{mp}\partial_p e^{2A}\partial_n e^{2A} \\ &\quad -e^{-4A}h_{\mu n}g^{pq}\partial_p e^{2A}\partial_q e^{2A} - \frac{1}{2}h_{\mu n}\Delta_{\mathcal{M}}\ ln\ e^{2A} \\ &\quad -e^{-4A}\tilde{g}^{\pi\rho}\tilde{\nabla}_\pi h_{\mu\rho}\partial_n e^{2A} + e^{-2A}g^{pq}\partial_\mu h_{np}\partial_q e^{2A} = 0 \end{aligned} \tag{1.50}$$

$$\begin{aligned} &e^{-2A}\tilde{\Box}_4 h_{mn} + \Delta_{\mathcal{M}}h_{mn} + 2e^{-2A}g^{pq}\partial_p e^{2A}\nabla_q h_{mn} \\ &\quad -2e^{-4A}g^{pq}\partial_p e^{2A}h_{qm}\partial_n e^{2A} - 2R^{s}{}_{mnp}g^{pq}h_{qs} \\ &-e^{-4A}\tilde{g}^{\pi\rho}\tilde{\nabla}_\pi h_{\rho m}\partial_n e^{2A} - e^{-4A}\tilde{g}^{\pi\rho}\tilde{\nabla}_\pi h_{\rho n}\partial_m e^{2A} - h_4\nabla_n\left(e^{-2A}\partial_m e^{2A}\right) = 0 \end{aligned} \tag{1.51}$$

The gauge condition $\mathcal{G}_N = 0$ that we imposed to obtain the previous equation can be written:

$$e^{-2A}\tilde{g}^{\pi\rho}\tilde{\nabla}_\pi h_{\rho\nu} - \frac{1}{2}e^{-2A}\tilde{\nabla}_\nu\tilde{h}_4 - \frac{1}{2}\nabla_\nu h_N + g^{pq}\nabla_p h_{q\nu} + 2h_{p\nu}g^{pq}e^{-2A}\partial_q e^{2A} = 0 \tag{1.52a}$$

$$g^{pq}\nabla_p h_{qr} - \frac{1}{2}\nabla_r h_N - \frac{1}{2}e^{-2A}\nabla_r\tilde{h}_4 + g^{\pi\rho}\tilde{\nabla}_\pi h_{\rho r} + 2h_{mr}g^{mp}e^{-2A}\partial_p e^{2A} = 0 \tag{1.52b}$$

Warp factor and effects on the cosmological constants

We assume a maximally symmetric four-dimensional space-time. Thus we can write, according to [28],

$$\tilde{R}^{\pi}{}_{\mu nu\sigma} = \frac{\Lambda_4}{3}\left(\delta^{\pi}_{\nu}\tilde{g}_{\mu\sigma} - \delta^{\pi}_{\sigma}\tilde{g}_{\mu\nu}\right) \tag{1.53}$$

with

$$\Lambda_4 = \frac{1}{4}\tilde{R}_4 \tag{1.54}$$

Then one can obtain the two following relations:

$$\frac{2D}{D-2}\Lambda_D = R^{(0)}_{D} = e^{-2A}\tilde{R}_4 + R_{\mathcal{M}} - e^{-4A}\left(\partial e^{2A}\right)^2 - 4e^{-2A}\Delta_{\mathcal{M}}e^{2A} \tag{1.55}$$

$$4\Lambda_4 = \tilde{R}_4 = \frac{4}{D-4}e^{2A}R_{\mathcal{M}} + 2\frac{D-2}{D-4}e^{-2A}\left(\partial e^{A}\right)^2 + 2\frac{D-8}{D-4}\Delta_{\mathcal{M}}e^{2A} \tag{1.56}$$

We see that Λ_4 is equal to a combination of $e^{2A}R_{\mathcal{M}}$, $\left(\partial e^A\right)^2$ and $\Delta_{\mathcal{M}}e^{2A}$ and that Λ_D is a equal to a combination of $e^{-2A}e^{2A}R_{\mathcal{M}}$, $e^{-2A}\left(\partial e^A\right)^2$ and $e^{-2A}\Delta_{\mathcal{M}}e^{2A}$. This overall factor e^{2A} can lead to a significant difference in the two cosmological constants.

In the next chapter we will assume a constant unitary warp factor and a Minkowski four dimensional space time. The assumption of a constant warp factor implies that Eq. (1.56) can now be written as:

$$\frac{2D}{D-2}\Lambda_D = R_D^{(0)} = \tilde{R}_4 + R_{\mathcal{M}} \tag{1.57}$$

$$4\Lambda_4 = \tilde{R}_4 = \frac{4}{D-4}R_{\mathcal{M}} \tag{1.58}$$

From this point, we deduce that for a four dimensional Minkowski space time, which is flat ($\tilde{R}_4 = 0 = \Lambda_4$), the scalar curvature and the cosmological constant in D dimension are both equal to zero. Moreover $\Lambda_D = 0$ implies through Eq. (1.27) that:

$$R_{MN}^{(0)} = 0 \tag{1.59}$$

Thus if we impose a constant unitary warp factor and a Minkowski four dimensional space time, the extra dimensions must be Ricci flat, i.e. $R_{mn}^{(0)} = 0$. We will make this assumption later on.

Chapter 2

Gravitational waves with extra dimensions

2.1 Wave equations with flat extra dimensions

2.1.1 Warp factor specification

The components (1.49), (1.50) and (1.51) of the wave equation in D dimensions look very complicated due to the presence of the warp factor. In order to simplify these equations, we will assume that the warp factor is constant, as mentioned in the previous chapter. Thus everywhere in the manifold $\mathcal{M}$ the infinitesimal element of length is strictly the same at the same location in each brane. We thus describes a infinite set of four-dimensional branes strictly identical considering only the background metric. All those branes are linked through the manifold $\mathcal{M}$. Only the perturbation metric will differ from one another.

We can set $e^{2A} = 1$ as every other value for the constant warp factor is equivalent. The four-dimensional metric $e^{2A}\tilde{g}_{\mu\nu}$ is now equal to $\tilde{g}_{\mu\nu} = g_{\mu\nu}$ so that one drops the tilde notation. The component of the Einstein equation (1.49), (1.50) and (1.51) can now be written:

$$\Box_4 h_{\mu\nu} + \Delta_{\mathcal{M}} h_{\mu\nu} = 2R^{\pi}{}_{\mu\nu\sigma} g^{\sigma\rho} h_{\rho\pi} \tag{2.1a}$$

$$\Box_4 h_{\mu n} + \Delta_{\mathcal{M}} h_{\mu n} = 0 \tag{2.1b}$$

$$\Box_4 h_{mn} + \Delta_{\mathcal{M}} h_{mn} = 2R^{s}{}_{mnp} g^{pq} h_{qs} \tag{2.1c}$$

The de Donder gauge condition can be written:

$$g^{\pi\rho}\nabla_\pi h_{\rho\nu} + g^{pq}\nabla_p h_{q\nu} - \frac{1}{2}\nabla_\nu h_4 - \frac{1}{2}\nabla_\nu h_N = 0 \tag{2.2a}$$

$$g^{\pi\rho}\nabla_\pi h_{\rho r} + g^{pq}\nabla_p h_{qr} - \frac{1}{2}\nabla_r h_4 - \frac{1}{2}\nabla_r h_N = 0 \tag{2.2b}$$

In the four-dimensional case, one usually sets the background metric to be Minkowski. The curvature of space-time caused by the Earth is negligible along the arm of an interferometer. Between the source and the Earth space is flat in the Friedmann-Lemaître-Robertson-Walker metric and one assumes that the expansion of the universe is negligible as the source only go to moderate redshifts. In order to compare the gravitational waves of the theory with extra dimensions with the ones of General Relativity, we also set $g_{\mu\nu} = \eta_{\mu\nu}$ in the theory with extra dimensions. Thus the right-hand side of equation (2.1a) vanishes. Also all the covariant derivatives with respect to four-dimensional coordinates are now equal to partial derivatives because these derivatives are built using only the four-dimensional metric. The gauge condition can be simplified further:

$$\partial^\rho h_{\rho\nu} + g^{pq}\nabla_p h_{q\nu} - \frac{1}{2}\partial_\nu h_4 - \frac{1}{2}\partial_\nu h_N = 0 \tag{2.3a}$$

$$\partial^\rho h_{\rho r} + g^{pq}\nabla_p h_{qr} - \frac{1}{2}\nabla_r h_4 - \frac{1}{2}\nabla_r h_N = 0 \tag{2.3b}$$

We notice that imposing a Minkowski background leads to the same residual gauge transformation for the four-dimensional perturbation $h_{\mu\nu}$. The decomposition of the metric into a background metric and a perturbation metric can be rewritten as:

$$\begin{pmatrix} g^D_{\mu\nu} & g^D_{\mu n} \\ g^D_{m\nu} & g^D_{mn} \end{pmatrix} = \begin{pmatrix} \eta_{\mu\nu} & 0 \\ 0 & g_{mn} \end{pmatrix} + \begin{pmatrix} h_{\mu\nu} & h_{\mu n} \\ h_{m\nu} & h_{mn} \end{pmatrix} \tag{2.4}$$

g^D being the metric of the D-dimensional manifold. Thus the transformations of $h_{\mu\nu}$ with respect to the four-dimensional coordinate x^μ that leave $g^D_{\mu\nu} = \eta_{\mu\nu} + h_{\mu\nu}$ unchanged are the same as for the four-dimensional theory. These are the Lorentz transformations and the infinitesimal gauge transformations.

2.1.2 Compactification

We must now discuss the compactification of the extra dimensions. Compactification is not required in order to reproduce General Relativity as shown in [29]. However the assumption of non-compact extra dimensions requires that the four-dimensional metric depends on the coordinates of the extra dimensions. As we impose $e^{2A(y)}$ to be constant, the metric is independent of the extra y^m coordinate and we must impose compact extra dimensions.

There are many possibilities. The extra dimensions are compact and this implies that the internal laplacian operator $\Delta_\mathcal{M}$ has a discrete basis of eigenfunctions. The compactification is formally imposed by choosing these eigenfunctions. We are restricted to a Ricci-flat manifold because we have made the assumption that the four-dimensional space-time is flat as discussed at the end of last chapter. Well-known examples are the Calabi-Yau manifolds used in string theory [30]. However we will turn to a much simpler type of manifold in the following: the flat torus T^N.

An N-dimensional flat torus corresponds to a manifold where each dimension has its beginning identified to its end. For example, a cube with each face identified to the opposite face is a three-dimensional flat torus. This implies the following Dirichlet boundary conditions on the perturbation metric:

$$h_{MN}(y^n = 0) = h_{MN}(y^n = l_n) \tag{2.5}$$

where l_n is the length of the n^{th} dimension. The solutions are combinations of the harmonic eigenfunctions of the discrete basis:

$$h_{MN}(x, y) = \sum_{\mathbf{k}} h^{\mathbf{k}}_{MN}(x)\omega_{\mathbf{k}}(y) \tag{2.6}$$

where $h^{\mathbf{k}}_{MN}$ are the Kaluza-Klein modes and the eigenfunctions $\omega_{\mathbf{k}}$ are solutions of the eigenvalue problem:

$$\Delta_\mathcal{M}\omega_{\mathbf{k}} = -m^2_{\mathbf{k}}\omega_{\mathbf{k}} \tag{2.7}$$

with $m_{\mathbf{k}}$ a real number. Equations (2.6) and (2.7) are general and in the case of the flat torus the eigenfunctions are simply given by $\omega_{\mathbf{k}} = e^{i\mathbf{k}\cdot\mathbf{y}}$ and $\{\mathbf{k}\}$ is a set of N-dimensional real vectors isomorphic to $\mathbb{Z}^N$. The eigenvalue associated to $\mathbf{k} = \mathbf{0}$ is by convention $m_{\mathbf{0}} = 0$ and we can write:

$$\mathbf{k} = \frac{2\pi k \hat{\mathbf{n}}}{L_{\hat{\mathbf{n}}}} \tag{2.8}$$

where k is an integer, $\hat{\mathbf{n}}$ a unitary vector of $\mathcal{M}$ and $L_{\hat{\mathbf{n}}}$ the length of $\mathcal{M}$ along the direction $\hat{\mathbf{n}}$.

In conclusion, in this thesis we shall study waves in a four-dimensional space-time with N extra dimensions, assuming

- A constant warp factor.
- A Minkowski four-dimensional space-time that implies a Ricci-flat manifold $\mathcal{M}$ and a null cosmological constant $\Lambda = 0$
- A flat torus manifold $\mathcal{M}$ that implies harmonic eigenfunctions as a basis of the internal laplacian operator $\Delta_{\mathcal{M}}$

Considering all these assumptions, the components of the wave equation in D dimension reads:

$$\Box_4 h^{\mathbf{k}}_{\mu\nu} - m^2_{\mathbf{k}} h^{\mathbf{k}}_{\mu\nu} = 0 \tag{2.9a}$$
$$\Box_4 h^{\mathbf{k}}_{\mu n} - m^2_{\mathbf{k}} h^{\mathbf{k}}_{\mu n} = 0 \tag{2.9b}$$
$$\Box_4 h^{\mathbf{k}}_{mn} - m^2_{\mathbf{k}} h^{\mathbf{k}}_{mn} = 2R^s{}_{mnp} g^{pq} h_{qs} \tag{2.9c}$$

where we recognise the Klein-Gordon equation. The expression of the gauge conditions (2.2a) and (2.2b) are unchanged.

2.2 Gravitational waves in 4 dimensions

As before, I will remind the reader of the main features of gravitational waves in 4 dimenions before discussing the case with extra dimensions. The devellopement presented here are based on [27]. We will study plane waves in the following for simplicity. A plane wave solution of equation (1.17) is:

$$\overline{h}_{\mu\nu} = A_{\mu\nu} \ \cos\left(k^\alpha x_\alpha\right) \tag{2.10}$$

with k_μ and $A_{\mu\nu}$ that must satisfy:

$$k_\alpha k^\alpha = 0 \tag{2.11}$$
$$A_{\mu\alpha} k^\alpha = 0 \tag{2.12}$$

The first constraint means that the velocity of the wave is the speed of light c due to the d'Alembertian operator of equation (1.17). The second is imposed by the de Donder (or Lorenz) gauge condition (1.16).

As seen in the first chapter the de Donder gauge condition leads to a wave equation but it doesn't fix completely the gauge because infinitesimal gauge transformation, Eq. (1.6),

$$\underline{x}^\alpha = x^\alpha + \xi^\alpha\left(x^\beta\right) \ , \ |\partial_\beta \xi^\alpha| \ll 1$$

are allowed. There are thus four degrees of freedom left to fix. A very common choice for gravitational waves is the *Transverse-Traceless gauge* or *TT gauge*. To impose the TT gauge condition, we must choose a 4-velocity u^α that is time-like. This 4-velocity corresponds to a choice of a Lorentz reference frame. This gauge choice implies further constraints on the solution which are:

$$A_{\mu\alpha}u^\alpha = 0 \tag{2.13}$$

$$A^\alpha{}_\alpha = 0 \tag{2.14}$$

In this gauge the amplitude of each mode of the solution and thus the solution $\overline{h}_{\mu\nu}$ is transverse to the direction u_μ and traceless. The equation (1.14) that defines $\overline{h}_{\mu\nu}$ implies:

$$h_{\mu\nu} = \overline{h}_{\mu\nu} + \frac{\overline{h}_\alpha{}^\alpha}{2}\eta_{\mu\nu} \tag{2.15}$$

so that $\overline{h}_{\mu\nu} = h_{\mu\nu}$ in this gauge and both are transverse and traceless.

Equation (2.13) is a set of four scalar equations but it adds only three constraints on $A_{\mu\nu}$ because they are linearly dependent due to Eq. (2.12) ($k^\alpha A_{\alpha\beta}u^\beta = 0$). Taking into account the scalar equation (2.14) adds another constraint on $A_{\mu\nu}$. So the transverse-traceless gauge add a total of four constraints and thus fixes completely the gauge.

Because $h_{\mu\nu} = \overline{h}_{\mu\nu}$, all the constraints on $A_{\mu\nu}$ can be express through constraints on $h_{\mu\nu}$ directly. There are eight of them. Choosing u^μ so that $u^0 = 1$ and $u^j = 0$ for simplicity (All the possible choice of u^α are linked by a Lorentz transformations):

$$h_{\mu 0} = 0 \tag{2.16}$$

$$\sum_{j=1}^{3} \partial_j h_{kj} = \sum_{j=1}^{3} ik_j h_{kj} = 0 \tag{2.17}$$

$$\sum_{k=1}^{3} h_{kk} = 0 \tag{2.18}$$

By choosing $k^\mu = (1, 0, 0, 1)$, so that the wave propagate in the z direction, Eq. (2.17) becomes $ik_z h_{kz} = h_{kz} = 0$. Thus we are left with only h_{xx}, h_{yy} and $h_{xy} = h_{yx}$ being non-zero. Taking into account the traceless condition (2.18), we eventually finds that the wave only has two degree of freedom h_+ and $h_\times$ such that:

$$h_{\mu\nu} = \begin{pmatrix} 0 & 0 & 0 & 0 \\ 0 & h_+ & h_\times & 0 \\ 0 & h_\times & -h_+ & 0 \\ 0 & 0 & 0 & 0 \end{pmatrix} \tag{2.19}$$

To visualize the effect of a gravitational wave, we can choose Fermi's normal coordinates system as the observer frame of reference (This implies that the observer is moving along a geodesic). In this coordinate system, the metric at the location of the observer is Minkowski and its first derivative is zero: it is the inertial frame of reference moving with a particle falling freely. In this reference frame, one can calculate the geodesic deviation of a ring of free falling particles centered on the observer. From the observer's point of view, the distances between him and all the particles of the ring oscillate so that the observer sees the ring changing according to the patterns of Fig. 2.1:

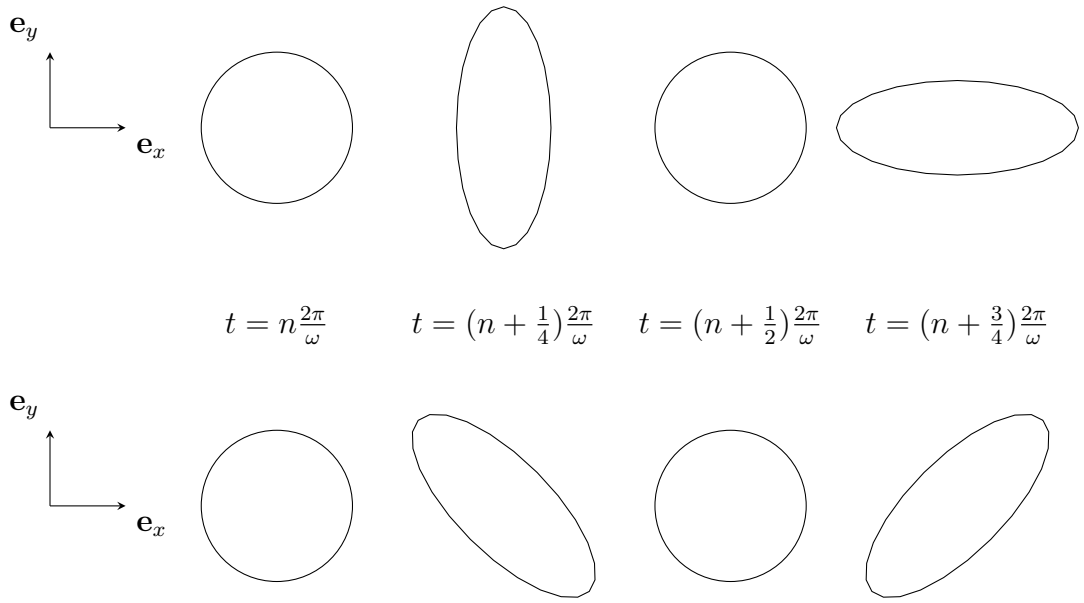

Figure 2.1: One period of the h_+ (above) and the $h_\times$ (below) modes

2.3 Gravitational waves in D dimensions

In this section, we calculate the solutions to equation (2.9). We are only interested in the solutions for $h_{\mu\nu}$ and need only to check compatibility with the other equations and the gauge conditions.

2.3.1 The massless mode

The first difference with the four-dimensional case is that we must solve an equation for each mode. As the zero-mode is associated with the eigenvalue $m_{\mathbf{0}} = 0$, the Klein-Gordon equation reduces to the wave equation for this mode. Also, we notice that the eigenfunction associated to the zero-mode is constant: $\omega_{\mathbf{0}} = e^{\mathbf{0}\cdot\mathbf{y}} = 1$. Equivalently the solution of the differential equation $\Delta_{\mathcal{M}}\omega_{\mathbf{0}} = 0$ is a linear function because it is a second order differential equation and the only way a linear function can satisfy the Dirichlet boundary conditions (2.5) is to be constant. Thus $\nabla_p h_{MN} = 0$, $\nabla_p h_4 = 0$, $\nabla_p h_N = 0$ and the gauge condition is simplified:

$$\partial^\rho h_{\rho\nu} - \frac{1}{2}\partial_\nu h_4 - \frac{1}{2}\partial_\nu h_N = 0 \tag{2.20a}$$

$$\partial^\rho h_{\rho r} = 0 \tag{2.20b}$$

The second gauge condition implies that $\Box_4 h_{\mu n} = 0$ is automatically satisfied. Moreover equations (2.9) and (2.20) contain no terms with $h_{\mu\nu}$ or h_{mn} such that it completely decouples from the other equations. As we are interested only in the behaviour of the four-dimensional part of the wave $h_{\mu\nu}$, the two equations discussed before can be omitted.

Furthermore, the four-dimensional wave is coupled to the extra dimensions only through h_N via the first gauge condition. We notice that taking the trace of equation (2.9c) by multiplying it with g^{mn} we obtain for the right-hand side:

$$
\begin{aligned}
2g^{mn}R^{s}{}_{mnp}g^{pq}h_{qs} &= 2g^{mn}g^{rs}R_{rmnp}g^{pq}h_{qs} \\
&= -2g^{mn}g^{rs}R_{mrnp}g^{pq}h_{qs} \\
&= -2g^{rs}R_{rp}g^{pq}h_{qs} \\
&= 0
\end{aligned}
$$

The last equality is due to the fact that we imposed the four-dimensional space-time to be Minkwoski and, as mentioned in the first chapter, this assumption implies that the manifold $\mathcal{M}$ is Ricci flat: $R_{rp} = 0$. Thus, we are left with:

$$\Box_4 h_{\mu\nu} = 0 \tag{2.21a}$$

$$\Box_4 h_N = 0 \tag{2.21b}$$

and the gauge condition (2.20a). From now on will note the zero mode amplitudes $h^{\mathbf{0}}_{\mu\nu}$ and $h^{\mathbf{0}}_N$

As mentioned before, $h^{\mathbf{0}}_{\mu\nu}$ transforms like in the four-dimensional case. The only difference is that the de Donder gauge is different due to the presence of the term $-\frac{1}{2}\nabla_\nu h^{\mathbf{0}}_N$. Thus the counting of the degrees of freedom is identical and the perturbation $h^{\mathbf{0}}_{\mu\nu}$ has two degree of freedom. The trace h_N has obviously one degree of freedom. We notice that $h^{\mathbf{0}}_N$ is a scalar field because the trace of a tensor is independent of the coordinate basis. The waves we study through this equation thus have 3 degrees of freedom, two in the four-dimensional space-time and one in the extra dimensions, linked to each other through the gauge condition.

Plane wave solutions of Eq. (2.21) are:

$$h^{\mathbf{0}}_{\mu\nu} = A^{\mathbf{0}}_{\mu\nu}\ \cos\left(k^\alpha x_\alpha\right) \tag{2.22}$$

$$h^{\mathbf{0}}_N = A^{\mathbf{0}}_N\ \cos\left(k^\alpha x_\alpha\right) \tag{2.23}$$

with k^μ, $A^{\mathbf{0}}_{\mu\nu}$ and $A^{\mathbf{0}}_N$ that must satisfy:

$$k^\alpha k_\alpha = 0 \tag{2.24}$$

$$k^\alpha A^{\mathbf{0}}_{\alpha\nu} - \frac{1}{2}k_\nu A^{\mathbf{0}}_4 - \frac{1}{2}A^{\mathbf{0}}_N = 0 \tag{2.25}$$

We can choose arbitrarily the propagation axis. Taking $k^\mu = (\omega/c, 0, 0, p)$, the gauge condition can be written:

$$\frac{\omega}{c}\ A^{\mathbf{0}}_{00} + k\ A^{\mathbf{0}}_{03} + \frac{1}{2}\frac{\omega}{c}\ A^{\mathbf{0}}_4 = -\frac{1}{2}\frac{\omega}{c}\ A^{\mathbf{0}}_N \tag{2.26a}$$

$$\frac{\omega}{c}\ A^{\mathbf{0}}_{10} + k\ A^{\mathbf{0}}_{13} = 0 \tag{2.26b}$$

$$\frac{\omega}{c}\ A^{\mathbf{0}}_{20} + k\ A^{\mathbf{0}}_{23} = 0 \tag{2.26c}$$

$$\frac{\omega}{c}\ A^{\mathbf{0}}_{30} - k\ A^{\mathbf{0}}_{33} + \frac{1}{2}k\ A^{\mathbf{0}}_4 = \frac{1}{2}k\ A^{\mathbf{0}}_N \tag{2.26d}$$

As in the four-dimensional case, we impose the transverse condition with respect to a direction given by the four-vector u^α. However, we notice that the de Donder condition doesn't imply

that the four scalar equations of the transverse condition are linearly dependent: $k^\beta h_{\beta\alpha} u^\alpha \neq 0$. The consequence is that there is no degree of freedom left to impose the traceless condition as the gauge is already completely fixed. Thus the presence of extra dimension forces the wave to have a non-zero trace. In fact all the calculations and hypotheses for the massless mode are identical to the four-dimensional case. However where we imposed a traceless condition in four dimensions we still impose a traceless condition but, this time, including the extra dimension in the computation of the trace. So we did impose the traceless condition exactly as in four dimensions but the difference here is that we are only interested in the four-dimensional part of the wave and not the whole wave.

Indeed, we impose the transverse condition:

$$A^{\mathbf{0}}_{\mu\alpha} u^\alpha = 0 \tag{2.27}$$

and choose the four-vector $u^\alpha = (1, 0, 0, 0)$ as in four dimensions so that $A^{\mathbf{0}}_{\mu 0} = A^{\mathbf{0}}_{0\mu} = 0$. Using this last result in equations (2.26) we find $A^{\mathbf{0}}_{13} = A^{\mathbf{0}}_{23} = A^{\mathbf{0}}_{33} = 0$ and $A^{\mathbf{0}}_4 = A^{\mathbf{0}}_{11} + A^{\mathbf{0}}_{22} = -A^{\mathbf{0}}_N$, so that:

$$A^{\mathbf{0}}_{\mu\nu} = \begin{pmatrix} 0 & 0 & 0 & 0 \\ 0 & A^{\mathbf{0}}_{11} & A^{\mathbf{0}}_{12} & 0 \\ 0 & A^{\mathbf{0}}_{21} & -A^{\mathbf{0}}_{11} - A^{\mathbf{0}}_N & 0 \\ 0 & 0 & 0 & 0 \end{pmatrix} \tag{2.28}$$

and

$$h^{\mathbf{0}}_{\mu\nu} = \begin{pmatrix} 0 & 0 & 0 & 0 \\ 0 & h^{\mathbf{0}}_{11} & h^{\mathbf{0}}_{12} & 0 \\ 0 & h^{\mathbf{0}}_{21} & -h^{\mathbf{0}}_{11} - h^{\mathbf{0}}_N & 0 \\ 0 & 0 & 0 & 0 \end{pmatrix} \cos(k^\alpha x_\alpha) = \begin{pmatrix} 0 & 0 & 0 & 0 \\ 0 & h^{\mathbf{0}}_{11} & h^{\mathbf{0}}_{12} & 0 \\ 0 & h^{\mathbf{0}}_{21} & -h^{\mathbf{0}}_{11} - h^{\mathbf{0}}_N & 0 \\ 0 & 0 & 0 & 0 \end{pmatrix} \cos\left(\omega\left(t - \frac{x^3}{c}\right)\right) \tag{2.29}$$

We know that any tensor can be split as follow:

$$(T_{\mu\nu}) = \frac{T}{N} \mathbb{1}_{N\times N} + (B_{\mu\nu}) \tag{2.30}$$

where T is the trace of the tensor $(T_{\mu\nu})$, N the number of dimension, $\mathbb{1}_{N\times N}$ the identity and $(B_{\mu\nu})$ a traceless tensor. The trace is thus linked to the isotropic part of the tensor. In this case, we expect that an isotropic mode in the transverse plane in addition to the two polarisation already present in the four-dimensional case. Thus we can decompose the expression of $h^{\mathbf{0}}_{\mu\nu}$ into a sum of an isotropic tensor and a traceless tensor as in (2.30) .The isotropic part has one degree of freedom and the traceless part has two degrees of freedom that can be identify to the two mode of the four-dimensional theory:

$$h^{\mathbf{0}}_{\mu\nu} = \left[\frac{-h^{\mathbf{0}}_N}{2} \begin{pmatrix} 0 & 0 & 0 & 0 \\ 0 & 1 & 0 & 0 \\ 0 & 0 & 1 & 0 \\ 0 & 0 & 0 & 0 \end{pmatrix} + \begin{pmatrix} 0 & 0 & 0 & 0 \\ 0 & h^{\mathbf{0}}_+ & h^{\mathbf{0}}_\times & 0 \\ 0 & h^{\mathbf{0}}_\times & -h^{\mathbf{0}}_+ & 0 \\ 0 & 0 & 0 & 0 \end{pmatrix} \right] \cos\left(\omega\left(t - \frac{x^3}{c}\right)\right) \tag{2.31}$$

As the additional mode is isotropic, we don't need to compute the geodesic deviation to find its effects. From the already known effects of the $h^{\mathbf{0}}_+$ and $h^{\mathbf{0}}_\times$, we deduce for $h^{\mathbf{0}}_\circ \equiv -h^{\mathbf{0}}_N/2$ that the effect seen by an observer at the center of a ring of particles is given by the patterns on Fig. 2.2. This oscillation mode is called the *breathing mode*.

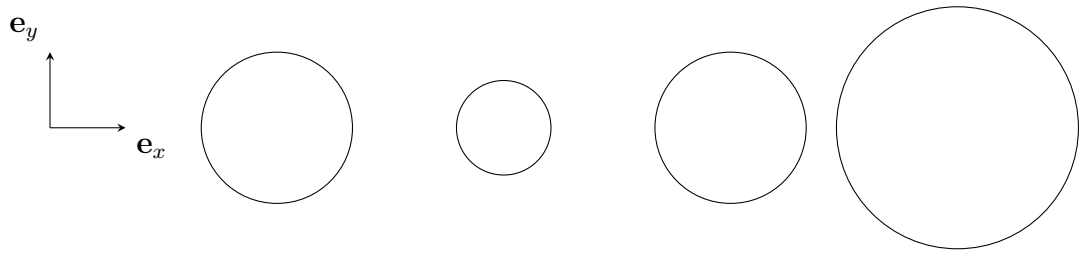

Figure 2.2: One period of the $h^{\mathbf{0}}_{\circ}$ mode

2.3.2 The massive modes

We consider now waves such that $m_{\mathbf{k}} \neq 0$. This means that the waves propagate partially, at least, in the manifold $\mathcal{M}$. We add to the amplitude of the massive mode a subscript $\mathbf{k}$: $h^{\mathbf{k}}_{\mu\nu}$. As before, we are interested only in the four-dimensional part of the waves. The equation for $h^{\mathbf{k}}_{\mu\nu}$ is given in (2.9a). We recognise the Klein-Gordon equation. A plane wave solution of this Klein-Gordon equation is:

$$h^{\mathbf{k}}_{\mu\nu} = A^{\mathbf{k}}_{\mu\nu} \cos\left(k^\alpha x_\alpha\right) \tag{2.32}$$

but this time $k^\mu = \left(\omega/c, \vec{k}\right)$ must satisfy:

$$\left(\frac{\omega}{c}\right)^2 = m^2_{\mathbf{k}} + \vec{k}^2 \tag{2.33}$$

which is a dispersion relation that prevents k^μ from being light-like. Thus all the mode with $m_{\mathbf{k}} \neq 0$ travel slower than light and previous four-dimensional gravitational waves. We call $m_{\mathbf{k}}$ a mass because the Klein-Gordon equation describes the behavior of massive particle despite the fact that the equation considered here is classical. However, as these modes travel slower than light their velocity depends on the observer reference frame as for any massive particle.

The gauge conditions (2.3a) and (2.3b) don't change. The difference with the massless mode is that the term $g^{pq}\nabla_p h_{q\nu}$ doesn't vanish because the four-dimensional part is no longer constant with respect to the extra dimensions. For a plane wave the de Donder gauge condition become:

$$\left(k^\alpha A^{\mathbf{k}}_{\alpha\nu} - \frac{1}{2}k_\nu A^{\mathbf{k}}_4\right)\cos\left(k^\alpha x_\alpha\right) = -\left(g^{mn}\nabla_m h_{n\mu}\right)^{\mathbf{k}} + \frac{1}{2}\partial_\nu h^{\mathbf{k}}_N \tag{2.34a}$$

$$\partial^\rho h_{\rho r} - \frac{1}{2}\nabla_r h_4 = -g^{pq}\nabla_p h_{qr} + \frac{1}{2}\nabla_r h_N \tag{2.34b}$$

In four dimensions, all the gauges that satisfy the de Donder gauge condition are linked by gauge transformations for which $\Box\xi^\mu = 0$. In the present situation, we deduce using the infinitesimal gauge transformations (1.26) that the de Donder gauge condition (2.3a) imposes that the gauge transformation satisfies:

$$\Box_4 \xi^{\mathbf{k}}_\mu - m_{\mathbf{k}}\xi^{\mathbf{k}}_\mu = 0 \tag{2.35}$$

We would like to proceeds like in the four-dimensional case and fix completely the gauge. At first sight it seems quite difficult because we need to take into account the gauge condition (2.3b). It turns out that equation (2.35) allows to impose:

$$\partial^\rho h^{\mathbf{k}}_{\rho\nu} = 0 \tag{2.36}$$

and

$$h^{\mathbf{k}\alpha}_{\ \ \alpha} \equiv h^{\mathbf{k}}_4 = 0 \tag{2.37}$$

Satisfying these two conditions adds the following constraints on the gauge transformations which are:

$$\Box_4 \xi^{\mathbf{k}}_\mu + \partial_\mu \partial^\nu \xi^{\mathbf{k}}_\nu = 0 \tag{2.38}$$

and

$$\partial^\nu \xi^{\mathbf{k}}_\nu = 0 \tag{2.39}$$

Taking into account all the constraints that a gauge transformation must satisfy to preserve the gauge conditions (2.35), (2.38) and (2.39) leads to:

$$m_{\mathbf{k}} \xi^{\mathbf{k}}_\mu = 0 \tag{2.40}$$

meaning that all the gauge conditions we imposed completely fix the gauge for the four-dimensional part. Moreover it is enough to study the four-dimensional part. We don't need to fix the extra dimensional part of the gauge degrees of freedom because the condition (2.38) and (2.39) imply that the left-hand side of the gauge condition (2.34a) is always equal to zero. So, the four-dimensional part of the wave is completely decoupled from the extra-dimensional part.

The de Donder gauge condition is imposed on the four-dimensional part and the extra-dimensional part of the wave such that it restricts the number of degrees of freedom of the whole wave. However as the four-dimensional part and the extra-dimensional part are still coupled if we consider only the de Donder condition, it doesn't reduce the number of degrees of freedom of the four-dimensional part. As a consequence, only the additional gauge condition (2.38) and (2.39) reduce the number of degrees of freedom of the four-dimensional part of the wave. There are five scalar constraints and a four by four symetric matrix has 10 degrees of freedom. So the four-dimensional massive modes have five degrees of freedom each.

Because of the dispersion relation (2.33) we can choose $k_\mu = (m_{\mathbf{k}}, 0, 0, 0)$ so that the gauge condition (2.38) leads to $A^{\mathbf{k}}_{0\nu} = 0$. Taking into account (2.38) we find:

$$A^{\mathbf{k}}_{\mu\nu} = \begin{pmatrix} 0 & 0 & 0 & 0 \\ 0 & A^{\mathbf{k}}_{11} & A^{\mathbf{k}}_{12} & A^{\mathbf{k}}_{13} \\ 0 & A^{\mathbf{k}}_{12} & A^{\mathbf{k}}_{22} & A^{\mathbf{k}}_{23} \\ 0 & A^{\mathbf{k}}_{13} & A^{\mathbf{k}}_{23} & -A^{\mathbf{k}}_{11} - A^{\mathbf{k}}_{22} \end{pmatrix} \tag{2.41}$$

so that

$$h^{\mathbf{k}}_{\mu\nu} = \begin{pmatrix} 0 & 0 & 0 & 0 \\ 0 & h^1_+ & h^1_\times & h^2_\times \\ 0 & h^1_\times & h^2_+ & h^3_\times \\ 0 & h^2_\times & h^3_\times & -h^1_+ - h^2_+ \end{pmatrix} \cos\left(m_{\mathbf{k}} c^2 t\right) \tag{2.42}$$

All the patterns of the modes are identical to the patterns shown previously. The oscillation mode denoted by a $+$ sign deforms a ring of particle into a ellipse with the axis along the background coordinates axes. The oscillation modes denoted by a $\times$ sign correspond to ellipses with axes rotated about 45 degrees with the spatial axes. The coordinates that correspond to one mode define the plane in which it deforms space. For example, the mode $h^3_\times$ deforms a ring of particles in the yz-plane as an ellipse with axes rotated about 45 degree with respect to the

directions y and z.

We see that the h_+ modes can generate breathing modes. For example, the h_+^1 and the h_+^2 modes generate a breathing mode in the xy-plane if these modes oscillate with the same amplitude and the same phase. As the only condition that couples the diagonal components of $h_{\mu\nu}^{\mathbf{k}}$ to each other is the traceless condition, we could have choose h_+^1 and h_+^3 to be arbitrary and h_+^2 would be equal to $-h_+^1 - h_+^3$. So the breathing mode can appear in any of the xy-plane, xz-plane and yz-plane.

These massive modes travel slower than light or massless gravitational waves as mentioned before. The reason behind that is that the massive modes travel at the same speed as other gravitational waves but partially in the extra dimensions whereas the massless modes travel purely in the four-dimensional brane. For a fixed frequency, the dispersion relation (2.33) tell us that the three-dimensional wave vector $\vec{k}$ can only take discrete values depending on the mass of the mode because the latter takes discrete values. For a fixed wave vector in the three-dimensional space the set of frequencies takes discrete values for the same reason. The mass is simply the wave vector of the mode in the extra dimensions and the dispersion relation imposes that the D-vector k^M is light-like.

Minimal frequency of the massive modes

The massive modes satisfy the dispersion relation (2.33). Hence there exist a minimal frequency for these massive modes. This frequency corresponds to a stationary wave, i.e. $\vec{k} = \vec{0}$. For such waves the dispersion relation is then:

$$\frac{\omega}{c} = m_{\mathbf{k}} \tag{2.43}$$

The masses $m_{\mathbf{k}}$ of the waves are linked to the size of the extra dimensions by Eq. (2.8). The relation between the frequency and the extra dimension is thus:

$$\frac{\omega}{c} = \frac{2\pi n}{L} \tag{2.44}$$

where L is given by:

$$L = \sqrt{\sum_{i=1}^{D} a_i L_i} \qquad , \qquad a_i \in \{0, 1\} \tag{2.45}$$

Hence the minimal frequency is evaluated by replacing L by its maximal value and setting $n = 1$:

$$\omega_{min} = \frac{c}{\sqrt{\sum_{i=1}^{D} L_i}} \equiv \frac{c}{L_{max}} \tag{2.46}$$

where ω_{min} is express in Hertz.

According to Fig. 3, current gravitational wave interferometers and those coming in the following years are able to detect frequencies that ranges roughly from 10^{-4} Hz to 10^4 Hz. We can take the logarithm of Eq. (2.46):

$$\log(\omega_{min}) = \log(c) - \log(L_{max}) \tag{2.47}$$

Now we suppose that all the extra dimensions have the same length so that we can easily introduce the number of extra dimension in the last equation. With this assumption we can write:

$$L_{max} = \sqrt{\sum_{i=1}^{D} L_i} = \sqrt{\sum_{i=1}^{D} L} = \sqrt{D}L \tag{2.48}$$

where L is the size of one extra dimension. Then we can write:

$$\log(\omega_{min}) = \log(c) - \log\left(\sqrt{D}L\right) \tag{2.49}$$

If there are only a few extra dimensions, we deduce that any potential signature of massive modes must have a high frequency because we suppose that the extra dimensions are small. For $L = 1\mu m$ and $D = 10$, we get $\omega_{min} \simeq 10^{14}\ Hz$. The frequency is thus too high to be detected by current or coming interferometers. For a frequency a few order of magnitude lower, the length of the extra dimensions must be a few order of magnitude larger than a micrometer. This is impossible because we suppose that we can't perceive them because of their small size.

On the other hand, if the number of extra dimensions is very large then we have no clue on the minimal frequency because it could belong to the frequency range that we can detect but it could also be much smaller. The frequencies of the massive modes are only bounded from below. Thus we could detect massive mode even if the minimal frequency is several orders of magnitude below the detection threshold of interferometers. However the number of extra dimensions becomes extremely high. For $L = 1\ \mu m$ and $\omega_{min} = 1\ Hz$, we find $D \simeq 10^{29}$...

Chapter 3

Existence of sources for the new modes

The mathematical developments in the previous chapters lead to differential equations allowing a new polarization and new modes - the Kaluza-Klein (KK) modes - of waves. We must now address the natural question: can we expect these new waves to be excited? The answer is not obvious because we will suppose that matter can only move in the four dimensional brane that we perceive. We will make this assumption because we are sure that matter can travel in four dimensions and thus our conclusions will only depend on the existence of the extra dimensions. In other words, we analyse whether or not gravitational waves in extra dimensions can be produced by matter that cannot move in these extra dimensions. Before that we will briefly review the emission of gravitational waves in General Relativity.

3.1 Sources in four-dimensional space-time

A source simply corresponds to a non-zero stress-energy tensor in the Einstein equation. The linearised Einstein equation with a source term is written:

$$\Box\overline{h}_{\mu\nu} = -16\pi T_{\mu\nu} \tag{3.1}$$

in the Lorenz gauge. We can define $h_{\mu\nu}$ and $\overline{h}_{\mu\nu}$ and impose the gauge condition as we did in the first chapter in order to linearise the theory. Far away from the source, the interpretation of $h_{\mu\nu}$ still holds because we consider space-time to be Minkowski there. However, in the region of space-time where the source is located the gravitational field could be strong (and is strong in the case of neutron star or black hole binaries that produce the waves that we are able to detect) and in this case the interpretation of $h_{\mu\nu}$ as a perturbation breaks down and the wave equation is false.

The stress-energy tensor satisfies the conservation relation:

$$\nabla_\alpha T^{\alpha\beta} = 0 \tag{3.2}$$

In the case of a Newtonian system, i.e. the gravitational field is well described by Newton's law of gravity (slow motion source), the last equation reduces to [27]:

$$\partial_\alpha T^{\alpha\beta} = 0 \tag{3.3}$$

The solution of the inhomogeneous equation (3.1) is given by:

$$\overline{h}_{\mu\nu} = 4\int_{\mathbb{R}^3} \frac{1}{\left|\vec{r}-\vec{r'}\right|} T_{\mu\nu}\left(t - \left|\vec{r}-\vec{r'}\right|, \vec{r'}\right)\ d^3\vec{r'} \tag{3.4}$$

The integration is made over all space but we assume that the curvature of space-time vanishes very quickly so that space-time between the source and the observer is Minkowski. Thus we can consider that $T_{\mu\nu} = 0$ outside a spherical spatial region V with a radius R containing the source so that the integration is made on this sphere. This implies that the integrand $\vec{r'}$ takes only values much smaller than $\vec{r}$ the distance to the source. The integral reduces to:

$$\overline{h}_{\mu\nu} = \frac{4}{r} \int_V T_{\mu\nu} \left(t - |\vec{r}| \, , \vec{r'} \right) \, d^3 r' \tag{3.5}$$

from which we deduce that the sources emit spherical waves as the expression of the amplitude $\overline{h}$ only depends on the modulus of the radius. Far away from the source the observer can thus assume that these waves are locally plane waves. The situation is represented schematically in Fig. 3.1.

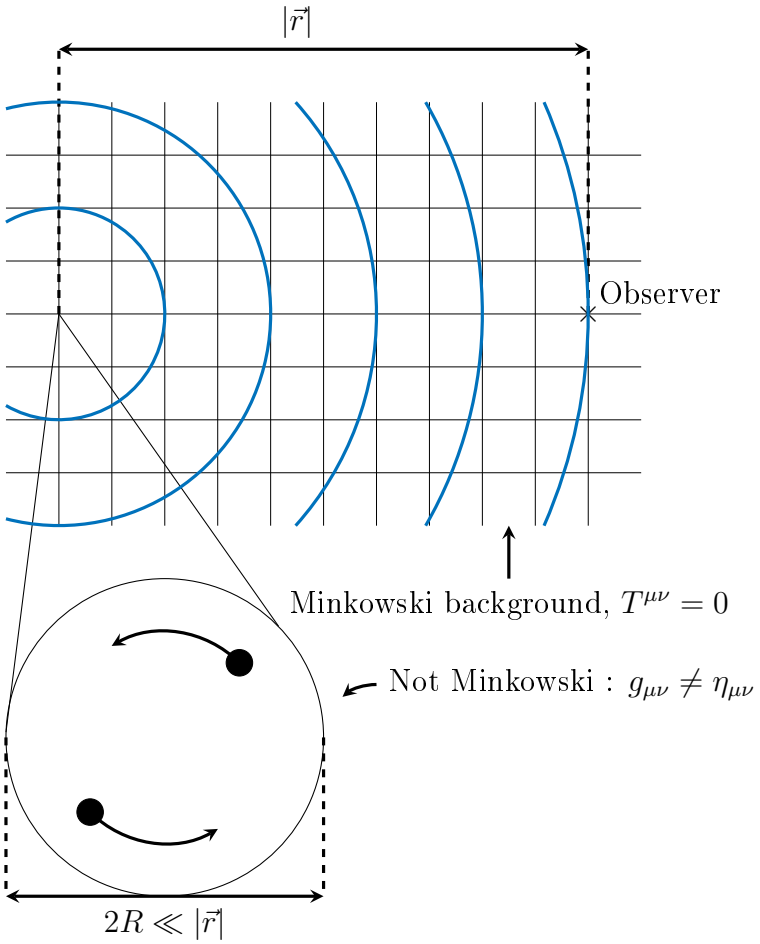

Figure 3.1: Gravitational wave from a binary system in the far field approximation

We will now evaluate this integral. To do that we define the quadrupole moment:

$$Q_{kl} = \int_V x_l \; x_k \; T_{00} \left(t, \vec{r'} \right) \; d^3 r' \tag{3.6}$$

and we calculate its second temporal derivative. We start with the first temporal derivative:

$$\begin{aligned}
\frac{\partial^2}{\partial t^2} Q_{kl} &= \int_V x_l \; x_k \; \partial^0 T_{00} \; d^3 r' \\
&= \int_V x_l \; x_k \; \left(-\partial^i T_{i0} \right) \; d^3 r' \\
&= -\int_V \left(\partial^i \left(T_{i0} \; x_k \; x_l \right) - T_{i0} \; \delta^i_l \; x_k - T_{i0} \; x_l \; \delta^i_k \right) \; d^3 r' \\
&= -\int_S T_{i0} \; x_k \; x_l \; d^2 r' - \int_V \left(-T_{i0} \; \delta^i_l \; x_k - T_{i0} \; x_l \; \delta^i_k \right) \; d^3 r' \\
&= \int_V \left(T_{l0} \; x_k + T_{k0} \; x_l \right) \; d^3 r'
\end{aligned}$$

where S is the boundary of the spherical region V. On this boundary the stress-energy tensor is everywhere equal to zero. We then calculate the second derivative:

$$\begin{aligned}
\frac{\partial^2}{\partial t^2} Q_{kl} &= \int_V \left(\partial^0 T_{l0} \; x_k - \partial^0 T_{k0} \; x_l \right) \; d^3 r' \\
&= \int_V \left(-\partial^i T_{li} \; x_k - \partial^i T_{ki} \; x_l \right) \; d^3 r' \\
&= \int_V \left(-\partial^i \left(T_{li} \; x_k \right) + T_{li} \; \delta^i_k - \partial^i \left(T_{ki} \; x_l \right) + T_{ki} \; \delta^i_l \right) \; d^3 r' \\
&= \int_S -T_{li} \; x_k \; d^2 r' + \int_V T_{li} \; \delta^i_k \; d^3 r' - \int_S T_{ki} \; x_l \; d^2 r' + \int_V T_{ki} \; \delta^i_l \; d^3 r' \\
&= 2 \int_V T_{kl} \; d^3 r'
\end{aligned}$$

From this results we obtain:

$$\overline{h}_{kl} = \frac{2}{r} \frac{\partial^2}{\partial t^2} Q_{kl} \left(t - \vec{r} \right) \tag{3.7}$$

This expression can be projected onto the TT gauge with the use of the projector:

$$P_{ij} = \delta_{ij} - n_i n_j \quad n_i = \frac{x_i}{r} \tag{3.8}$$

We obtain:

$$h^{TT}_{kl} = \frac{2}{r} \frac{\partial^2}{\partial t^2} \left(P_{ki} Q_{ij} P_{jl} - \frac{1}{2} P_{kl} \left(P_{ij} Q_{ji} \right) \right) \tag{3.9}$$

where $P_{ki} Q_{ij} P_{jl}$ is the projection on the transverse plane and $\frac{1}{2} P_{kl} \left(P_{ij} Q_{ji} \right)$ is the trace.

3.2 Sources of the new waves

We suppose that matter can't travel in the extra dimensions. This implies that $T_{MN} \neq 0$ only if $M = \mu$ and $N = \nu$. Thus we have to solve the following equations:

$$\Box_4 h_{\mu\nu} + \Delta_{\mathcal{M}} h_{\mu\nu} = -16\pi T_{\mu\nu} \tag{3.10a}$$
$$\Box_4 h_{\mu n} + \Delta_{\mathcal{M}} h_{\mu n} = 0 \tag{3.10b}$$
$$\Box_4 h_{mn} + \Delta_{\mathcal{M}} h_{mn} = 0 \tag{3.10c}$$

We are only interested in the four-dimensional waves. The solution is given by:

$$h_{\mu\nu} = 4\int_{\mathbb{R}^{D-1}} \frac{1}{\left|\vec{R}-\vec{R'}\right|} T_{\mu\nu}\left(t-\left|\vec{R}-\vec{R'}\right|, \vec{R'}\right)\ d^{D-1}\vec{R'} \tag{3.11}$$

where $\vec{R}$ and $\vec{R'} \in \mathbb{R}^{D-1}$.

As matter can't travel in the extra dimensions, this implies that we live exclusively in one of the four-dimensional branes. We set $y^m = 0$ as the position of our brane in the manifold $\mathcal{M}$. For each point with $y^m \neq 0$ there is a four-dimensional brane that could be filled with matter. But if the extra dimension exists we don't know whether or not the other branes contains matter. So we will suppose that these branes are empty in order to see if the matter of our brane is sufficient to create waves with an extra dimensional signature. Mathematically this means that the previous integral reduces to a three-dimensional integral as in General Relativity because we suppose a energy-impulse tensor of the form:

$$T_{\mu\nu}\left(t-\left|\vec{R}-\vec{R'}\right|, \vec{R'}\right) = T_{\mu\nu}\left(t-\left|\vec{r}-\vec{r'}\right|, \vec{r'}\right)\delta^{D-4}\left(\vec{y}\right) \tag{3.12}$$

where $\vec{r}$ and $\vec{r'} \in \mathbb{R}^3$ and $\vec{y} \in \mathcal{M}$.

$$h_{\mu\nu} = 4\int_{\mathbb{R}^3} \frac{1}{\left|\vec{r}-\vec{r'}\right|} T_{\mu\nu}\left(t-\left|\vec{r}-\vec{r'}\right|, \vec{r'}\right)\ d^3\vec{r'} \tag{3.13}$$

The right-hand side is exactly the same as in the previous section so that we can conclude:

$$h_{\mu\nu} = \frac{2}{r}\frac{d^2}{dt^2} Q_{kl}\left(t-\vec{r}\right) \tag{3.14}$$

The previous result is obvious because we supposed that the source is the same as in the four-dimensional theory. The difference is on the left hand side of the equation. The term $h_{\mu\nu}$ contains all the modes and polarizations discussed in the previous chapter. Thus the answer to the question *Can a source in four-dimension excite the new waves ?* is yes.

We could also deduce those results without calculation. The four dimensional matter can bend space-time in various ways. But not all types of curvature of space-time can lead to a wave. To create a wave, the dynamics of the geometry must allow a particular deformation of space-time to propagate. In General Relativity only the two polarizations h_+ and $h_\times$ can propagate. With our hypothesis of extra dimensions and the restriction that matter travels only in four dimensions we simply add a new mechanism that allows new waves to propagate from four dimensional sources. However, the addition of this new possibility for gravitational waves to propagate mean that the energy of the sources will be distributed between more possible kind of waves. If we express $h_{\mu\nu}$ in terms of all the modes we can write:

$$\sum_{\mathbf{k}=0}^{\infty}\left[\Box_4 h^{\mathbf{k}}_{\mu\nu} - m^2_{\mathbf{k}} h^{\mathbf{k}}_{\mu\nu}\right]\exp\left(i\mathbf{k}\cdot\mathbf{y}\right) = \frac{2}{r}\frac{\partial^2}{\partial t^2} Q_{kl}\left(t-\vec{r}\right) \tag{3.15}$$

3.3 Propagation of the new waves

We would like now to determine the amplitude of the excitation of each mode. We will thus calculate the Green function $h_{\mu\nu}(x,y) = G_{\mu\nu}(x,y)$ that is the solution of the differential equations with a pulse as the source term:

$$\sum_{\mathbf{k}} \left[\Box_4 G^{\mathbf{k}}_{\mu\nu} - m^2_{\mathbf{k}} G^{\mathbf{k}}_{\mu\nu}\right] \exp\left(i\mathbf{k}\cdot\mathbf{y}\right) = \sum_{\mathbf{k}} \eta_{\mu\nu}\delta^{(4)}\left(x - x_0\right)\exp\left(i\mathbf{k}\cdot\mathbf{y}\right) \tag{3.16}$$

x_0 is the location of the pulse and is located in the brane at $y^m = 0$. From now on $x_0 = 0$. For simplicity we now consider a scalar wave $G^{\mathbf{k}}$ and only one extra dimension as in [31] such that $\mathbf{k} \in \mathbb{R}^N \to k \in \mathbb{R}$. The retarded Green function corresponding to the differential problem:

$$\Box_4 G^k - m_k^2 = \delta^{(4)}(x) \tag{3.17}$$

is given in [31]:

$$G^k_R = -\frac{1}{4\pi r}\frac{\partial}{\partial r}\left[J_0\left(m_k\sqrt{t^2 - r^2}\right)\theta\left(t - r\right)\right] \tag{3.18}$$

with J_0 the Bessel function of the first kind of order 0, t and r are the time and the radius coordinates respectively and θ is the Heaviside step function. The sum of the J_0 function over all the Kaluza-Klein masses is also given in [31]:

$$\sum_{k=-\infty}^{+\infty} J_0\left(\frac{2k\pi}{L}\sqrt{t^2 - r^2}\right) = \frac{2L}{\pi}\sum_{k=-\infty}^{+\infty}\frac{\theta\left(t - \sqrt{r^2 + 8k^2L^2}\right)}{\sqrt{t^2 - r^2 - 8k^2L^2}} \tag{3.19}$$

so that the retarded Green function summed over all the masses, which is also given in [31], is:

$$G_R = -\frac{1}{2\pi^2}\sum_{k=-\infty}^{+\infty}\frac{1}{r}\frac{\partial}{\partial r}\frac{\theta\left(t - \sqrt{r^2 + 16k^2L^2}\right)}{\sqrt{t^2 - r^2 - 16k^2L^2}} \tag{3.20}$$

We now evaluate the derivative and find:

$$G_R = -\frac{1}{2\pi^2}\sum_{k=-\infty}^{+\infty}\left(-\frac{1}{\sqrt{r^2 + 16k^2L^2}}\frac{\delta\left(t - \sqrt{r^2 + 16k^2L^2}\right)}{\sqrt{t^2 - r^2 - 16k^2L^2}} + \frac{\theta\left(t - \sqrt{r^2 + 16k^2L^2}\right)}{\left(t^2 - r^2 - 16k^2L^2\right)^{\frac{3}{2}}}\right) \tag{3.21}$$

This retarded Green function is quite hard to interpret. However we can compare the expression of the Green function for the massless mode and the massive modes. The two mathematical expression

$$\frac{\delta\left(t - \sqrt{r^2 + 16k^2L^2}\right)}{\sqrt{t^2 - r^2 - 16k^2L^2}}, \qquad \theta\left(t - \sqrt{r^2 + 16k^2L^2}\right) \tag{3.22}$$

take the same value in the massless and the massive cases. The difference is that in the massive cases these expression are shifted towards the light cone interior. We thus expect the massless signal to be followed by copies of itself. But these copies will have a smaller amplitude because the two expression in 3.22 are respectively multiplied by

$$-\frac{1}{\sqrt{r^2 + 16k^2L^2}} < -\frac{1}{r} \qquad \forall k \neq 0 \tag{3.23}$$

$$\frac{1}{\left(t^2 - r^2 - 16k^2L^2\right)^{\frac{3}{2}}} < \frac{1}{\left(t^2 - r^2\right)^{\frac{3}{2}}} \qquad \forall k \neq 0 \tag{3.24}$$

Hence we expect echoes of the massless signal with an amplitude decreasing as the mass of the wave that produced these echoes increases. The decreasing rate of the echoes will be mentioned later in this chapter.

3.3.1 Propagation of the isotropic massless mode

The isotropic polarization propagates exactly like the other massless modes: they travel within a brane at the speed of light while stretching and squeezing space in directions perpendicular to their propagation direction. The difference with General Relativity is the presence of other spatial directions perpendicular to the propagation: the extra dimension. As we have seen this allows an isotropic transverse polarization because the traceless condition applies to the extra dimension as well.

However we must keep in mind that we did not discuss the deformation of the extra dimension when deriving the isotropic polarization. If there are more than one extra dimension then the isotropic polarization is degenerate because different deformations of the extra dimensions can lead to an isotropic deformation of the dimensions we perceive. Obviously we can't distinguish them because we cannot observe directly the extra dimensions.

Hence the isotropic transverse polarizations share all the features of the usual gravitational waves predicted by General Relativity. This is just an new polarization of the massless gravitational waves and thus presents no exotic behaviour unlike the massive modes. For example massive modes create echoes of a gravitational waves. These echoes are created due to the fact that these massive modes propagate in the extra dimensions as we will see. Massless modes are thus unable to create echoes because they travel exactly like gravitational waves from General Relativity.

3.3.2 Visualization of the propagation of massive modes

In order to visualize the propagation of the massive modes which are D-dimensional gravitational waves let us consider a hyperspherical shell wave as illustrated in Fig. 3.2. The abscissa corresponds to the modulus of the three dimensional position vector and the ordinate corresponds to the modulus of the position vector in the manifold $\mathcal{M}$. The wave is represented by the gray area. Because the extra dimensions are compact there is a correspondence between each interval separated by a dotted line.

Each value of $|\vec{y}|$ corresponds to a continuous set of points each associated to a four dimensional brane. In particular, $|\vec{y}| = nL$ is an (N-1)-sphere that includes our brane. The points on this (N-1)-sphere that correspond to our brane satisfy:

$$L = \sqrt{\sum_{k=1}^{D-4} (\alpha_k l_k)^2} \quad , \quad \alpha_k \in \mathbb{N} \tag{3.25}$$

with l_k the length of the flat k^{th} extra dimension. This condition is easily seen in Fig. 3.3. To each of these points corresponds a three-dimensional spherical wave.

We can decompose the hyperspherical wave into the harmonic basis of the extra dimension. This signal in D dimension can then be seen as a combination of massive modes moving through the extra dimension different copies of the four dimensional signal at different times. Instead of a one-dimensional pulse on a string the initial image that is transported is now a spherical shell (in 3D). This shell is then filled with the echoes propagating through the extra dimensions.

I now discuss whether or not the whole wave travelling in the D dimensions, which is assumed to be emitted from our brane, crosses periodically our brane and when it does if there

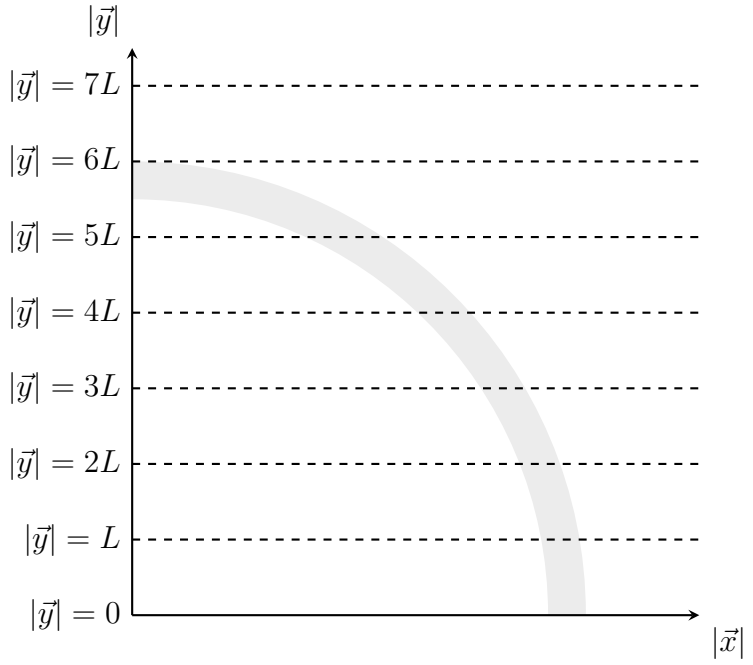

Figure 3.2: Hyper spherical wave

is a limit on the period.

Considering the case of a two-dimensional flat manifold $\mathcal{M}$ and setting the extra coordinates of our brane as $(y^1, y^2) = (0, 0)$, the situation can be visualized in Fig. 3.3. The angle θ determines a direction in the extra dimensions. Along that path, each time a wave travels the distance l_1 along y^1 it travels $l_1 \tan(\theta)$ along y^2. In order to cross our brane the angle has to satisfy the equation:

$$n_1 \; l_1 \; \tan(\theta) = n_2 \; l_2 \quad , \quad n_1, n_2 \in \mathbb{N} \tag{3.26}$$

which implies that

$$\frac{n_2}{n_1} = \frac{l_1 \; \tan(\theta)}{l_2} \quad \in \mathbb{Q} \tag{3.27}$$

In the case of an N dimensional manifold $\mathcal{M}$ this reasoning can easily be generalised by induction. For a three-dimensional $\mathcal{M}$ we just needs to consider a direction in the plane y^1y^2 that satisfies Eq. (3.27) and consider a two-dimensional plane $y^{12}y^3$ where y^{12} is the linear combination of y^1 and y^2 that corresponds to the chosen direction.

Hence not the whole D-dimensional wave will come back to our three dimensional space. Some parts of it will be lost in the extra dimensions. For those that will cross our brane there is no limit on the period because for each ratio n_2/n_1 there exists a wave corresponding to the ratio $n_2/(n_1 + 1)$. We thus expect echoes emitted indefinitely. However we also expect that geometrical dilution in $\mathcal{M}$ will make these massive mode practically undetectable after some time. The decaying amplitude of the echoes is the geometrical dilution of the hypersphere wave seen from our four-dimensional perspective.

Now we would like to know how fast the amplitude decreases. The decaying signal formed by the echoes of an initial finite duration signal with a constant unit amplitude is calculated

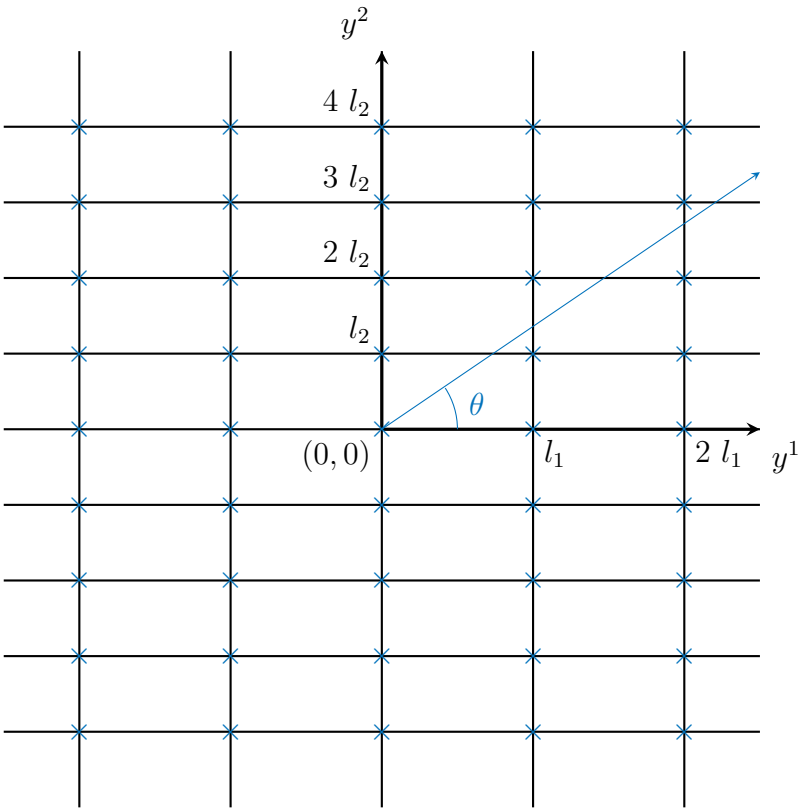

Figure 3.3: Two dimensional flat manifold $\mathcal{M}$, each blue cross corresponds to our brane

in [31] in the case of one compact extra dimension and was called *tail*. A screening effect at the forefront of the pulse is also highlighted in the article. The two effects can be seen in Fig. 3.4. Because the tail of the signal is a part of the initial pulse that travelled through the extra dimension, it is linked to the missing part of the signal at the forefront: the four-dimensional pulse looses part of its amplitude to produce images that travel in the extra dimension eventually coming back to produce the tail.

The decreasing rate of the tail is evaluated in [31] and is:

$$\langle \Phi(t,\vec{x}) \rangle_{tail} = (2^{\frac{5}{2}} - 5)\frac{G_4}{2\pi^2}\frac{L^{\frac{1}{2}}T}{t^{\frac{5}{2}}} \tag{3.28}$$

for $t \gg r$ and $t \gg T$. $G_4 = G_5/L$ is an effective four-dimensional gravitational constant, T is the duration of the pulse and L is the size of the extra dimension. The brackets means that the quantity is averaged over time. The reason for that is that the echoes are made of a discrete set of images which are singularities. The temporal averaging implies that the duration of the pulse is sufficiently long to create multiple images ($T \gg L/c$). The temporal averaging of these singularities is finite. We see that this average amplitude decreases with time as a power law $t^{-\frac{5}{2}}$. In the conclusion of [31], this average amplitude of the tails is compared with the amplitude of the four dimensional part of the signal $\Phi_0(t,r) = G_4/4\pi r$. The upper bound on this ratio is given by:

$$\chi \sim cT\sqrt{\frac{L}{r^3}} \tag{3.29}$$

with $t \geq r$. As in [31], we consider a signal with a duration $T \sim 10^4\ s$ which corresponds to the inverse of lowest frequency that could be detected by the future LISA space-borne

interferometer. With $L \sim 10^{-6}\ m$, $r \sim 10\ Mpc$ we find $\chi \sim 10^{-26}$. Hence we don't expect to observe the massive modes.

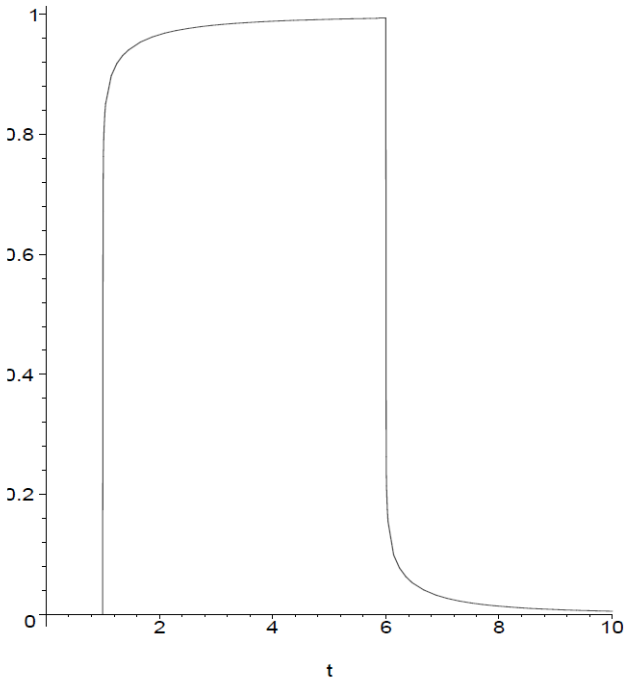

Figure 3.4: Amplitude $\langle \Phi(t, \vec{x}) \rangle$ with respect to time t, from [31]. The amplitude of the wave is dimensionless and the time coordinate is ct with c set to 1. The plot corresponds to $cT = 5$ and $L = 0.1$. The units of t on the abscissa depends on the unit chosen for T and L. Note that the ration cT/L is not so large so that we can see the typical shape of the signal. With realistic value for T and L we have seen that the upper bound of the tail is of the order $\chi \sim 10^{-26}$.

Chapter 4

Detection of the new modes

The new features that can reveal a D-dimensional gravitational wave with $D > 4$ are an isotropic massless polarization and new massive modes. We have just seen in the previous chapters that these new modes and polarizations can be excited by four-dimensional sources living in our brane. We would like to know if the new gravitational wave astronomy could be able to collect evidence for extra compact dimensions.

4.1 Massless mode

4.1.1 Effect on one interferometer

Current detections of gravitational waves are performed using interferometers. We must now analyse the effect of the new polarizations on the detectors. A gravitational wave interferometer has two arms. On one side of each arm lies the beam splitter and on the other side lies a mirror. We will now analyse the effect of a gravitational wave on one arm of the interferometer, following [32].

We derived the expression of the gravitational waves in the transverse gauge. In this gauge, we suppose that the beam splitter is at rest, meaning that it corresponds to its local inertial frame. The mirror is considered to be initially (before the gravitational wave reaches the detector) at rest:

$$\left.\frac{dx^i}{d\tau}\right|_{\tau=0} = 0 \tag{4.1}$$

The movement of the mirror in this coordinates system is given by the geodesic equation:

$$\frac{d^2x^\alpha}{d\tau^2} + \Gamma^\alpha_{\mu\nu}\frac{dx^\mu}{d\tau}\frac{dx^\nu}{d\tau} = 0 \tag{4.2}$$

Especially, at $\tau = 0$:

$$\left.\frac{d^2x^i}{d\tau^2}\right|_{\tau=0} = -\Gamma^i_{\mu\nu}\left.\frac{dx^\mu}{d\tau}\frac{dx^\nu}{d\tau}\right|_{\tau=0} = -\Gamma^i_{00}\left.\frac{dx^0}{d\tau}\frac{dx^0}{d\tau}\right|_{\tau=0} \tag{4.3}$$

with

$$\Gamma^\alpha_{\mu\nu} = \frac{1}{2}\eta^{\alpha\beta}\left(\partial_\mu h_{\nu\beta} + \partial_\nu h_{\mu\beta} - \partial_\beta h_{\mu\nu}\right) \tag{4.4}$$

In the transverse gauge $h_{0\mu} = h_{\mu 0} = 0$ which leads to $\Gamma^\alpha_{00} = 0$ and

$$\left.\frac{d^2x^i}{d\tau^2}\right|_{\tau=0} = 0 \tag{4.5}$$

This expression is thus independent of τ. This implies that the mirror stays at the same coordinate in the transverse gauge reference frame:

$$\frac{dx^i}{d\tau} = 0 \tag{4.6}$$

The spatial coordinates of the mirror being fixed, the proper time is thus equal to the time coordinate of the mirror. Indeed, the proper time is given by:

$$c^2 d\tau^2 = c^2 dt^2(\tau) - \left(\delta_{ij} + h_{ij}^{TT}\right) dx^i(\tau) dx^j(\tau) \tag{4.7}$$

with

$$dx^i dx^j = \frac{dx^i}{d\tau}\frac{dx^j}{d\tau} d\tau^2 \tag{4.8}$$

As the mirror is static in this coordinate system, i.e. $\frac{dx^i}{d\tau} = 0$, we obtain:

$$d\tau = dt \tag{4.9}$$

The physical effect of the gravitational wave is to change the distance between the beam splitter and the mirror:

$$\begin{aligned} ds^2 = -c^2dt^2 &+ \left[1 + \left(h_\circ^{\mathbf{0}} + h_+^{\mathbf{0}}\right)\cos\left(\omega\left(t - \frac{x^3}{c}\right)\right)\right] dx^2 \\ &+ \left[1 + \left(h_\circ^{\mathbf{0}} - h_+^{\mathbf{0}}\right)\cos\left(\omega\left(t - \frac{x^3}{c}\right)\right)\right] dy^2 \\ &+ 2h_\times^{\mathbf{0}}\cos\left(\omega\left(t - \frac{x^3}{c}\right)\right) dxdy + dz^2 \end{aligned} \tag{4.10}$$

for a plane wave propagating along the z axis. Assuming that the beam splitter and the mirror are initially located along the x axis at x_1 and x_2, the distance between the them is given by:

$$\int_{x_1}^{x_2} ds = \int_{x_1}^{x_2} \left[1 + \left(h_\circ^{\mathbf{0}} + h_+^{\mathbf{0}}\right)\cos\left(\omega\left(t - \frac{x^3}{c}\right)\right)\right]^{\frac{1}{2}} dx \tag{4.11}$$

$$= (x_2 - x_1)\left[1 + \left(h_\circ^{\mathbf{0}} + h_+^{\mathbf{0}}\right)\cos\left(\omega\left(t - \frac{x^3}{c}\right)\right)\right]^{\frac{1}{2}} \tag{4.12}$$

The separating distance oscillates between $L(1 + (h_\circ^{\mathbf{0}} + h_+^{\mathbf{0}}))$ and $L(1 - (h_\circ^{\mathbf{0}} + h_+^{\mathbf{0}}))$ with $L \equiv (x_2 - x_1)$.

More generally, if the beam splitter and the mirror are separated by the spatial three vector $\vec{L}$, we can write:

$$s = \left(L^2 + h_{ij}L_iL_j\right)^{\frac{1}{2}} \tag{4.13}$$

that we can approximate to its first order Taylor development in h_{ij}:

$$s \simeq L + \frac{1}{2}h_{ij}\frac{L_iL_j}{L} \tag{4.14}$$

An interferometer compares the lengths of its two arms by measuring the phase difference of two light beams that travels back and forth along these two arms. Hence the important quantity is the difference in length between the two arms. If we consider an interferometer with one arm along x and the other along y and a gravitational wave with a + polarization moving along z, we can use Eq. (4.14) to write:

$$s_x - s_y = L_x + \frac{1}{2} h_{xx} \frac{L_x L_x}{L_x} - L_y - \frac{1}{2} h_{yy} \frac{L_y L_y}{L_y} \tag{4.15}$$

If the two arms have the same length then:

$$s_x - s_y = \frac{1}{2} \left(h_{xx} - h_{yy} \right) L \tag{4.16}$$

We can rewrite the last equation as follow:

$$\frac{s_x - s_y}{L} = \frac{1}{2} \left(\vec{e}_x \vec{e}_x - \vec{e}_y \vec{e}_y \right) : \mathbf{h} \tag{4.17}$$

where ":" is the scalar product of two tensor ($\mathbf{A} : \mathbf{B} = \sum_{i,j} A_{ij} B_{ij}$) and with

$$\mathbf{h} = \begin{pmatrix} h_+ & 0 & 0 \\ 0 & h_+ & 0 \\ 0 & 0 & 0 \end{pmatrix} \tag{4.18}$$

This tensorial expression remains valid if we consider other massless polarizations.

4.1.2 Antenna pattern functions

We would like to determine the antenna pattern functions of an interferometer and their angular dependence. We first define $(O', \vec{e}_{x'}, \vec{e}_{y'}, \vec{e}_{z'})$ as the basis in which the propagation direction of the wave corresponds to the $\vec{e}_{z'}$ axis. In this basis a superposition of the three massless polarizations can be written as:

$$\begin{pmatrix} h_\circ(t) + h_+(t) & h_\times(t) & 0 \\ h_\times(t) & h_\circ(t) - h_+(t) & 0 \\ 0 & 0 & 0 \end{pmatrix} = h_\circ(t)\ \mathbf{e}_\circ + h_+(t)\ \mathbf{e}_+ + h_\times(t)\ \mathbf{e}_\times \tag{4.19}$$

where we defined:

$$\mathbf{e}_\circ \equiv \vec{e}_{x'} \vec{e}_{x'} + \vec{e}_{y'} \vec{e}_{y'} \tag{4.20}$$

$$\mathbf{e}_+ \equiv \vec{e}_{x'} \vec{e}_{x'} - \vec{e}_{y'} \vec{e}_{y'} \tag{4.21}$$

$$\mathbf{e}_\times \equiv \vec{e}_{x'} \vec{e}_{y'} + \vec{e}_{y'} \vec{e}_{x'} \tag{4.22}$$

A detector will give us a signal $h(t)$ as the output corresponding to the input (4.19). We can thus characterize the detector with the tensor $\mathbf{D}$ that satisfies:

$$h(t) \equiv \mathbf{D} : \left(h_\circ(t)\ \mathbf{e}_\circ + h_+(t)\ \mathbf{e}_+ + h_\times(t)\ \mathbf{e}_\times \right) \tag{4.23}$$

and we also define the detector pattern functions:

$$F_{\circ,+,\times} \equiv \mathbf{D} : \mathbf{e}_{\circ,+,\times} \tag{4.24}$$

The definitions of $\mathbf{e}_\circ$, $\mathbf{e}_+$ and $\mathbf{e}_\times$ rely on the choice of the basis vector $\vec{e}_{x'}$ and $\vec{e}_{y'}$. These two vectors are arbitrary (but must be orthogonal to $\vec{e}_{z'}$) whereas the vector $\vec{e}_{z'}$ must be along the

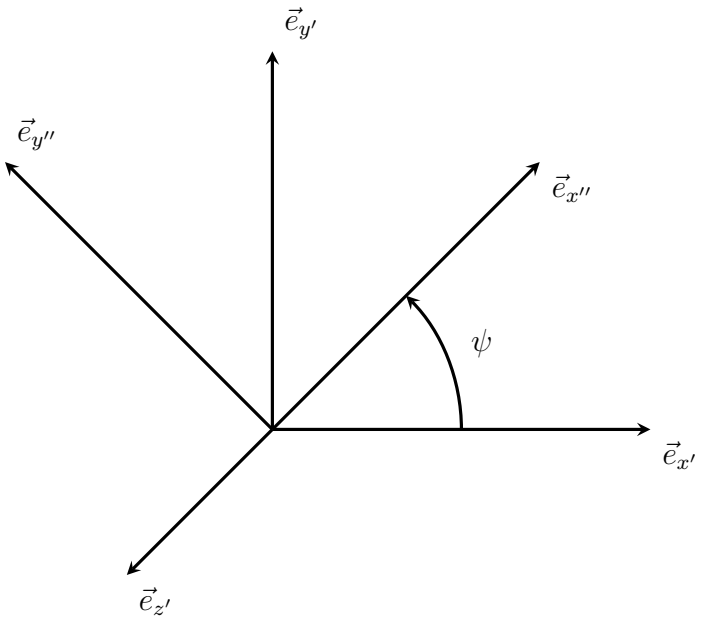

Figure 4.1: Rotation in the transverse plane

propagation direction. A unitary change of basis in the plane perpendicular to the propagation direction is given by a rotation of angle ψ around $\vec{e}_{z'}$:

$$\mathbf{R}_\psi = \begin{pmatrix} \cos\ \psi & -\sin\ \psi & 0 \\ \sin\ \psi & \cos\ \psi & 0 \\ 0 & 0 & 1 \end{pmatrix} \tag{4.25}$$

In this new basis, the polarization tensors $\mathbf{e}_\circ$, $\mathbf{e}_+$ and $\mathbf{e}_\times$ are given by $\mathbf{R}_\psi \mathbf{e}_{\circ,+,\times} \mathbf{R}_\psi^T$:

$$\mathbf{e}_\circ(\psi) = \begin{pmatrix} 1 & 0 & 0 \\ 0 & 1 & 0 \\ 0 & 0 & 0 \end{pmatrix} \tag{4.26}$$

$$\mathbf{e}_+(\psi) = \begin{pmatrix} \cos\ 2\psi & \sin\ 2\psi & 0 \\ \sin\ 2\psi & -\cos\ 2\psi & 0 \\ 0 & 0 & 0 \end{pmatrix} \tag{4.27}$$

$$\mathbf{e}_\times(\psi) = \begin{pmatrix} -\sin\ 2\psi & \cos\ 2\psi & 0 \\ \cos\ 2\psi & \sin\ 2\psi & 0 \\ 0 & 0 & 0 \end{pmatrix} \tag{4.28}$$

We now define the basis $(O, \vec{e}_x, \vec{e}_y, \vec{e}_z)$ such that the interferometer is located at the origin O and has its two arms aligned with $\vec{e}_x$ and $\vec{e}_y$. An interferometer is only sensitive to a difference of length between its arms. Hence the matrix $\mathbf{D}$ for an interferometer in this basis is:

$$\mathbf{D} = \frac{1}{2}\left(\vec{e}_x \vec{e}_x - \vec{e}_y \vec{e}_y\right) \tag{4.29}$$

according to Eq. (4.17).

In order to calculate the detector pattern functions we must express $\mathbf{e}_\circ$, $\mathbf{e}_+$ and $\mathbf{e}_\times$ in the basis $(O, \vec{e}_x, \vec{e}_y, \vec{e}_z)$. We can perform the change of basis by rotating $\vec{e}_{x'}$, $\vec{e}_{y'}$ and $\vec{e}_{z'}$ around three different axis.

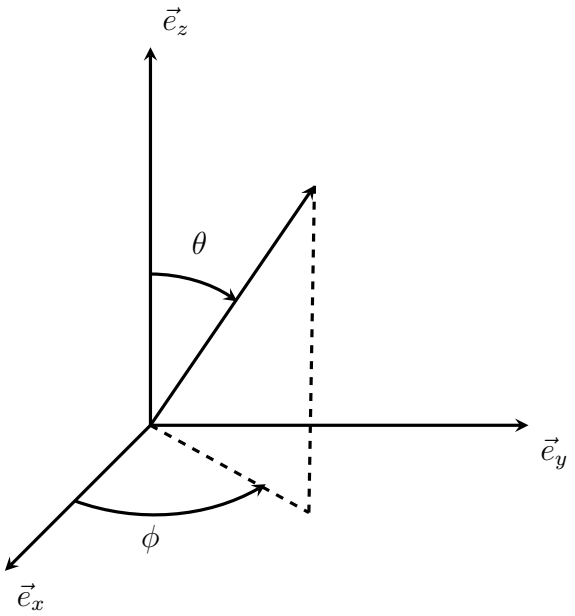

Figure 4.2: Rotation of the source position in the sky

First we find the matrix that allows us to express the propagation direction $\vec{e}_{z'}$ in the $(O, \vec{e}_x, \vec{e}_y, \vec{e}_z)$ basis. We define θ as the angle between $\vec{e}_{z'}$ and $\vec{e}_z$, and ϕ as the angle between $\vec{e}_x$ and the orthogonal projection of $\vec{e}_{z'}$ on the $\vec{e}_x\vec{e}_y$-plane. The vector $\vec{e}_{z'}$ is expressed in the interferometer basis via:

$$\mathbf{R} = \mathbf{R}_\phi \mathbf{R}_\theta = \begin{pmatrix} \cos\ \phi & \sin\ \phi & 0 \\ -\sin\ \phi & \cos\ \phi & 0 \\ 0 & 0 & 1 \end{pmatrix} \begin{pmatrix} \cos\ \theta & 0 & \sin\ \theta \\ 0 & 1 & 0 \\ -\sin\ \theta & 0 & \cos\ \theta \end{pmatrix} \tag{4.30}$$

Indeed, in the interferometer basis the expression of the propagation vector is given by $\mathbf{R}\vec{e}_{z'}$. Thus the expression of $\mathbf{e}_\circ$, $\mathbf{e}_+$ and $\mathbf{e}_\times$, which are tensors, in the interferometer basis are given by $\mathbf{R}\mathbf{e}_{\circ,+,\times}(\psi)\mathbf{R}^T$. We then find:

$$F_\circ = \mathbf{D} : \mathbf{e}_\circ(\psi) = -\frac{1}{2}\sin^2\theta\cos\ 2\phi \tag{4.31}$$

$$F_+ = \mathbf{D} : \mathbf{e}_+(\psi) = \frac{1}{2}\left(\cos^2\ \theta + 1\right)\cos\ 2\phi\ \cos\ 2\psi + \cos\ \theta\ \sin\ 2\phi\ \sin\ 2\psi \tag{4.32}$$

$$F_\times = \mathbf{D} : \mathbf{e}_\times(\psi) = -\frac{1}{2}\left(\cos^2\ \theta + 1\right)\cos\ 2\phi\ \sin\ 2\psi + \cos\ \theta\ \sin\ 2\phi\ \cos\ 2\psi \tag{4.33}$$

We see that an interferometer is blind to the isotropic mode if it travels along the direction perpendicular to the plane in which the detector lies. Considering $\theta = \pi/2$ the patterns functions of the isotropic polarization is maximum when $\phi = n\pi/2$, i.e. when the propagation axis and one of the arms of the interferometer are aligned.

With three detectors we can detect this isotropic polarization if they are not parallel to each other. Each interferometer sees the same gravitational wave with a different direction with respect to its arms, i.e. with different angles θ and ϕ. The angle ψ is the same for all interferometers and defines the amplitude of the $+$ and $\times$ polarizations. Let us choose $\psi = 0$. Then the antenna pattern functions of each interferometer is given by:

$$F_\circ = -\frac{1}{2}\sin^2\theta\cos\ 2\phi \tag{4.34}$$

$$F_+ = \frac{1}{2}\left(\cos^2\ \theta + 1\right)\cos\ 2\phi \tag{4.35}$$

$$F_\times = \cos\ \theta\ \sin\ 2\phi \tag{4.36}$$

The ideal situation is the following. One detector would see the isotropic polarization with its maximal amplitude : $\theta_1 = \pi/2$, $\phi = 0$. For this interferometer $F_\circ = -1/2$, $F_+ = 1/2$ and $F_\times = 0$. The observed signal of the first interferometer $S_1(t)$ is then given by:

$$S_1(t) = F_\circ S_\circ(t) + F_+ S_+(t) = -\frac{1}{2}S_\circ(t) + \frac{1}{2}S_+(t) \tag{4.37}$$

where $S_{\circ,+,\times}(t)$ are the temporal evolution of the amplitude of the corresponding polarization.

Still in the ideal situation, the two other detectors would be blind to the isotropic polarization. If we choose $\theta_{2,3} = 0$ then maximize the + response of the second detector and the $\times$ response of the third by setting $\phi_2 = 0$ and $\phi_3 = \pi/4$ respectively. This gives:

$$S_2(t) = F_\circ S_\circ(t) + F_+ S_+(t) + F_\times S_\times(t) = 0 + 1S_+(t) + 0 = S_+(t) \tag{4.38}$$

$$S_3(t) = F_\circ S_\circ(t) + F_+ S_+(t) + F_\times S_\times(t) = 0 + 0 + 1S_\times(t) = S_\times(t) \tag{4.39}$$

In this idealised situation the three signal observed would appear clearly as linearly independent.

4.1.3 Detection of the isotropic polarization

We now consider real interferometers: LIGO Hanford, LIGO Livingston and Virgo. The two LIGO interferometers are almost anti-parallel so the situation is far from ideal for polarization measurements. The location and orientation of the three observatories are

Detector	Latitude	Longitude	Azimuth	
			X Arm	Y Arm
LIGO Hanford	$46°27'19''N$	$119°24'28''W$	$N36°W$	$W36°S$
LIGO Livingston	$30°33'46''N$	$90°46'27''W$	$W18°S$	$S18°E$
Virgo	$43°37'53''N$	$10°30'16''E$	$N19°E$	$W19°N$

Figure 4.3: Coordinates and orientation of the three current gravitational waves detectors. Note on the azimuth: $N36°W$ means a direction between local North and West, 36 degrees away from North [33]

We must now find the relation between $(\phi_{Virgo}, \theta_{Virgo})$, $(\phi_{LLO}, \theta_{LLO})$ and $(\phi_{LHO}, \theta_{LHO})$. First we can express the unit vector corresponding to the propagation direction of the wave in a reference frame at Virgo location but with the x direction towards the North pole

$$\begin{pmatrix} \sin(\theta_{Virgo})\cos(\phi_{Virgo}) \\ \sin(\theta_{Virgo})\sin(\phi_{Virgo}) \\ \cos(\theta_{Virgo}) \end{pmatrix} \rightarrow \begin{pmatrix} \sin(\theta_{Virgo})\cos(\phi_{Virgo} - 19°) \\ \sin(\theta_{Virgo})\sin(\phi_{Virgo} - 19°) \\ \cos(\theta_{Virgo}) \end{pmatrix} \tag{4.40}$$

Now we will rotate the propagation direction of the wave so that we get the relative orientation of the propagation direction with respect to an interferometer located at LIGO Hanford

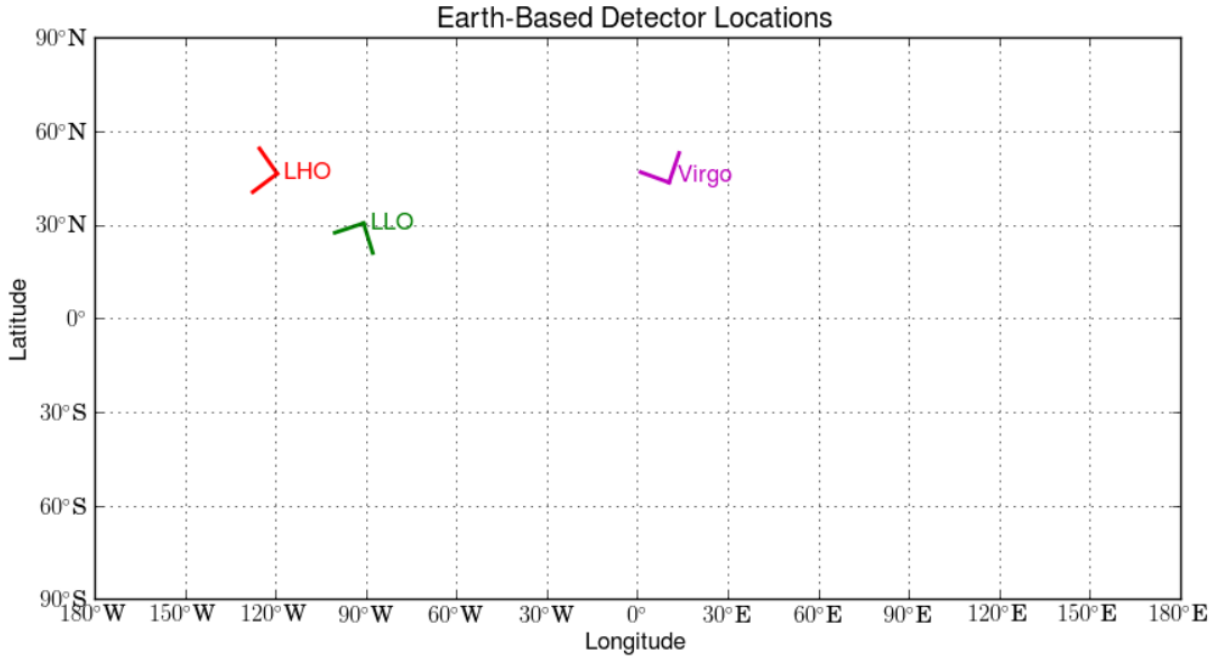

Figure 4.4: Location and orientation of LIGO and Virgo, from [33]. Note that the arm directions do not take into account any map projection effects, they simply indicate the direction of the arms relative to local north.

(resp. Livingston) but with its x arm pointing towards the North pole. This will be done in three steps. After these rotations we will correct the azimuth.

First we perform a rotation of the propagation direction in order to obtain the relative orientation of the wave with respect to an interferometer located at the Equator, at the same longitude as Virgo, with its x arm pointing towards the North pole. Then we perform a rotation that give us the propagation direction relative to an interferometer located at the Equator, at the same longitude as LIGO Handford (resp. Livingston) with its x arm pointing towards the North pole. The last rotation gives us the orientation of the propagation direction with respect to an interferometer at the same location as LIGO Hanford (resp. Livingston) but with its x arm pointing towards the North pole. These three rotations are given by:

$$\mathbf{R}_{Eq->LHO} = -\begin{pmatrix} \cos(l_{LHO}) & 0 & \sin(l_{LHO}) \\ 0 & 1 & 0 \\ -\sin(l_{LHO}) & 0 & \cos(l_{LHO}) \end{pmatrix} \tag{4.41}$$

$$\mathbf{R}_{Eq} = \begin{pmatrix} 1 & 0 & 0 \\ 0 & \cos(L_{LHO} - L_{Virgo}) & \sin(L_{LHO} - L_{Virgo}) \\ 0 & -\sin(L_{LHO} - L_{Virgo}) & \cos(L_{LHO} - L_{Virgo}) \end{pmatrix} \tag{4.42}$$

$$\mathbf{R}_{Virgo->Eq} = \begin{pmatrix} \cos(l_{Virgo}) & 0 & \sin(l_{Virgo}) \\ 0 & 1 & 0 \\ -\sin(l_{Virgo}) & 0 & \cos(l_{Virgo}) \end{pmatrix} \tag{4.43}$$

Taking into account the azimuth of Virgo and LIGO Handford (resp. Livingston) we find the

following relation between the propagation direction with respect to Virgo and LIGO Handford:

$$\begin{pmatrix} \sin(\theta_{LHO})\cos(\phi_{LHO}+36°) \\ \sin(\theta_{LHO})\sin(\phi_{LHO}+36°) \\ \cos(\theta_{LHO}) \end{pmatrix} = \mathbf{R}_{Eq->LHO}\mathbf{R}_{Eq}\mathbf{R}_{Virgo->Eq} \begin{pmatrix} \sin(\theta_{Virgo})\cos(\phi_{Virgo}-19°) \\ \sin(\theta_{Virgo})\sin(\phi_{Virgo}-19°) \\ \cos(\theta_{Virgo}) \end{pmatrix} \tag{4.44}$$

with and $l_{Virgo} \simeq 43.6314°$, $l_{LHO} \simeq 46.4553°$, $L_{Virgo} \simeq 10.5044°$ and $L_{LHO} \simeq -119.4078°$. For the observatory located at Livingston $l_{LLO} \simeq 30.5628°$, $L_{LLO} \simeq -90.7714$ and $+36° \rightarrow +108°$. From equation (4.44) we can find the angle ϕ_{LHO}, θ_{LHO}, ϕ_{LLO} and θ_{LLO} as functions of ϕ_{Virgo} and θ_{Virgo}. Thus we can easily compute the antenna pattern functions of $LIGO$ and $Virgo$ as functions of the two angle associated to Virgo. The absolute value of the antenna pattern function of the isotropic polarization of each observatory is plotted in Fig. 4.5, 4.6 and 4.7, as function of ϕ_{Virgo} and θ_{Virgo}. The amplitude of the polarization is set to unity: $S_\circ(t) = 1$.

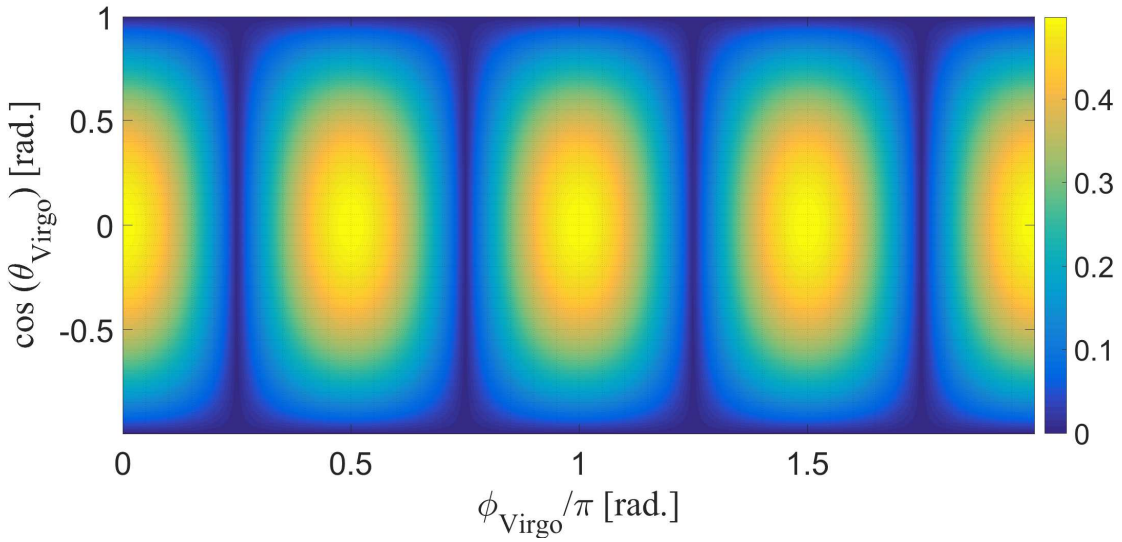

Figure 4.5: Virgo : Antenna pattern function of the isotropic polarization.

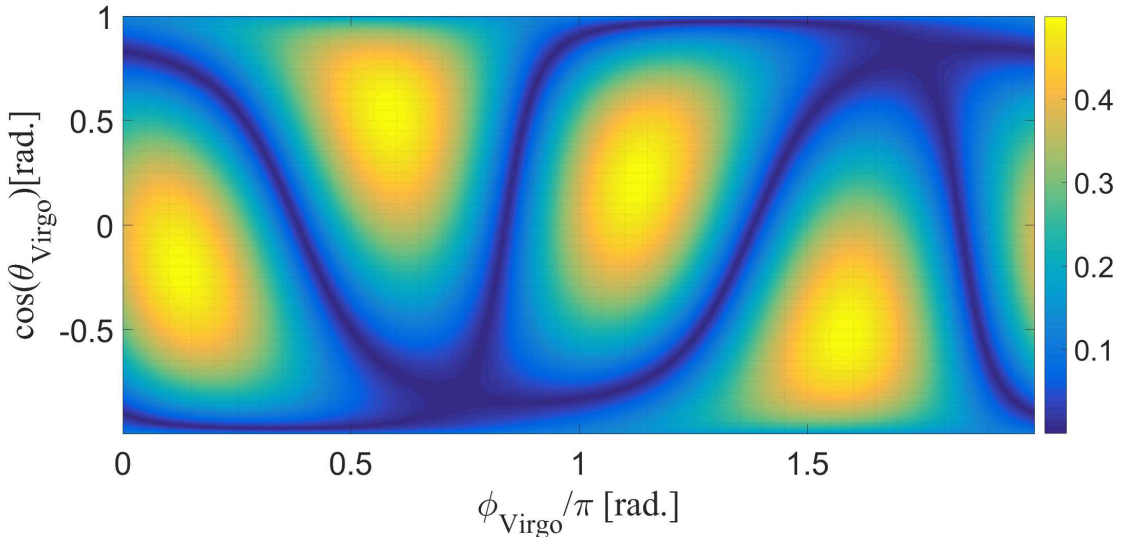

Figure 4.6: LIGO Hanford : Antenna pattern function of the isotropic polarization.

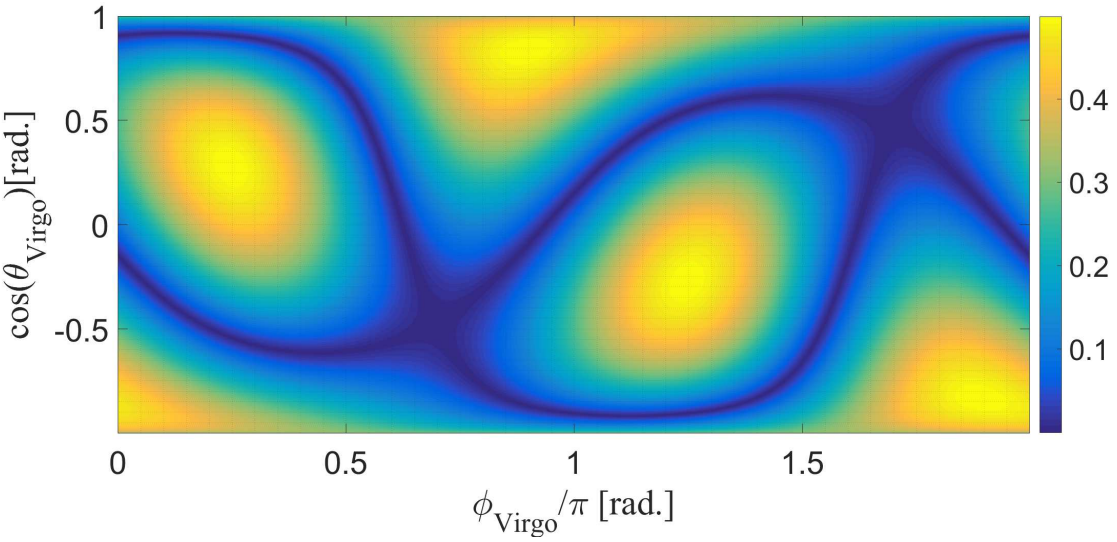

Figure 4.7: LIGO Livingston : Antenna pattern function of the isotropic polarization.

We see on Fig. 4.5, 4.6 and 4.7 the antenna patterns functions of each interferometers. The antenna pattern functions corresponding to the + and × polarizations can be found in the appendix. We want to know if there is a propagation direction that allows the three interferometers to detect the isotropic polarizations with a high amplitude.

In Fig. 4.8, we can see the sum of the square of the amplitude $F_\circ$ of each interferometers normalized by a factor $\sqrt{3}$.

$$F \equiv \frac{F^2_{\circ Virgo} + F^2_{\circ LHO} + F^2_{\circ LLO}}{3} \tag{4.45}$$

This facilitates the identification of propagation directions for which the response of the whole system $LIGO - Virgo$ is maximum. We see that there are four local maxima. The location of these maxima and the corresponding amplitudes are summarized in the table 4.3.

We can now study the linear dependence of the three interferometer antenna pattern functions in order to determine whether or not the new isotropic polarization could be identified. The response of the three interferometers can be written:

$$\begin{pmatrix} S_{Virgo}(t) \\ S_{LHO}(t) \\ S_{LLO}(t) \end{pmatrix} = S_\circ(t) \begin{pmatrix} F_{\circ Virgo} \\ F_{\circ LHO} \\ F_{\circ LLO} \end{pmatrix} + S_+(t) \begin{pmatrix} F_{+Virgo} \\ F_{+LHO} \\ F_{+LLO} \end{pmatrix} + S_\times(t) \begin{pmatrix} F_{\times Virgo} \\ F_{\times LHO} \\ F_{\times LLO} \end{pmatrix} \tag{4.46}$$

where

$$\vec{F}_\circ = \begin{pmatrix} F_{\circ Virgo} \\ F_{\circ LHO} \\ F_{\circ LLO} \end{pmatrix}, \quad \vec{F}_+ = \begin{pmatrix} F_{+Virgo} \\ F_{+LHO} \\ F_{+LLO} \end{pmatrix}, \quad \vec{F}_\times = \begin{pmatrix} F_{\times Virgo} \\ F_{\times LHO} \\ F_{\times LLO} \end{pmatrix} \tag{4.47}$$

are three vectors in a three dimensional vectorial space with three basis vectors that correspond to a unit signal measured at Virgo, LIGO Hanford and LIGO Livingston respectively. Each vector of (4.47) characterises the response of the system composed of the three interferometers to a particular polarization. We want to know whether some directions of propagation of gravitational waves with respect to the three observatories produce three responses (one for each

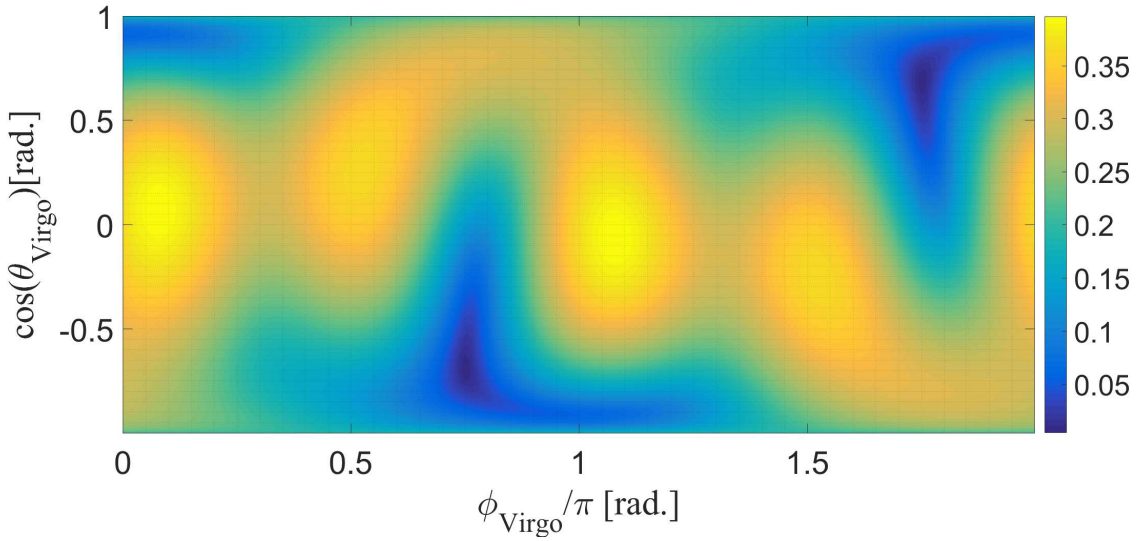

Figure 4.8: Map of $F \equiv \sqrt{F_{\circ Virgo}^2 + F_{\circ LHO}^2 + F_{\circ LLO}^2}/\sqrt{3}$. The factor $\sqrt{3}^{-1}$ is present so that the value plotted on the map represents the amplitude of the isotropic polarization that would be seen by one interferometer if all the interferometers measure this polarization with the same amplitude.

polarization) of the system that are linearly independent. Hence we want some measure of the linear dependence of the three vectors of (4.9) as a function of ϕ_{Virgo} and θ_{Virgo}.

Three vectors in a three-dimensional space are linearly independent if and only if the determinant of the matrix with each column that corresponds to one of these three vectors is different from zero. If we normalize the three vector then the determinant can take value between 0 and 1. The case $det = 1$ corresponds to an orthogonal basis. In our case we write:

$$D\left(\phi_{Virgo}, \theta_{Virgo}\right) \equiv \frac{1}{\| \vec{F}_\circ \| \| \vec{F}_+ \| \| \vec{F}_\times \|} det \left[\begin{pmatrix} F_{\circ Virgo} & F_{+Virgo} & F_{\times Virgo} \\ F_{\circ LHO} & F_{+LHO} & F_{\times LHO} \\ F_{\circ LLO} & F_{+LLO} & F_{\times LLO} \end{pmatrix} \right] \tag{4.48}$$

The value of $D\left(\phi_{Virgo}, \theta_{Virgo}\right)$ is plotted in Fig. 4.9. We see that, expect two regions located approximately at $\phi_{Virgo} = \pi/4$ and $\phi_{Virgo} = 5\pi/4$ and some meanders linked to them, all the directions gives a value of $D > 0.3$ approximately.

We would like to know if the regions where the isotropic polarization is detected with a high amplitude correspond to regions where the response to this polarization is linearly independent from the two polarizations $+$ and $\times$. In table 4.10 are the values of $F_\circ$ for each interferometer and D, at the center of each region corresponding to a local maximum of F. We see that two maxima correspond to $D \sim 0.1$ and the two others correspond to $D \sim 0$. Hence the three interferometers don't seem well suited for polarization measurements but it doesn't seem impossible either. A more detailed analysis of the interferometer responses, including noise for example, would be needed. In addition, for long signals the rotation of the Earth could help to increase the linear independence of the response but this also requires a deeper analysis beyond the scope of this thesis.

So far we have assumed that we know precisely the propagation direction of the wave. This is far from true when there is no electromagnetic counter part. Unfortunately only neutron star

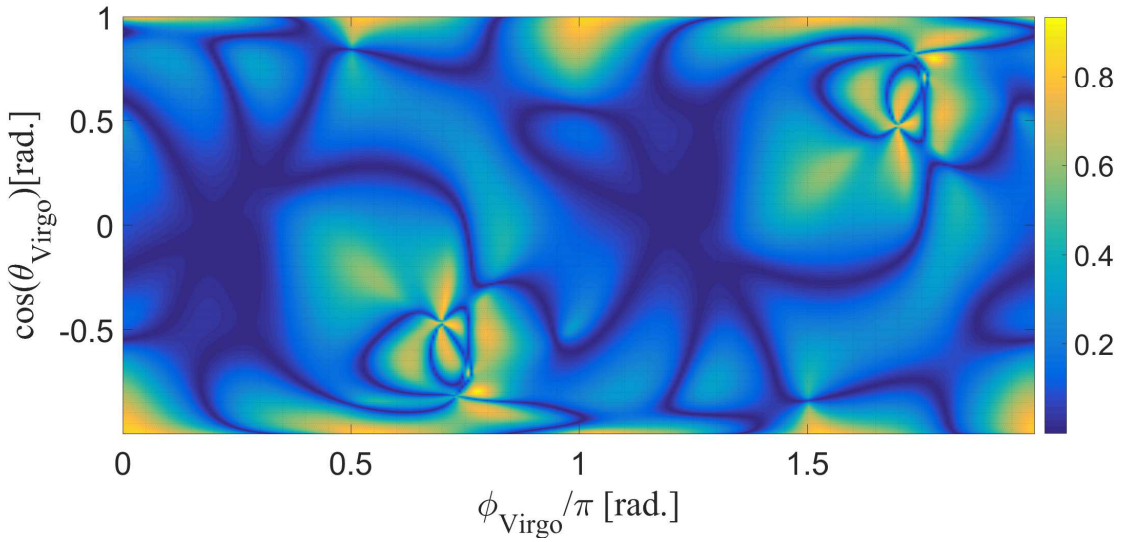

Figure 4.9: Absolute value of $D\left(\phi_{Virgo}, \theta_{Virgo}\right)$, the determinant of the three polarization vectors as a function of the propagation axis direction (θ, ϕ) with respect to Virgo's arms.

	$\sqrt{\frac{F_{\circ Virgo}^2+F_{\circ LHO}^2+F_{\circ LLO}^2}{3}}$	$F_{\circ Virgo}$	$F_{\circ LHO}$	$F_{\circ LLO}$	D
$\phi_{Virgo} = 0.07639\pi$ $\cos\left(\theta_{Virgo}\right) = 0.07074$	0.3962	0.4413	0.4472	0.2759	0.08464
$\phi_{Virgo} = 0.522\pi$ $\cos\left(\theta_{Virgo}\right) = 0.2579$	0.3649	0.4623	0.4084	0.1374	0.02207
$\phi_{Virgo} = 1.076\pi$ $\cos\left(\theta_{Virgo}\right) = -0.06915$	0.3962	0.4421	0.4474	0.2742	0.08446
$\phi_{Virgo} = 1.522\pi$ $\cos\left(\theta_{Virgo}\right) = -0.2563$	0.4629	0.4072	0.1389	0.3649	0.02377

Figure 4.10: Propagation directions corresponding to local maxima of $LIGO - Virgo$ response and the amplitude seen by each interferometer.

mergers produce electromagnetic counterpart that we can detect. Currently, only two of these mergers have been detect by gravitational wave observations as can be seen in Fig. 4.11. The scarcity of these detections reduces the probability to observe a neutron star mergers well oriented for polarization measurements. The forthcoming new interferometers will solve this issue.

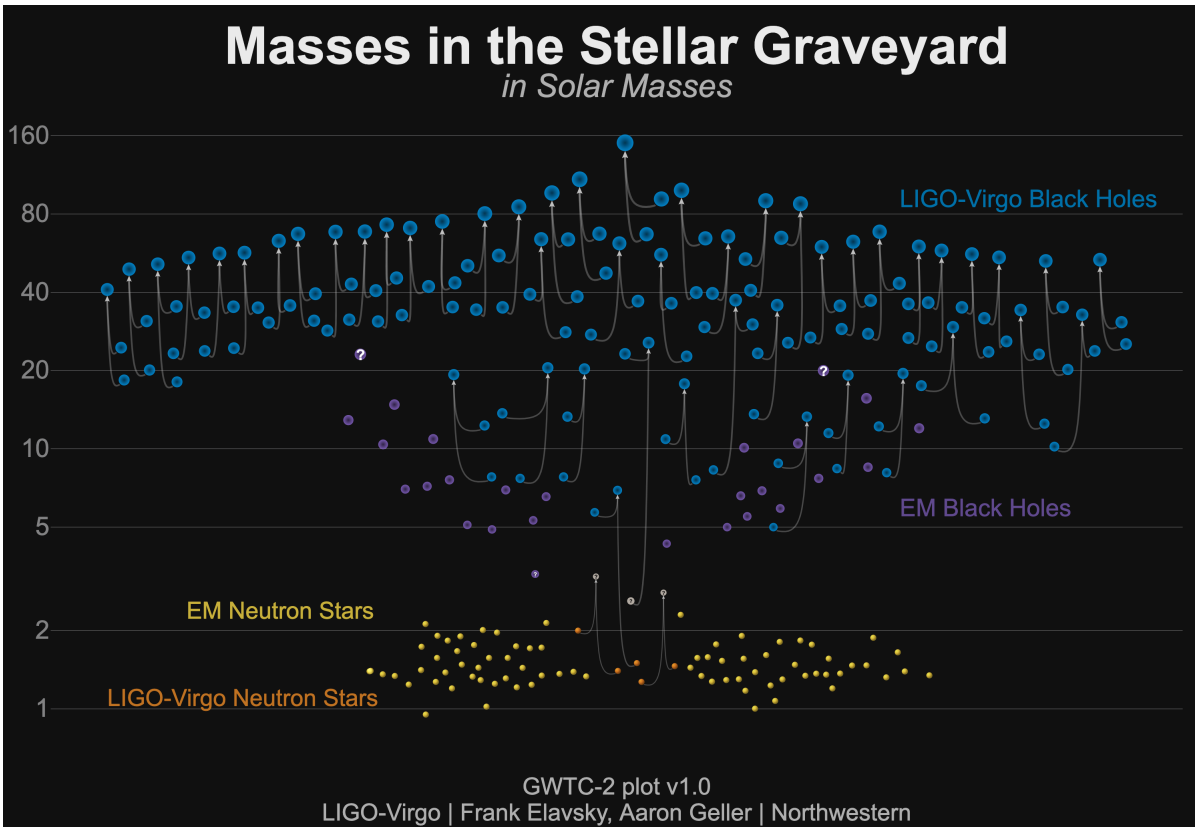

Figure 4.11: Masses of detected LIGO/Virgo compact binaries. Neutron stars detected by gravitational waves are represented by orange dots. From [34].

4.2 Massive modes

The massive modes are expected to be undetectable due to their possibly very high frequency and the power law decrease of their amplitude as discussed in chapter 2 and 3 respectively. However, we made a lot of simplifying hypotheses and we don't know whether other hypotheses on the extra dimensions could lead to detectable waves with a longitudinal polarization similar to the polarization of the massive modes in our simplified theory. Hence it can be interesting to look for other polarizations before worrying about which modified theory can produce them.

Generically a four by four space-time metric can have six polarizations. In addition to the three mode $\circ, +, \times$ are a longitudinal scalar mode L and two vectorial mode X, Y. Their patterns functions are given by [35]:

$$F_L = \frac{1}{2}\sin^2\ \theta\ \cos\ 2\phi \tag{4.49}$$

$$F_X = -\sin\ \theta\,(\cos\ \theta\ \cos\ 2\phi\ \cos\ 2\psi + \sin\ 2\phi\ \sin\ \psi) \tag{4.50}$$

$$F_Y = -\sin\ \theta\,(-\cos\ \theta\ \cos\ 2\phi\ \sin\ 2\psi + \sin\ 2\phi\ \cos\ \psi) \tag{4.51}$$

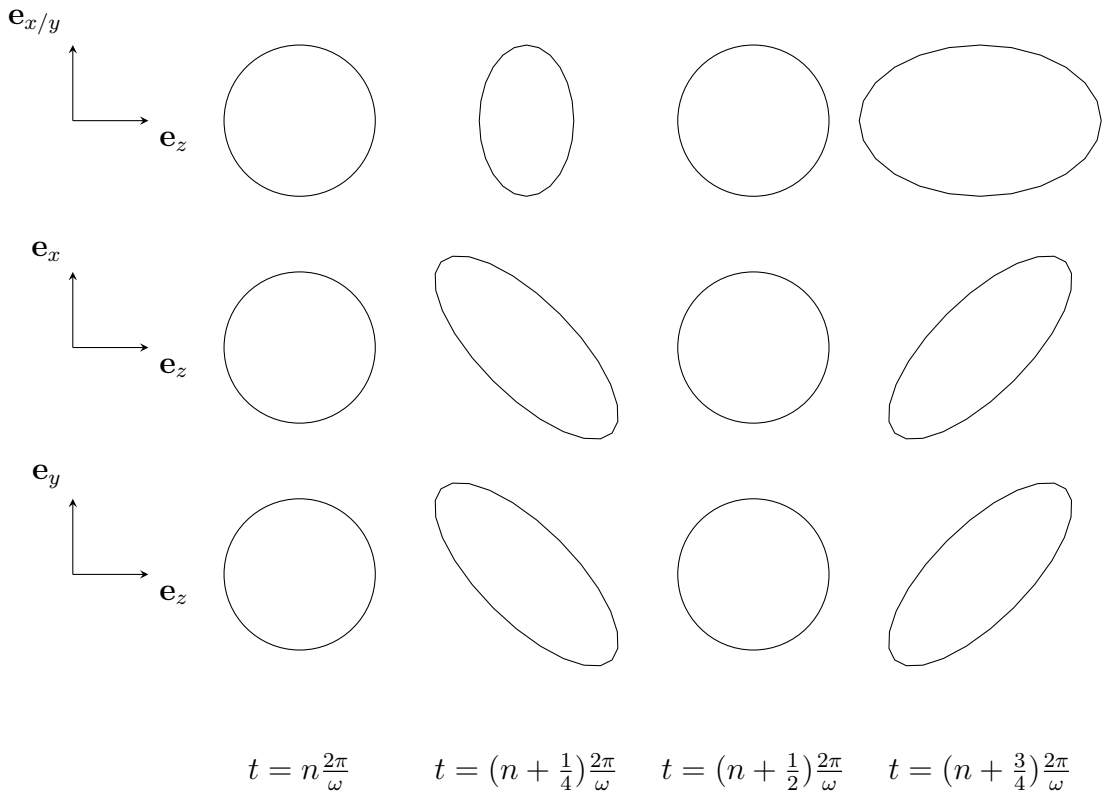

Figure 4.12: One period of the h_L (upper), the h_X (middle) and the h_Y (lower) modes

4.3 Polarization measurements

If we want to determine the presence of more polarizations than the two predicted by General Relativity we need at least five detectors. Indeed, the output signal of one interferometer is given by:

$$h(t) = F_\circ h_\circ(t) + F_L h_L(t) + F_X h_X(t) + F_Y h_Y(t) + F_+ h_+(t) + F_\times h_\times(t) + n(t) \tag{4.52}$$

where $n(t)$ is the noise. The signal $h(t)$ is thus a basis of patterns functions. The patterns functions $F_\circ$ and F_L are linearly dependent because they have the same analytical expression with opposite signs. The patterns functions basis is thus 5 dimensional.

If we assume that we know the location in the sky of the source from an electromagnetic counterpart, we know how to shift in time the signals of a set of N interferometers. Thus we can write:

$$\vec{h}(t) = \mathbf{F} \cdot \vec{h}_{pol}(t) + \vec{n}(t) \tag{4.53}$$

with

$$\vec{h}(t) = \begin{pmatrix} h_1(t) \\ h_2(t) \\ \vdots \\ h_N(t) \end{pmatrix} \qquad \vec{h}_{pol}(t) = \begin{pmatrix} h_\circ(t) \\ h_L(t) \\ \vdots \\ h_\times(t) \end{pmatrix} \qquad \vec{n}(t) = \begin{pmatrix} n_1(t) \\ n_2(t) \\ \vdots \\ n_N(t) \end{pmatrix} \tag{4.54}$$

and

$$\mathbf{F} = \begin{pmatrix} F_{\circ 1} & F_{L1} & F_{X1} & F_{Y1} & F_{+1} & F_{\times 1} \\ F_{\circ 2} & F_{L2} & F_{X2} & F_{Y2} & F_{+2} & F_{\times 2} \\ : & : & : & : & : & : \\ F_{\circ N} & F_{LN} & F_{XN} & F_{YN} & F_{+N} & F_{\times N} \end{pmatrix} \tag{4.55}$$

In order to determine the full composition of the signal in the five polarizations modes one needs at least five interferometers so that the matrix $\mathbf{F}$ can be inverted. With a high quality signal one can thus detect and measure all polarizations in principle.

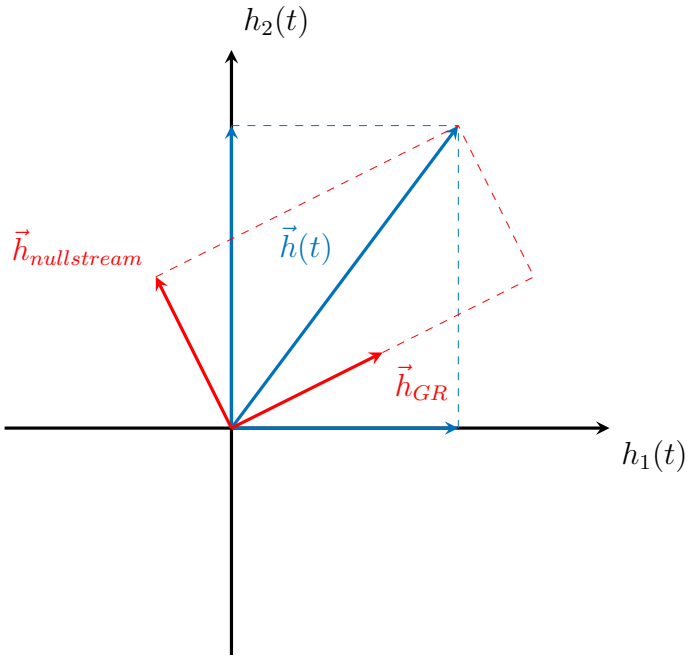

Figure 4.13: Representation of the signal measured by two interferometer in a two dimensional vectorial space. This vectorial space is a subspace of the five dimensional vectorial space of polarization and it is given by the antenna pattern functions of the two interferometers. $\vec{h}_{nullstream}$ is the projection of the signal on the null stream vector $\vec{e}_{nullstream}$. $\vec{h}_{GR}$ is the projection of the signal on the subspace containing only the + and × polarizations.

A way to separate the signal from the noise in gravitational wave data is the null stream method. We have seen that there are five linearly independent antenna pattern functions. The signal observed by an interferometer $\vec{h}(t)$ thus belongs to a vectorial space with five functions as basis vectors. The idea is to project the vector $\vec{h}(t)$ onto a subspace orthogonal to some polarizations. This can be used with less than 5 detectors to test the presence of new polarizations without knowing precisely the composition of the gravitational wave signal in term of polarizations, as explained in the following.

Currently, only three interferometers are operational the two that constitute LIGO and Virgo. The two LIGO interferometers are antiparallel and thus are equivalent to one detector as far as polarization measurements are concerned. Despite the fact that gravitational wave events are observed with fewer than five interferometers, we can use the null-stream method to search for new polarizations. With this method one can project the data on a subspace orthogonal to the plane determined by the basis function F_+ and $F_\times$. Indeed, with two interferometer the system of equations (4.53) becomes:

$$\begin{pmatrix} h_1(t) \\ h_2(t) \end{pmatrix} = \begin{pmatrix} F_{\circ 1} & F_{L1} & F_{X1} & F_{Y1} & F_{+1} & F_{\times 1} \\ F_{\circ 2} & F_{L2} & F_{X2} & F_{Y2} & F_{+2} & F_{\times 2} \end{pmatrix} \begin{pmatrix} h_\circ(t) \\ h_L(t) \\ h_X(t) \\ h_Y(t) \\ h_+(t) \\ h_\times(t) \end{pmatrix} \tag{4.56}$$

The signal $\vec{h}(t)$ in the five dimensional vectorial space of polarizations is projected onto a two dimensional plane corresponding to the LIGO and Virgo response. Hence we can define the vector $\vec{e}_{nullstream}$ in the polarization vectorial space such that $\vec{e}_{nullstream} \cdot \vec{e}_+ = \vec{e}_{nullstream} \cdot \vec{e}_\times = 0$. The vectors $\vec{e}_+$ and $\vec{e}_\times$ are the two basis vectors of the five dimensional vectorial space that correspond to the + and × polarizations respectively.

The projection of the signal $\vec{h}(t)$ on $\vec{e}_{nullstream}$ should be constituted only of noise if the gravitational wave is composed only of the two polarizations of General Relativity. If there was no noise the projection on $\vec{e}_{nullstream}$ would be zero in the theory of General Relativity. That's why it is called "null stream".

If the projected signal is significantly different from the noise projection on the null stream vector it means that other polarizations are present in the wave. A similar method (the null energy method) was used in [36] for the signal GW170817. The results are in favor of the presence only of the two polarizations predicted by General Relativity with a p-value of 0.315.

Another way to test for the presence of other polarizations is to perform a coherent Bayesian analysis of a GW signal. This consists in the comparison of the probability that one model generates the data observed and the probability that another model generates the same data. The comparison is given by the Bayes factor:

$$K = \frac{\mathcal{P}(D|M_1)}{\mathcal{P}(D|M_2)} \tag{4.57}$$

where $\mathcal{P}(D|M_1)$ and $\mathcal{P}(D|M_2)$ are the probabilities that the data D is produces by the models M_1 and M_2 respectively.

This is was done in [37] and [38] for the signals GW170814 and GW170817 respectively. They both compared the case with only the two tensor modes to the case with the two vector modes only and the two scalar modes only. Both results are in favor of General Relativity. In [37], the tensor case vs the vector case gives a Bayes factor of more than 200 and for the tensor case vs the scalar case the Bayes factor is 1000. In [38], the results are more precise due to the determination of the sky position of the event thanks to its electromagnetic counterpart. The Bayes factors are $10^{20.81 \pm 0.08}$ and $10^{23.09 \pm 0.08}$ for the tensor vs vector case and the tensor vs scalar case respectively.

Conclusion

We have seen that the introduction of extra dimensions is motivated by the "Kaluza-Klein miracle". However there are lots of possibilities for a theory of physics implying extra dimensions. In addition, N dimensional physics is not intuitive at all. So it is very hard to select a criterion to prefer a specific theory with respect to another. On the other hand, if one wants to keep a general reasoning, calculations get very quickly hard to handle especially geometrodynamics calculations as can be seen by looking at the equations in the first chapter. For this reason we imposed many simplifying hypotheses. The theory we analysed is thus a toy model to get an idea of the consequences of adding extra dimensions. However assuming a constant warp factor is a strong simplification and it would be interesting to analyse the non constant case.

In our simplified theory, the new features are intuitive despite the fact that the extra dimensions are not: the traceless condition extends to more spatial dimensions allowing a transverse isotropic polarization and waves travelling partially in the extra dimensions are seen as massive modes simply because we perceive only some component of their velocity in the D dimensional space-time. Unfortunately the power law decreasing amplitude of the massive mode and their probably too high frequencies implies that they are not very interesting in view of searching for new physics from gravitational wave observations. However, more complex theories with extra dimensions could lead to non vanishing massive modes and that is why looking for new polarizations is interesting.

Currently there are only few constraints on polarization due to the low number of observatories as explained. The new interferometers will not only allows to test more precisely the polarizations but they will also increase the diversity of the sources observed (and obviously increase the number of observations).

Among the next generation of ground-based interferometers is the Einstein telescope [39]. The telescope will have a much higher sensitivity than the current observatories LIGO and Virgo. The reasons of this higher sensitivity are the length of the arms on the one hand and new technologies to reduce the different sources of noise on the other hand. The arms of the Einstein telescope will measure 10 km in length. For comparison Virgo arms measure 3 km in length. This increased sensitivity with respect to the second generation of ground-based interferometers will allow to observed earlier epochs of the universe as seen in Fig. 4.14 The Einstein telescope will be able to observe the entire spectrum of stellar and intermediate black holes and determine their stellar or primordial origin. It will also detect neutron star inspirals and tidal effects. The observatory will be sensitive to higher and lower frequencies than LIGO and Virgo. The first observations are expected in 2035.

LIGO-India [40] is an improved version of the advanced LIGO observatory. The arm length will be the same as for LIGO. Thus the improvements concern the technologies of noise reduction [41]. The main purpose of this telescope is to extend the gravitational wave detector network in order to improve the sky location determination and polarization measurements.

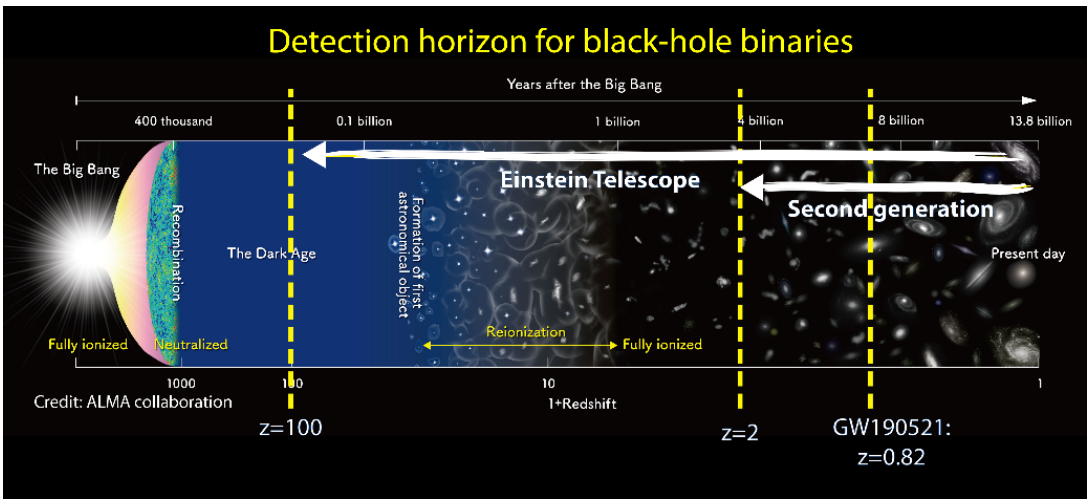

Figure 4.14: Epochs of the Universe that will be observed by the Einstein telsecope, from [39]

The Japanese telescope KAGRA [42] is already built. The telescope started its operations in 2020. However the sensitivity of KAGRA needs to be improved through real time debugging before reaching the expected sensitivity. The observatory is thus less sensitive than LIGO and Virgo for now. The length of the arms of KAGRA is 3 km. The telescope is thus similar to Virgo. As for LIGO India the improvements with respect to the second generation of detectors concerns not only the noise reduction technologies, but also cryogeny, and a location underground.

Cosmic Explorer [43] is a future third generation U.S. ground-based detector. Its arms will be 40 km in length. These are 10 times longer than the arms of LIGO. Hence the sensitivity of Cosmic Explorer will be much higher than LIGO's.

The LISA interferometer [44] is a space-borne gravitational wave detector led by ESA and an international scientific consortium. It will observe gravitational waves with frequencies between 0.1 mHz and 1 Hz. These frequencies correspond to sources with a wider orbit than those we can detect with ground-based observatories. These sources are potentially much heavier also. Hence LISA will be able to detect supermassive black hole mergers. The observatory is expected to be launched in the early 2030s.

The need for different gravitational waves observatories to measure polarization comes from the necessity to observe a signal with different orientation with respect to the detectors. However, as the Earth rotates on itself, the ground-based observatories rotate with it. Hence, for a long enough signal, the interferometer relative orientation can change significantly.

The time until coalescence of a binary system is given in [45]:

$$\tau_c = \frac{5}{256\eta}\frac{GM}{c^3}\left(\frac{\pi G M f_0}{c^3}\right)^{-8/3} \tag{4.58}$$

where $\eta = \mu/M$ is the symmetric mass ratio and f_0 is the initial frequency of the gravitational wave emitted by the binary system. M is the total mass of the system $m_1 + m_2$ and μ is the reduced mass:

$$\mu = \frac{m_1 m_2}{m_1 + m_2} \tag{4.59}$$

We see from Eq. (4.58) that the time until coalescence decrease with the mass of the total mass of the system M. Thus longer signal are from neutron star binaries. For two neutron star of mass 1.5 $M_\odot$ for example and starting with a frequency $f_0 = 10Hz$ that corresponds to the lower bond of current interferometers we find:

$$\tau_c \simeq 900\ s \tag{4.60}$$

This corresponds to approximately 15 minutes. The interferometer will not rotates significantly with respect to the gravitational wave. However τ_c is very sensitive to the initial frequency value f_0. If we consider now a signal stating with 1 Hz that would be detectable by the Einstein detector in principle, we find:

$$\tau_c \simeq 4 \cdot 10^5 s \tag{4.61}$$

This corresponds to approximately 110 hours. We see that neutron star inspiral signals can be very long if we can detect them at frequencies between 1 and 10 Hz. This duration would lead to a significant variation of the sky position of the source for the same interferometer.

Eventually massless new polarizations are of particular interest for future observations. The origin of the isotropic mode is the relaxation of the traceless condition on the two spatial component in the plane transverse to the propagation. This is a direct effect of the introduction of new dimensions that has nothing to do with the physics in these dimensions. Thus we expect that any theory with gravity in extra dimensions should present such new polarizations and we can expect them to have an amplitude similar to the tensor massless mode we already detected. Hence, the construction of new interferometers in the following years or decades will gives us key results on the existence of extra dimensions.

Appendix

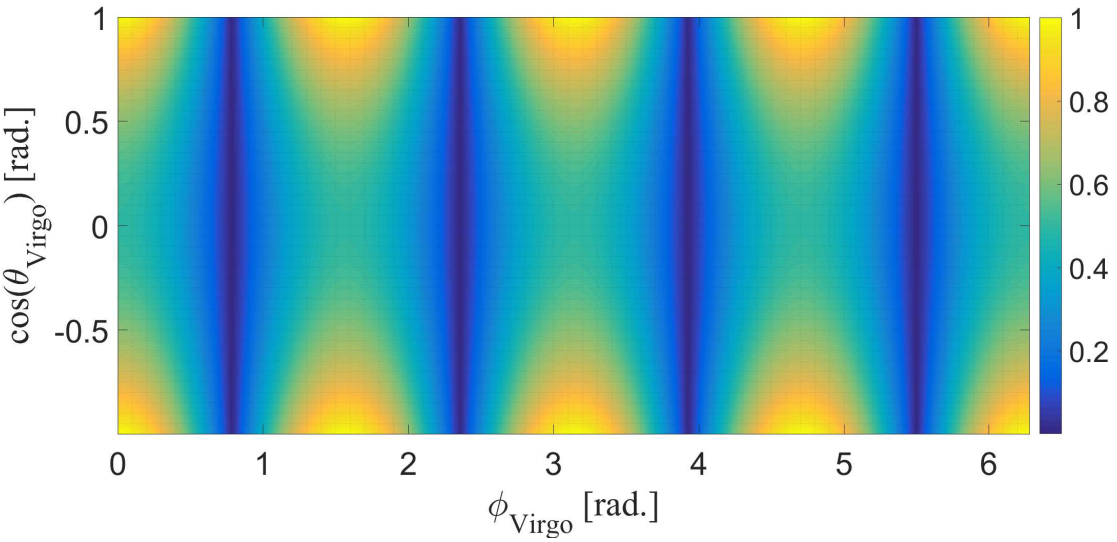

Figure 4.15: Absolute value of the F_+ antenna pattern function of Virgo

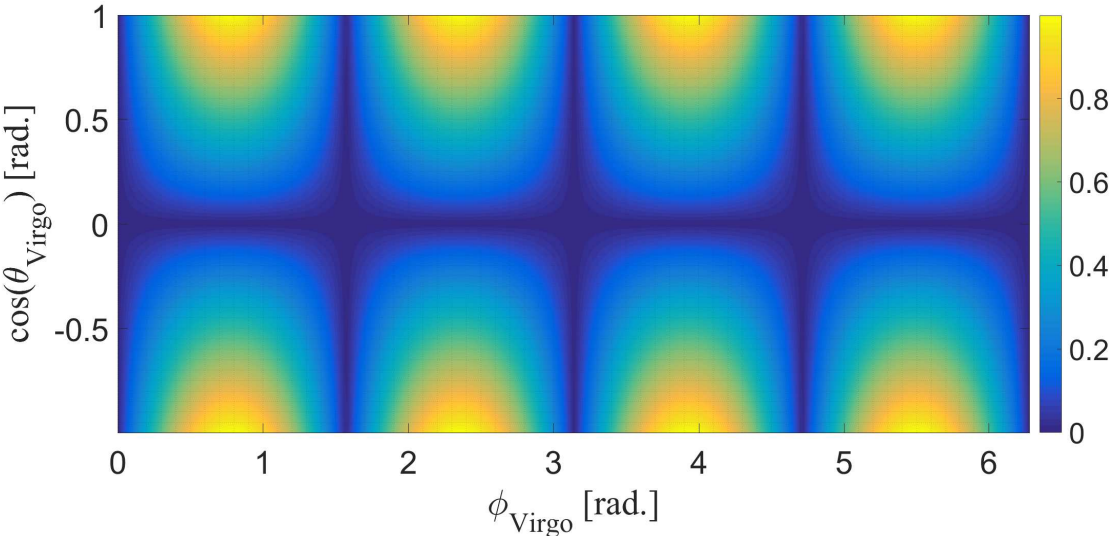

Figure 4.16: Absolute value of the $F_\times$ antenna pattern function of Virgo

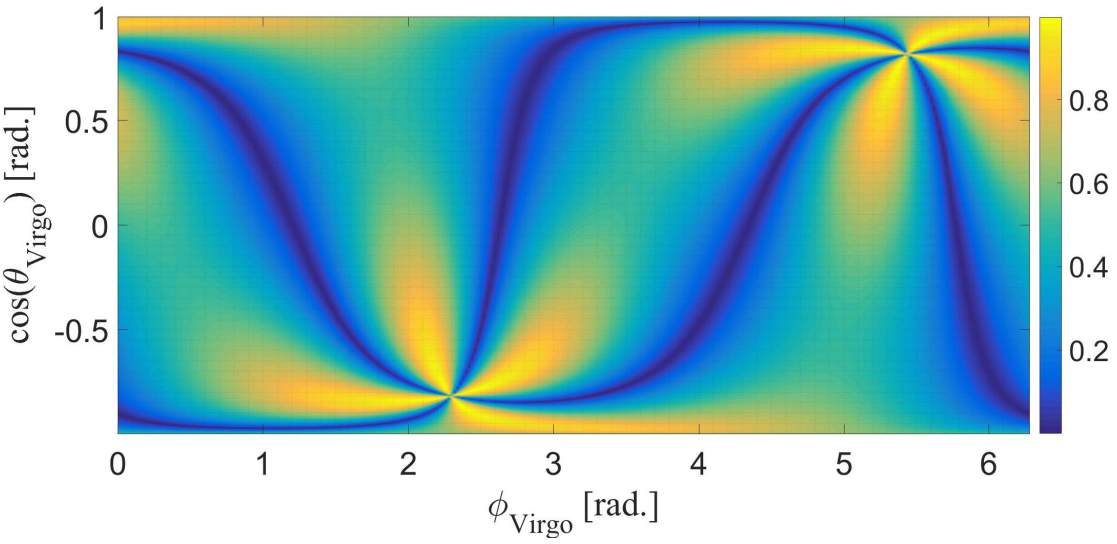

Figure 4.17: Absolute value of the F_+ antenna pattern function of LIGO Hanford

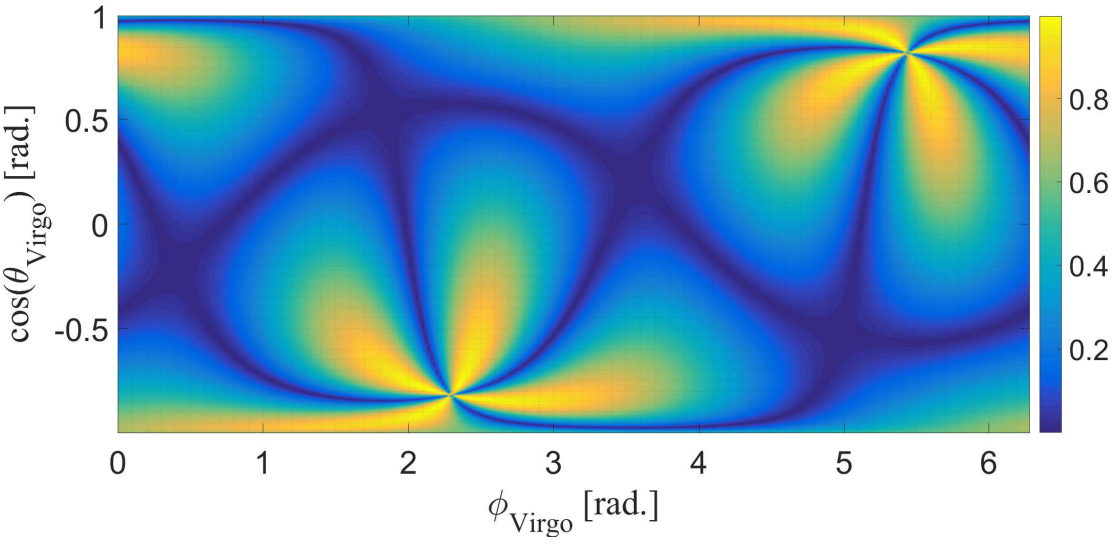

Figure 4.18: Absolute value of the $F_\times$ antenna pattern function of LIGO Hanford

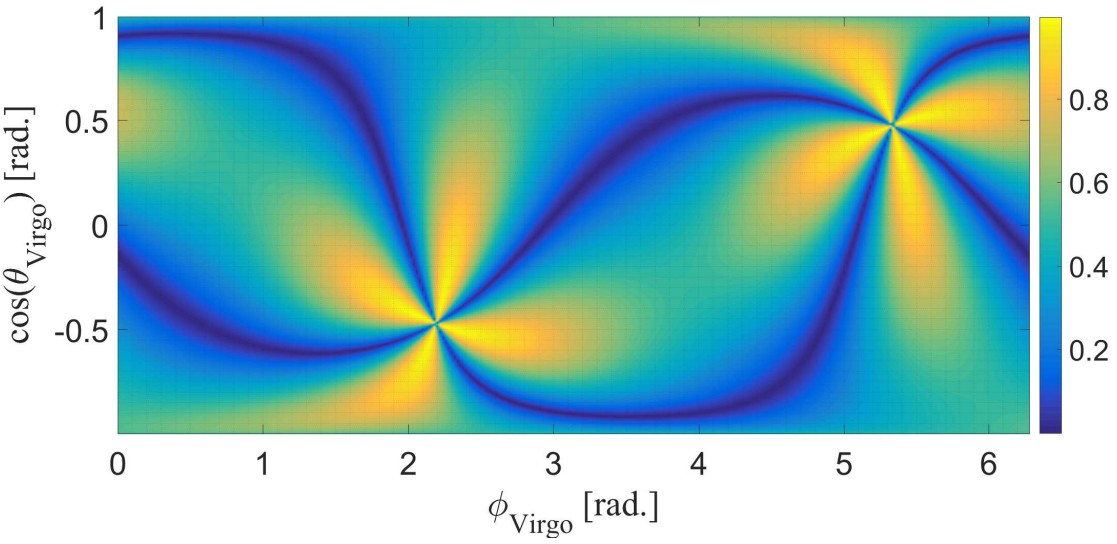

Figure 4.19: Absolute value of the F_+ antenna pattern function of LIGO Livingston

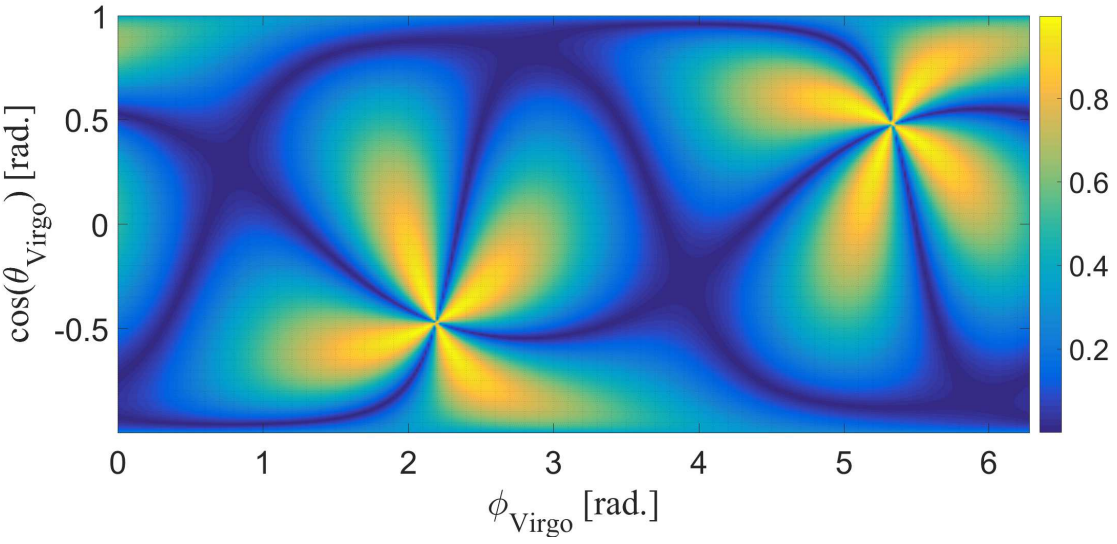

Figure 4.20: Absolute value of the $F_\times$ antenna pattern function of LIGO Livingston

Bibliography

[1] Jorge Cervantes-Cota, Salvador Galindo-Uribarri, and George Smoot. A Brief History of Gravitational Waves. *Universe*, 2(3):22, Sep 2016. ISSN 2218-1997. doi: 10.3390/universe2030022. URL `http://dx.doi.org/10.3390/universe2030022`.

[2] The Nobel Commitee for Physics. The laser interferometer gravitational-wave observatory and the first direct observation of gravitational waves, 2017. https://www.nobelprize.org/uploads/2018/06/advanced-physicsprize2017-1.pdf.

[3] Albert Einstein. Zur Elektrodynamik bewegter Körper. *Annalen Phys*, 17:891–821, 1905.

[4] Henri Poincaré. Sur la dynamique de l'électron. *Comptes rendus de l'Académie des sciences*, 140:1504–1508, 1905.

[5] Albert Einstein. *The Collected Papers of Albert Einstein. The Berlin Years: Correspondence, 1914-1918*, volume 8. Robert Schulmann and Martin J. Klein, July 1998. ISBN 9780691048413. (German) Available at: https://einsteinpapers.press.princeton.edu/vol8-trans/224.

[6] Albert Einstein. *The Collected Papers of Albert Einstein. The Berlin Years: Writings, 1914-1917*, volume 6. Robert Schulmann and Martin J. Klein, July 1996. ISBN 9780691010861. (German) Available at: https://einsteinpapers.press.princeton.edu/vol6-doc/.

[7] Albert Einstein. *The Collected Papers of Albert Einstein. The Berlin Years: Writings, 1918-1921*, volume 7. Robert Schulmann and Martin J. Klein, July 2002. ISBN 9780691057187. (German) Available at: https://einsteinpapers.press.princeton.edu/vol7-doc/.

[8] Daniel Kennefick. Einstein versus the physical review. *Physics Today - PHYS TODAY*, 58, 09 2005. doi: 10.1063/1.2117822.

[9] Dean Rickles Cécile M. DeWitt. *The Role of Gravitation in Physics, Report form the 1957 Chapel Hill Conference*. 2011. ISBN 3945561299. Available at : https://edition-open-sources.org/sources/5/index.html.

[10] J. Weber. Evidence for discovery of gravitational radiation. *Phys. Rev. Lett.*, 22:1320–1324, Jun 1969. doi: 10.1103/PhysRevLett.22.1320. URL `https://link.aps.org/doi/10.1103/PhysRevLett.22.1320`.

[11] J.H. Taylor, L.A. Fowler, and P.M. McCulloch. Measurements of general relativistic effects in the binary pulsar psr1913+16. *Nature*, 277:437–440, Feb 1979. doi: https://doi.org/10.1038/277437a0.

[12] M.E. Gertsenshtein and V.I. Pustovoit. On the detection of low frequency gravitational waves. *Sov. J. Exp. Theor. Phys.*, 43:605–607, 1962.

[13] Robert L. Forward. Wideband laser-interferometer graviational-radiation experiment. *Phys. Rev. D*, 17:379–390, Jan 1978. doi: 10.1103/PhysRevD.17.379. URL https://link.aps.org/doi/10.1103/PhysRevD.17.379.

[14] R. Weiss. Quarterly progress report. Technical Report 105, Research Laboratory of Electronics, MIT, 1972. Available at : http://dspace.mit.edu/bitstream/handle/1721.1/56271/RLE_QPR_105_V.pdf?

[15] F. A. E. Pirani. On the Physical significance of the Riemann tensor. *Acta Phys. Polon.*, 15:389–405, 1956. doi: 10.1007/s10714-009-0787-9.

[16] Collins Harry. Interview with peter kafka, 1976. see WEBQUOTE under "Kafka reviews Weiss's Proposal" Available at : http://sites.cardiff.ac.uk/harrycollins/webquote/.

[17] David Shoemaker, R Schilling, L Schnupp, W Winkler, K Maischberger, and Albrecht Rüdiger. Noise behavior of the garching 30-meter prototype gravitational-wave detector. *Physical review D: Particles and fields*, 38:423–432, 08 1988. doi: 10.1103/PhysRevD.38.423.

[18] Collins Harry. *Gravity's Shadow, The search for gravitational waves*. University of Chicago Press, 2004. ISBN 0226113787.

[19] R. Weiss, P. Linsay, and Saulson P. A study of long baseline gravitational wave antenna system, 1983. Available at : https://dcc.ligo.org/public/0028/T830001/000/NSF_bluebook_1983.pdf.

[20] . LIGO webpage of Caltech : https://www.ligo.caltech.edu/page/ligo-gw-interferometer.

[21] Menner. LIGO Interferometer simplified, February 2016. Availble at: https://commons.wikimedia.org/wiki/File:LIGO_simplified.svg.

[22] R. Abbott et al. (The LIGO Scientific Collaboration and the Virgo Collaboration). GWTC-2: Compact binary coalescences observed by LIGO and Virgo during the first half of the third observing run. *arXiv e-prints*, page arXiv:2010.14527, 2021.

[23] NASA Goddard Space Flight Center. The gravitational wave spectrum, sources and detectors, January 2012. Source : https://science.gsfc.nasa.gov/663/research/index.html, Availble at: https://en.wikipedia.org/wiki/File: The_Gravitational_wave_spectrum_Sources_and_Detectors.jpg.

[24] K. Riles. Gravitational waves: Sources, detectors and searches. *Progress in Particle and Nuclear Physics*, 68:1–54, Jan 2013. ISSN 0146-6410. doi: 10.1016/j.ppnp.2012.08.001. URL http://dx.doi.org/10.1016/j.ppnp.2012.08.001.

[25] R. Abbott et al. (The LIGO Scientific Collaboration and the Virgo Collaboration). Tests of general relativity with binary black holes from the second LIGO-Virgo gravitational-wave transient catalog. *arXiv e-prints*, page arXiv:2010.14529, 2020.

[26] Matthias Blau. Lecture notes on General Gelativity. Available at: http://www.blau.itp.unibe.ch, December 2020. Accessed : 01-31-2021.

[27] C.W. Misner, K.S. Thorne, and J.A. Wheeler. *Gravitation*. W.H.Freeman & Co Ltd, 1973. p. 974-1044.

[28] David Andriot and Gustavo Lucena Gómez. Signatures of extra dimensions in gravitational waves. *Journal of Cosmology and Astroparticle Physics*, 2017(06): 048–048, Jun 2017. ISSN 1475-7516. doi: 10.1088/1475-7516/2017/06/048. URL http://dx.doi.org/10.1088/1475-7516/2017/06/048.

[29] Lisa Randall and Raman Sundrum. An Alternative to Compactification. *Physical Review Letters*, 83(23):4690–4693, Dec 1999. ISSN 1079-7114. doi: 10.1103/physrevlett.83.4690. URL http://dx.doi.org/10.1103/PhysRevLett.83.4690.

[30] Shing-Tung Yau. Calabi's conjecture and some new results in algebraic geometry. *Proceedings of the National Academy of Sciences*, 74(5):1798–1799, 1977. ISSN 0027-8424. doi: 10.1073/pnas.74.5.1798. URL https://www.pnas.org/content/74/5/1798.

[31] A.O. Barvinsky and Sergey N. Solodukhin. Echoing the extra dimension. *Nuclear Physics B*, 675(1-2):159–178, Dec 2003. ISSN 0550-3213. doi: 10.1016/j.nuclphysb.2003.10.011. URL http://dx.doi.org/10.1016/j.nuclphysb.2003.10.011.

[32] M. Maggiore. *Gravitational Waves : Volume 1 : Theory and experiments*. OUP Oxford, 2007. p. 339-241 and 494-495.

[33] . Location and orientation of LIGO and Virgo: https://www.ligo.org/scientists/GW100916/GW100916-geometry.html.

[34] Frank Elavsky and Aaron Geller. Masses in the stellar graveyard. Stellar Graveyard : https://media.ligo.northwestern.edu/g.

[35] Clifford M. Will. The confrontation between general relativity and experiment. *Living Reviews in Relativity*, 17(1), Jun 2014. ISSN 1433-8351. doi: 10.12942/lrr-2014-4. URL http://dx.doi.org/10.12942/lrr-2014-4.

[36] Peter T.H. Pang, Rico K.L. Lo, Isaac C.F. Wong, Tjonnie G.F. Li, and Chris Van Den Broeck. Generic searches for alternative gravitational wave polarizations with networks of interferometric detectors. *Physical Review D*, 101 (10), May 2020. ISSN 2470-0029. doi: 10.1103/physrevd.101.104055. URL http://dx.doi.org/10.1103/PhysRevD.101.104055.

[37] R. Abbott et al. (The LIGO Scientific Collaboration and the Virgo Collaboration). GW170814: A three-detector observation of gravitational waves from a binary black hole coalescence. *Physical Review Letters*, 119(14), Oct 2017. ISSN 1079-7114. doi: 10.1103/physrevlett.119.141101. URL http://dx.doi.org/10.1103/PhysRevLett.119.141101.

[38] R. Abbott et al. (The LIGO Scientific Collaboration and the Virgo Collaboration). Tests of general relativity with gw170817. *Physical Review Letters*, 123 (1), Jul 2019. ISSN 1079-7114. doi: 10.1103/physrevlett.123.011102. URL http://dx.doi.org/10.1103/PhysRevLett.123.011102.

[39] Official website of the Einstein telescope: http://www.et-gw.eu/.

[40] . Caltech website, LIGO India page: https://www.ligo.caltech.edu/page/ligo-india.

[41] . Official website of the LIGO India observatory, Detector specifications: https://www.ligo-india.in/activities/research/detector/.

[42] Caltech website, KAGRA Begins Initial Observations:
https://www.ligo.caltech.edu/news/ligo20200304.

[43] Cosmic Explorer website: https://cosmicexplorer.org/#.

[44] ESA website, LISA page: https://www.sci.esa.int/web/lisa.

[45] Jolien D. E. Creigthon and Warren G. Anderson. *Gravitational-wave Physics and Astronomy: Introduction Theory, Experiment and Data Analysis*. Wiley VCH, 2011. p. 88.